W. van der Zee

Flushing Basins

A study of the effect of geometric parameters on the performance of a flushing basin system

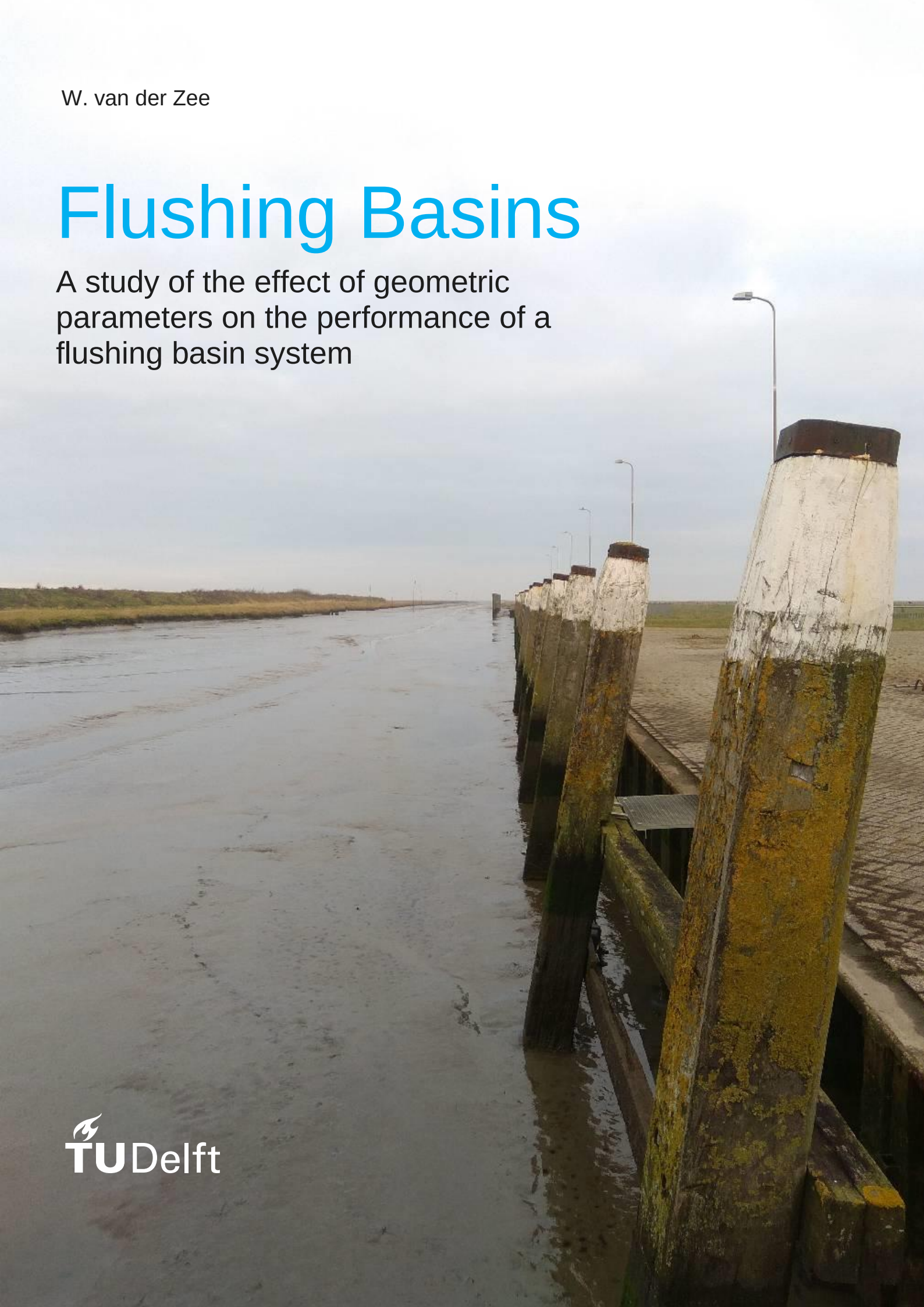

TU Delft

FLUSHING BASINS

A study of the effect of geometric parameters on the performance of a flushing basin system

By:

W. van der Zee

in partial fulfilment of the requirements for the degree of

Master of Science
in Civil Engineering

at the Delft University of Technology, Faculty of Civil Engineering and Geosciences

Date:	19/10/2017	
Student number:	1354582	
Graduation committee:	Prof.dr.ir. S.G.J. Aarninkhof	Professor of Coastal Engineering, TU Delft
	Prof.dr.ir. J.C. Winterwerp	Professor of Environmental Fluid Mechanics, TU Delft
	Ir. T.J. Zitman	Assistant Professor of Coastal and Hydraulic Engineering, TU Delft
	Dr. J. Cleveringa	Senior specialist, WAT - Deltasystemen & Waterveiligheid, ARCADIS

TU Delft

ARCADIS Design & Consultancy for natural and built assets

The cover image: The harbour of Noordpolderzijl, made during a visit at 19-12-2016, 9:53 h

PREFACE

The boundary between land and water has many configurations. In the Netherlands, the Dutch try to protect and conserve the unique natural morphology of tidal flats and channels in the Wadden Sea as much as possible. Nevertheless, when the natural net residual transport causes navigational problems (silting up), human intervention is inevitable to protect economic interests. In this era of environmental awareness, the trend is to search for sustainable solutions and the ideal would be to develop a system allowing the maintenance of the navigational channels in the Wadden Sea at their original depth with minimal human interference.

In this thesis, I describe such a system: the so-called flushing basin system. I asked myself the question: "Is it an obsolete outdated solution or can it be reintroduced?" My personal curiosity has been a strong driving force to write this thesis. I was intrigued to research a method that uses the force of nature (tidal force) to optimize the navigability of a tidal harbour channel. A method which brings the philosophy of 'Building with Nature' into practice.

This thesis is a part of the master Coastal Engineering, one of the specializations of Civil Engineering and Geosciences of Delft University of Technology. In cooperation with Arcadis BV, an engineering company in Zwolle, I worked on the topic of the function of flushing basins.

I would like to thank all colleagues of Arcadis Zwolle, my hosting company, for their involvement and help. Especially Jelmer Cleveringa: not only for his expert knowledge, but also for his good sense of humour and patience at all times.

Moreover, I would like to thank all members of the committee for their guidance and supervision of my thesis. For discussing the progress with Tjerk, regular visits have been made to Delft. These meetings had been an important aid. Unfortunately, most of the time ending up with cold coffee.

The hospitality of my aunt and uncle to invite me to stay at their place for the total duration of my thesis has been unlimited. They offered not only a place to stay moreover a special time. Especially the *Haute Cuisine* and the relaxing evenings watching old movies my uncle bought at the various second-hand shops.

Last but not least, this thesis could not have been made without the support of my close family and friends. My parents that gave me the possibility to study.

ABSTRACT

Flushing basins have been used at several locations in Germany, Belgium, and the Netherlands in the past centuries to maintain the navigational depths of harbour channels. These locations are not in use anymore or are only partly responsible for channel maintenance. This thesis encompasses a study to optimize the geometric parameters of a flushing basin system in a tidal back barrier basin. Although flushing basins are known as an effective method to prevent siltation, used in the past, full comprehension of their functioning is still lacking. The addition of a flushing basin behind a tidal harbour channel (see Figure 1) is meant to affect the sediment regime in the channel from a flood-dominant towards an ebb-dominant regime. This ebb-dominant regime implies a net export of sediment and therefore it prevents the siltation of the tidal harbour channel. With a one-dimensional model of a schematized reference situation, the role of three parameters in the tide-residual sediment transport is investigated for the flushing basin system sketched in Figure 1. The examined parameters are: the sluice width, the horizontal area of the flushing basin and the ratio between the tidal amplitude and the channel depth. The last parameter has been studied and concluded to be an important parameter for the tide-residual transport. The other two presumed to be important parameters as these determine the channel-basin interaction.

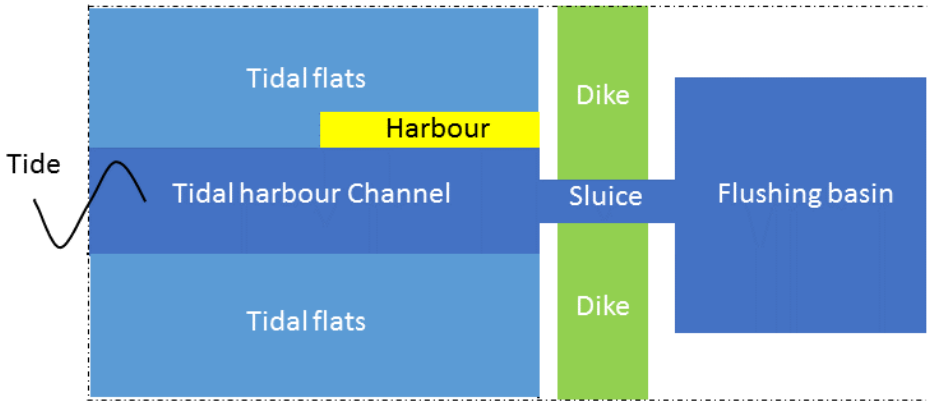

Figure 1 - Top view of schematization of the flushing basin system

For the reference location of Noordpolderzijl, representative values for a flushing basin system have been defined. The functioning of a flushing basin is simulated by using a one-dimensional hydrodynamic model. This model has longitudinal constant cross section representing a tidal channel including tidal flats. Results of the peak velocity should show asymmetry, this is used as an indicator for the optimal function of the flushing basin system.

Based upon this research and numerous simulations, varying the key parameters in the model, it can be concluded that three conditions need to be met simultaneously to create ebb dominance along the total length of the channel:

- **a sufficiently large flushing basin area**:
  an increased flushing basin area results in larger current velocities as result of the increased phase lag of the water level in the basin compared to the water levels in the channel. The positive effect of an increase of the flushing basin area, decreases for larger flushing basin area.
- **a small sluice width, compared to the channel width.**
  The sluice width is most important for an optimal function of the flushing basin. The sluice width must be sufficiently small, to create a tide-residual ebb transport. For sluice widths of about one fifth of the width of the channel. For higher values of the width, flood dominance is present in part of the channel. In combination with a relatively shallow channel, the net transport quantities are larger than for the situation without the presence of a flushing basin.
- **a relatively deep channel compared to the tidal amplitude.**
  Considering a tidal amplitude of 1 m and a depth of 5 m, result in a tide-residual transport for the total length of the channel in the seaward direction which is maximum.

For each combination of the key parameters another tide-residual transport over the channel is present. Fulfilling the above three combined conditions an optimal design can be created. The added value of this study: by a one-dimensional description of the flushing basin system, the effect of the geometric key design parameters can be quantified to optimize the design of a flushing basin system.

CONTENTS

1 INTRODUCTION

The objective of this study is to gain insight in the functioning of 'flushing basins' to counteract channel siltation in tidal basins. The Dutch local board of Eemsmond and the water board of Noorderzijlvest initiated to implement a flushing basin at Noordpolderzijl at the Dutch Wadden Sea. The involvement of ARCADIS in the feasibility study for a flushing basin allowed me to choose Noordpolderzijl specifically as a reference situation.

What is a flushing basin?

A flushing basin (in Dutch: 'Spoelmeer' or 'Spuikom') is an artificial tidal basin that enables extra tidal flow through a tidal channel by filling and emptying the basin. The enlarged tidal flow through the tidal channel affects the tide-residual sediment transport and the erosion and sedimentation pattern within the channel. The function of a flushing basin is its ability to counteract detrimental sedimentation within the tidal channel, and so to maintain the navigability of the tidal channels to harbours. A schematic overview of the flushing basin is given in Figure 2. In the upper panel, a top view of a flushing basin system is visualized. The main elements are indicated by dark blue: a tidal channel, a sluice, and the flushing basin. Along the channel and connected to the shore, a harbour is situated. Alongside the tidal channel tidal flats are present. The tidal flats at either side of the channel are submerged only during high water only. In this study, it is assumed that the channel remains flooded at all times.

In the lower panel, the cross-section AA' of the upper panel is given. Cross-section AA' is indicated in the upper panel by a horizontal dashed line. On the left-hand side, the system is forced by the tide. The exchange of water between the channel and the flushing basin results in different water levels and current velocities in the channel than for the situation without a flushing basin. The sluice will affect the exchange of water too.

Research in Ostend in Belgium (Hubrechtsen, 2000) confirms the difficult optimization of a flushing basin system. In Ostend, several basins have been constructed and used simultaneously to optimize the effects. In Germany at Nessmersiel, the effects are optimized with an open/closure regime. But despite the use of the flushing basin at Nessmersiel agitation dredging is needed to increase the effect of the flushing basin (Coldewey, Erchinger, & Probst, 1987). Recently, a feasibility study for Holwerd in the Netherlands, confirms marginal effects of a flushing basin (P.C.P. Vellinga et al., 2015) and (P.C.P. Vellinga et al., 2016).

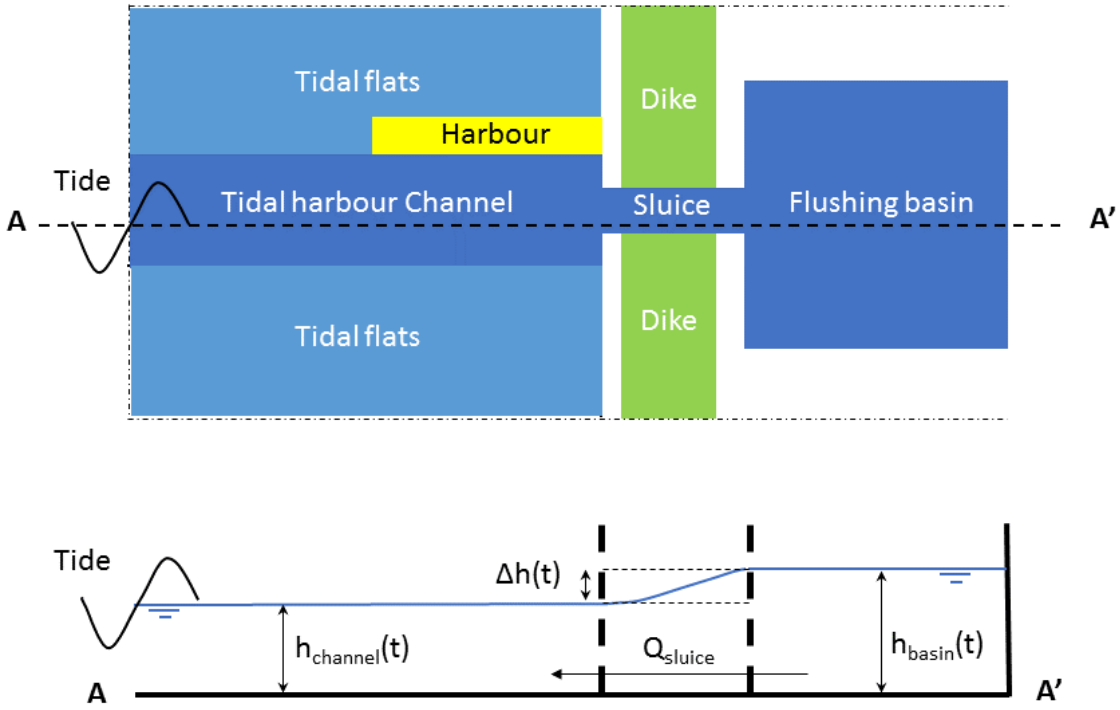

Figure 2 - Top view (upper panel) and cross-section (lower panel) of a flushing basin system

1.1 Problem definition

Within tidal basins a system of flats and channels is present, sometimes with salt marshes along the shore. Close to these shores and the tidal watersheds, the current velocities are lower than elsewhere in the basin. Due to the decreased current velocities, finer sediment can be found here. In the past, harbours were built at the ends of natural tidal channels. The siltation causes problems for the navigability of the tidal channels. Moreover, the required depth for navigational purposes is in most cases larger than the equilibrium depth, from morphological point of view. Therefore, these channels are dredged frequently to maintain the required depth. The use of a flushing basin can form an alternative or addition to dredging. The idea is that, due to the water storage capacity a basin provides at the landward end of a tidal channel the flow in that channel changes to a regime that exports sediment and, hence, prevents siltation.

In the historical past, flushing basins have been used along the North Sea, the Western Scheldt and the Wadden Sea. However a proper design of these basins has been a difficult challenge (for example in Ostend (Hubrechtsen, 2000)). Nowadays a flushing basin is present at the harbour of Nessmersiel, in the German part of the Wadden Sea. There, the required depth of the harbour channel is maintained partly by use of the flushing basin. The depth is further increased by agitation dredging (Coldewey et al., 1987).

1.2 Research objective

The promising concept of flushing basins has not resulted in a complete alternative for dredging. The basic question is therefore:

Could flushing basins form an alternative solution to dredging in counteracting tidal harbour channel siltation problems?

To answer this question, the function and/or design of the flushing basin must be determined and optimized. This has been described already in a study for the flushing basin of Nessmersiel (Germany). The opening regime of the sluice has been changed to determine an optimum for the tide-residual suspended sediment transport. Based on the given geometries of the channel, the sluice and the basin, the effect of the various sluice regimes has been determined. However, for a new design of a flushing basin in other places, the geometric dimensions are not prescribed. By changing the width of a permanently open sluice in combination with the dimensions of the flushing basin, the integrated sediment transport in the channel considering one tidal period might be influenced positively. The second question therefore is:

What is the influence of the geometry (shape and dimensions) of the flushing basin system upon the residual tidal transport in the harbour channel?

In this thesis, the effect of the geometric parameters on the performance of the flushing basin system is investigated. The aim is to identify values of these parameters for which this performance reaches its optimum, given the local tidal conditions.

1.3 Methodology

Within a tidal basin the residual transport is dominated by the asymmetry of the tidal wave (see for example (van Straaten, 1957), (Dronkers, 1998) and (Wang, Jeuken, & de Vriend, 1999)). To determine the change of the residual transport in the channel by using a flushing basin, the focus therefore lies also on the asymmetry of the tide.

Most of the harbours located in tidal basins are close to or along the shore or dike and at the end of a tidal channel. For this study, it is assumed that the flushing basin is located at the landward end of the harbour channel and on shore or behind the dike. Between the harbour channel and the basin, a sluice is used to allow manipulation of the discharge between channel and basin by narrowing the width of the sluice (see upper panel of Figure 2).

To simulate the tidal flow in the tidal channel, the cross-sectionally integrated shallow water equations are used. As the variations of the bathymetry along the channel are small, a one-dimensional representation with a one-dimensional hydrodynamic model is sufficient. With this one-dimensional approach, the effect of the geometric parameters: area of the basin, depth of the channel and width of the sluice, on the asymmetry of the peak velocities can be quantified. With the variation of the values of these geometric parameters the effect on the performance of the flushing basin system is investigated. The values of these parameters are identified for which the performance reaches its optimum, given the local tidal conditions.

At Noordpolderzijl, implementation of a flushing basin has been inventoried (Danel, 2014) as part of the initiative: 'Programma naar een Rijke Waddenzee'[1]. It is one of the harbour channels in the Wadden Sea that has a large siltation problem. Although the tidal harbour channel to Noordpolderzijl is used as a reference case, the approach is still generic by using the geometric parameters.

In this theoretical study, the access channel to the flushing basin is straight and has a flat, horizontal bottom. The channel width varies with the water level to account for the presence of tidal flats at either side of the channel. The sluice connecting the channel and the flushing basin acts as a weir in the sense that its width determines the discharge through the sluice in relation to the difference in water level over it.

Results of the hydrodynamic model are used to quantify the asymmetry and related tide-residual sediment transport. For the sediment transport fine sediments are assumed to be present. For fine sediments and an alluvial bed, which provides an unlimited amount of available sediments, the asymmetry of the peak flow velocities is the dominant factor for the residual transport. The length of slack water durations is therefore not relevant, as would be the case for starved bed conditions. For extreme concentrations of cohesive sediments flocculation can occur, but this is not considered in the present study. Neither is he consolidation of fine sediments on the bed considered.

The analysis demonstrates how the geometric parameters of flushing basins influence the asymmetry of the tides and what the consequences are for the tide-residual transport. The theoretical results provide a first insight in the performance of flushing basins.

1.4 Outline

This document comprises a theoretical part, a model methodology part and a results part. The first chapter: literature survey, describes what a flushing basin is, and where and why they have been used. This part ends with the functional aspects identified in literature.

In the second part, the theory of tidal propagation and the asymmetry is presented in chapter 3. A description of the generation and forms of tidal asymmetry is given and the link to sediment transport is made.

The use of the hydrodynamic model is described in the next chapter (4). The set-up of the model, assumptions and the chosen variables and their variations are presented. In the last section: 'Check; linear solution, the model performance is checked for a channel with a very deep rectangular cross section.

In the following chapter 5: model-results, the results for the reference situation of Noordpolderzijl are depicted, comparing the initial situation without a flushing basin and with a flushing basin. In the subsequent sections each geometric parameter is described separately. An overview of the variations is given in section 5.7. This chapter ends with a conclusion on the effects of parameter variations.

Chapter 6 starts with an introduction of the limitations of the method. Finally, the conclusions and recommendations for further research are presented in chapter 7.

[1] 'Programma naar een rijke Waddenzee' has the ambition to restore and enrich the natural value of the Wadden Sea. The economic activities should not harm the environment. One of the strategies is to make a transition to a sustainable harbour and approach-channel management. The created extra value for nature and at the same time influence the morphology in such a way that it is suitable for navigational, are important for the success of each project within the Wadden Sea.

2 LITERATURE SURVEY

Flushing basins are not a new concept. Although they have been used at several locations in the past and at least at one location still today, flushing basins are not used often. Flushing basin seem a promising alternative or addition to dredging. However, optimising the design still proves to be difficult. In this chapter, a description of a flushing basin is given in 2.1. Where and how they have been used is discussed in 2.2. The aspects that are important for an optimal performance of flushing basins are presented in 2.3.

2.1 What is a flushing basin?

A flushing basin is an artificial tidal basin which enables extra tidal flow through a tidal channel by filling and emptying the basin. The aim of a flushing basin is to prevent the channel from silting up. Without the presence of a flushing basin the current velocities decrease to zero in the direction of the channel-end (landward end).

The flushing basin is located at the landward end of the channel and connected with the channel by a discharge sluice. The discharge sluice has a width that is narrower than the channel width. The narrow discharge sluice between the channel and the flushing basin results in locally enlarged current velocities at either side of the discharge sluice. The effect of a discharge sluice resembles that of a weir. The effect of the discharge sluice must be considered when studying functioning of a flushing basin system. A weir can be used to close off the flushing basin in storm situations and to influence the in- and outflow. However, the closing or partial closing of a weir is not discussed in this study. Locally the effect of the discharge sluice as part of a flushing basin system, can be described by the equation of Torricelli, see Equation 1. The equation describes the exchange of water through the sluice between the basin and channel. This is schematically visualized in Figure 3, showing a longitudinal cross-section. At the left-hand side, the channel and at the right side the basin are located. The discharge sluice is situated In between. The sluice is schematized as two vertical lines, which is generally a long structure with at either side bottom protection. As a result of the relatively narrow discharge sluice and wide channel and flushing basin, a difference in water levels can arise; $\Delta h(t)$. This level difference results in a discharge at the sluice (Q_{sluice}) determined by:

Equation 1 - sluice discharge

$$Q_{sluice}(t) = A_{effective}\sqrt{2g\Delta h(t)}$$

With:

Equation 2 - Cross-sectional area of the sluice

$$A_{effective}\ (t) = W_{sluice}\ h_{channel-end}(t)$$

and

Equation 3 - water level difference

$$\Delta h(t) = Z_{channel-end}(t) - Z_{basin}(t) = cos(\omega_{M2}t) - cos(\phi)cos(\omega_{M2}t - \phi)$$

With:

ω_{M2} = semi-diurnal wave frequency
ϕ = phase difference, with $0 < \phi < \frac{\pi}{2}$

To determine the effective cross-sectional area of the sluice ($A_{effective}$), in which all dissipative effects are excluded, the lowest water level of the channel and the basin is used. For the situation depicted in Figure 3 $h_{channel}(t)$ is used. In this study the sluice is permanently open. The discharge through the sluice is partly defined by the width of the sluice and therefore a design parameter. In this study, the effect of various sluice widths is determined, see section 5.3. The sluice width is not managed.

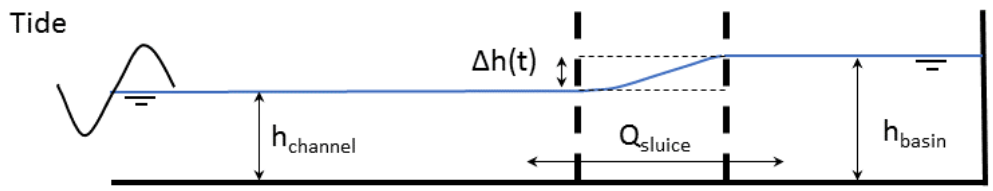

Figure 3 - Schematic visualization of the functioning of a weir as result of tidal variation in the channel at a moment in time.

In Figure 4, the variation of the water level of the basin Z(t) in orange, and the channel Z(t) in black, combined with the time variable discharge at the sluice, are illustrated. Due to a semi-diurnal tidal water level variation in the channel, see Figure 4 in orange, the water level in the flushing basin is varied, see Figure 4 in black. Although this periodically variation is rather theoretical, it is illustrative. As the discharge sluice is relatively narrow, the water level variation of the basin is delayed and reduced compared to the variation in the channel. As result of the variable water level difference between the channel and the basin, the sluice discharge varies with time. The maximum discharge in grey is halfway the basin water level variation. This is when the water level difference between basin and channel is at its maximum.

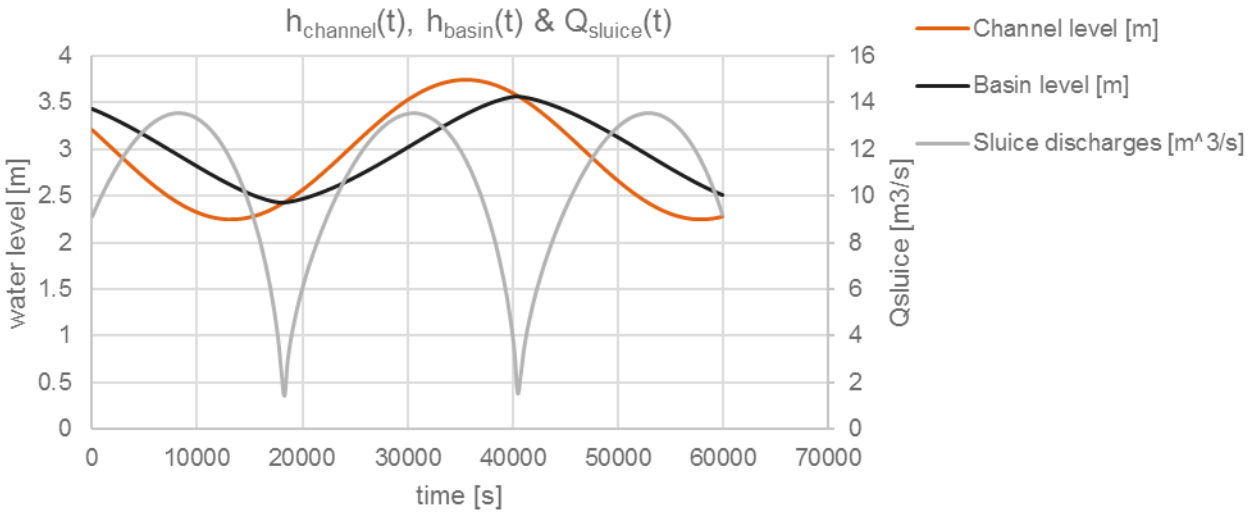

Figure 4 - Sluice discharge $Q_{sluice}(t)$ as result of the water level difference of the channel; $h_{channel}(t)$ and basin; $h_{basin}(t)$

2.2 Locations with a flushing basin

Flushing basins have been used in the past to maintain the depth of approach channels of harbours. Some are still in use today. In Table 1, some of these locations are enumerated. In the next section, the flushing basins at Nessmersiel and Ostend are described.

Table 1 - Locations with flushing basin

The Netherlands	Belgium	Germany
Breskens	Ostend	Nessmersiel
Goes	Doel	Dornumersiel
Middelburg	Blankenberge	Harlesiel
Vlissingen (in English: “Flushing”)		Greetsiel
Sluis		Norddeich
Den Helder		Norderney

2.2.1 Ostend

The city of Ostend has a rich history of using flushing basins to maintain the depth of the harbour approach channel (Hubrechtsen, 2000). For several centuries land is subsequently sacrificed and retaken to adjust the basin area to obtain current velocities in the harbour more appropriate for maintaining the required depth. The next few sections describe this sequence.

2.2.1.1 Historical description

In the early 16th century a discharge sluice was used to flush the harbour with surplus water from the hinterland. At the end of the century a new entrance was created through a breach in the dunes east of Ostend. A large intertidal area was created: a polder-flushing-system. This system, called the Catharina polder, consisted of several polders, indicated in Figure 5 with different colours. Due to the construction of several dikes (the Steense Dijk in 1608, the Groene Dijk in 1612 and the Legaards Dijk in 1626) the area of the Catharina polder reduced. This resulted in unintentional siltation of the harbour.

To increase the depth of the channel ones again, the polders Zwaenhoekschorre (see Figure 5, nr. 2) and the Nieuwe Zandvoordepolder (see Figure 5, nr. 3) were added to the system in 1664, enlarging the flushing basin to 1500 ha. Although large depths originated by the increased current velocities through the harbour channel, the subsequent large currents resulted in erosional problems to the embankments and the city. The city council supported in 1697 new dikes that landowners demanded to protect their land. And, the Nieuwe Zandvoordepolder had to be closed off again.

In 1720 complaints about the reduced depth had to be solved by a breakthrough of the Snaaskerkepolderdijk (see Figure 5, nr.4). In 1744 the Catharinapolder was closed due to siltation and subsequent closure of other polders resulted in the end of this Polder-flushing-systems.

In the nineteenth century, the construction of discharge sluices in Ostend resulted in a resurrection of the use of flushing basins, see Figure 6. The discharge sluice 'Écluse de Chasse' with a basin area of 25.5 ha behind it and the 'Military sluice' with a basin of 12 ha were not sufficient to counteract the siltation of a bank in front of the harbour. In 1863, closer to the harbour entrance, the construction of the Leopoldsluice with a basin of 17.2 ha had to solve the problem. Operational problems resulted in a few uses only. The last flushing basin of 85 ha was created in 1912, indicated with nr. 5 in Figure 6. This basin, however, has also been used a few times only due to the creation of the steam engine and dredging equipment as an alternative for maintaining the depth of the channel.

Figure 5 - Ostend Polder-flushing-system (Hubrechtsen, 2000)

Figure 6 - Ostend flushing basins anno 1897 (Hubrechtsen, 2000)

2.2.1.2 Concluding notes about Ostend

To the history of the flushing basin at Ostend, a few remarks can be made:

- The entrance channel of the harbour of Ostend has been changed frequently as result of adjustments to the geometries of the harbour. The use of a flushing basin system created by inundation of existing polders, had been an effective method to increase the current velocities in the entrance channel. Too large polder areas resulted however in too large current velocities, that not only resulted in the erosion of the channel bed but also of the channel embankments.
- In addition, banks present on the bed of the harbour channel had been a recurring problem. With consecutive constructions of multiple basins at several locations and simultaneous usage, Ostend tried to get rid of these banks. However, without good results.
- The decreased basins areas of Ostend resulted in decreased current velocities in the channel. At the same time, the depth reduced in the channel. An increased basin or polder area resulted in larger current velocities in the channel and larger channel depth. A relation between the channel depth and basin area seems to be present.

The optimization of a flushing basin should consider a mechanism that only creates bottom erosion without erosion of the embankment of the channel. In addition, banks at the entrance of the channel should be resolved. Is an optimal design possible? Or, are measures to protect the embankments still required?

2.2.2 Nessmersiel

At Nessmersiel a flushing basin has been used since 1979. Nessmersiel is in the German part of the Wadden Sea. The harbour channel to Nessmersiel is connected to the deeper channel called Nessmersieler Balje, in the Wadden Sea. The alignment of the channel is perpendicular to the dike. The harbour of Nessmersiel is located close to the dike at the end of the channel. This harbour is used by the ferry to Baltrum and by smaller fishing and recreational vessels.

The flushing basin has an area of about 14 ha., a storage volume of 80 – 100 km^3 and a channel length of 2 km. Along the channel there is a dam: Leitdamm, see Figure 7. This dam prevents siltation as result of the tidal cross-currents. The deeper access channel starts at the end of the dam, indicated with Nessmersieler Balje.

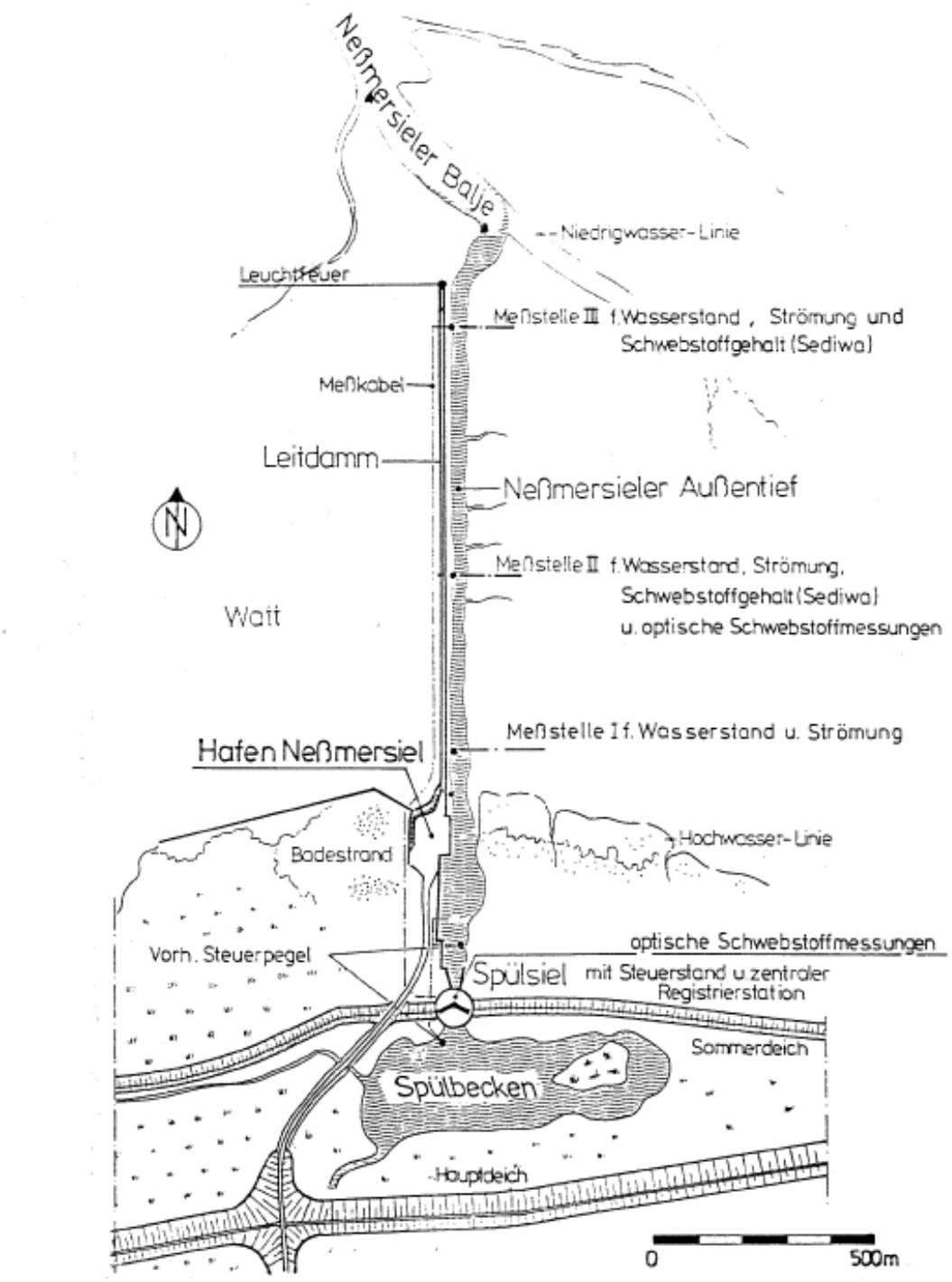

Figure 7 - Plan view of the flushing basin Nessmersiel, original figure from (Coldewey et al., 1987)

In the past, other flushing basins have been constructed along the German shore but total siltation of the basin resulted in non-functioning flushing basin systems, e.g. at Norddeich, Norderney und Greetsiel. No documentation considering these basins is known. The impact of today's flushing basin of Nessmersiel has been researched by the Bauamt fur Küstenschutz Norden in the period of 1984 – 1986 (Coldewey et al., 1987). All values mentioned in the section are from this research. In the next section, a short summary of the findings is given.

2.2.2.1 Concluding notes about Nessmersiel

There is a sluice with multiple gates that can be used to close or open the sluice partly or entirely. The flow can thus be forced through upper or lower part of the water column. During one tidal cycle, a closing regime can be used to influence the net sediment transport.

To investigate the effect of the flushing basin of Nessmersiel, measurements on water level, current velocity in longitudinal and cross-channel direction, suspended sediment concentration, turbidity and oxygen-temperature have been executed. By measuring the temporal variation of concentration at various locations, an indication of the removal of sediments has been obtained. Various closing regimes have been investigated (Coldewey et al., 1987).

To maximize the net residual transport in the ebb direction, delayed flushing is used. For a few hours directly following high water, the sluice is closed. When the water levels in the channel have been lowered to almost the lowest level, the sluices are opened. See Figure 8, in which the dashed line indicates the basin level. As result of an increased head difference the discharge at the sluice increases, as described in section 2.1.

To gain insight into the effectiveness of the flushing basin, the concentration of the suspended sediment in the water column was measured at two locations in the channel. Various moments for flushing has been investigated, to determine the effect on the net sediment transport. Depending on the delay of flushing an optimum is determined. The optimum in net suspended sediment transport is obtained at 2.2 hours before low water, see Figure 9.

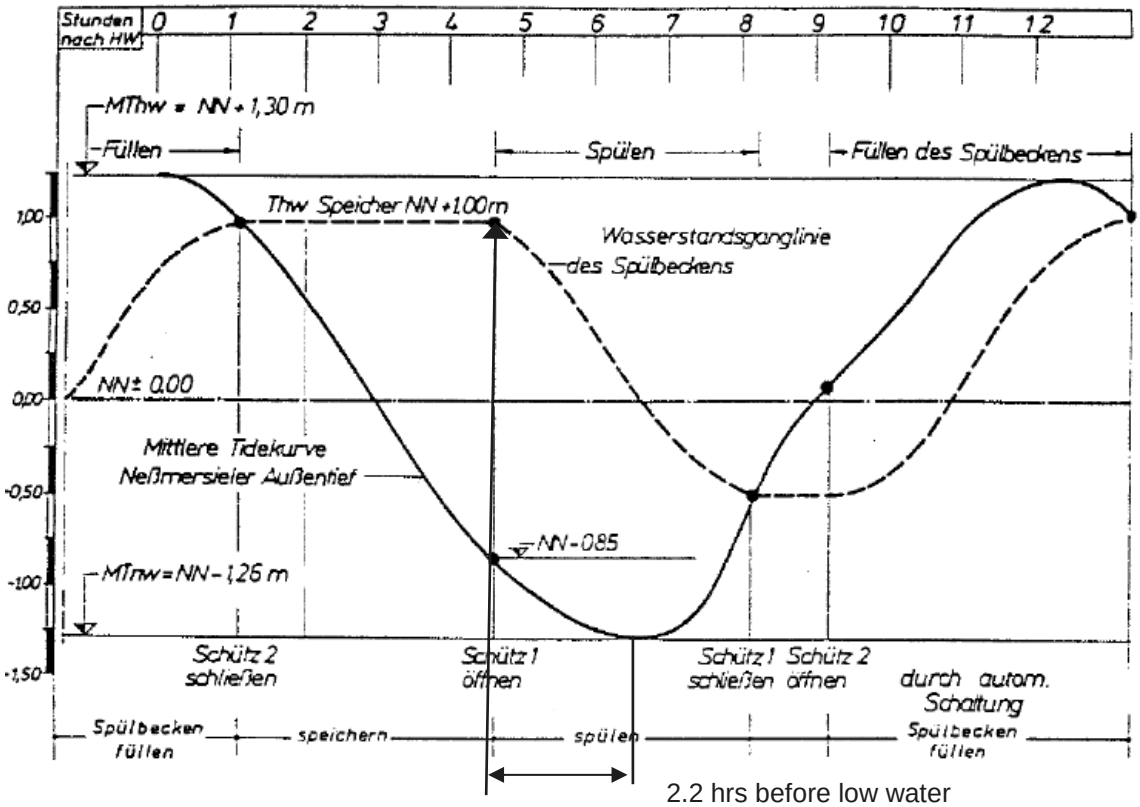

Figure 8 - Water levels in the channel and the basin of Nessmersiel, from (H.G. Coldewey et al., 1987) Füllen =filling, Speicher = storing, Spülen = flushing and Spülbecken = flushing basin. Black line: average water level of Nessmersiel, Dashed line: water level of the flushing basin.

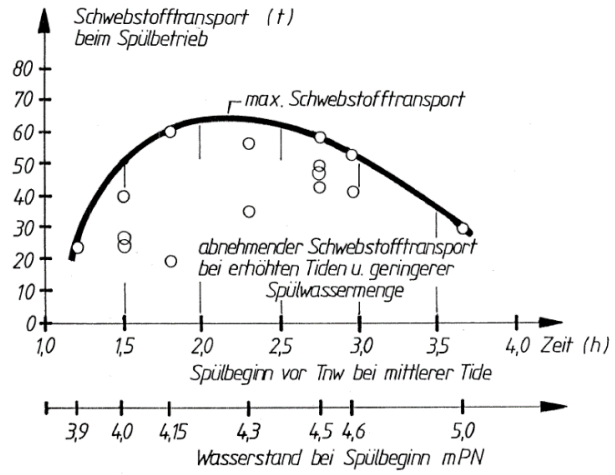

Figure 9 - Suspended sediment transport for various sluice regimes at Nessmersiel. (H.G. Coldewey et al., 1987)

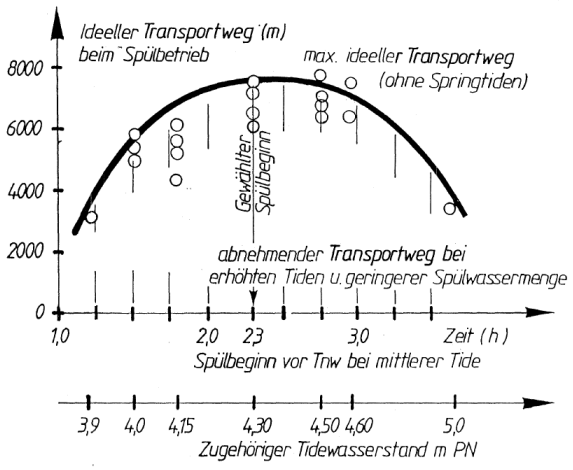

Figure 10 - Transport length of suspended sediment. (Coldewey et al., 1987)

Concluding notes about Nessmersiel research are:

- The presence of a flushing basin increases the current velocities in the channel. These velocities can be increased furthermore by temporal closure of the sluice. The closure of the sluice, results in a water level difference between the basin and the channel. Due to the water level difference at the sluice the current velocities in the channel will increase. A longer closure increases the water level difference between the channel and the basin. However, the available duration of flushing will reduce when the closure time will increase as the water levels will rise during flushing. An optimum is determined for the closure time of the sluice to maximize the net residual transport during one flushing cycle. A minimum duration of two hours and a velocity larger than 0.5 m/s is recommended. For Nessmersiel flushing should be delayed from high water to 2.2 hours before low water.
- Flushing should be started when the water levels in the channel are lowered beneath the tidal flats, to prevent spreading of discharge water from the basin over these tidal flats. When the flushing duration becomes too short, earlier flushing is needed.
- During the erosion phase a sufficiently large transport length should be obtained such that the material can be captured and transported in seaward direction by the natural tidal flows and does not come back to the harbour channel.
- The filling of the basin should occur during the second half of the flood tidal period as the suspended sediment content in the water column is lower in than in the first half of the flood tidal period.
- Initial deepening of the basin as a buffer is needed, as the basin is sediment trap.
- Transport of sediment during flushing may be increased by deployment of boats to stirr up material. A volume of 300 t transported sediment, is measured at one location in the channel, that was created by the ebb currents for a duration of 3.5 hours and current velocities up to 1.1 m/s.

The findings above can optimize the tide-residual suspended sediment transport, for example by defining an optimal sluice regime (opening and closing time) of the flushing basin of Nessmersiel. With a sluice, delayed flushing is possible. The delayed flushing results in a head difference between the channel and the flushing basin. This water level difference results in an increased discharge at the sluice as explained in section 2.1.

Delayed flushing is advantageous as it is attended with larger current velocities than without a delay. Simultaneously, a delay results in a decrease of the flushing period as the sum of the delay and the flushing period is bounded by the duration of ebb. The contradiction of these two effects with respect to sediment transport calls for an optimization of the delay.

3 TIDAL ASYMMETRY

When a tidal wave with equal flood and ebb velocities enters shallow water, the magnitudes of flood and ebb velocities becomes unequal due to non-linear processes. This inequality is called tidal asymmetry. Because there is a direct relation between the velocities and the sediment transport, the tidal asymmetry results in a tide-residual sediment transport. The inequality is caused by the generation of higher harmonics, which are multiplications of the base frequency. Their generation depends on the geometry of the channel or basin. The tidal waves can be described by using the cross-sectionally integrated shallow water equations considering an idealized prismatic channel, see 3.1.1. These equations comprise various non-linear terms, e.g. the friction and the advective inertia, for which their relative importance is shown.

The generation of higher harmonics as a result of the non-linear terms in the shallow water equations is discussed in 3.2.1. The resulting asymmetry can be quantified by determining the subsequent multiplications of the base frequency. To get an indication of the tide-residual sediment transport direction, the magnitude and phase shift between the base frequency and it first higher harmonic are used. Depending on the type of sediment different asymmetries and phases are of importance, see 3.2.2 for a description.

3.1 Tidal waves

Waves can be classified in terms of their period and wave length. Tidal waves are waves which are generated by the interaction of the ocean with the moon and the sun. These waves have one of the longest time and length scales of all types present in the ocean waves. When a wave enters shallow water, with a relative small depth h compared to the wavelength L, the wave can be can be called a shallow water wave when h/L < $1/20$. For these type of waves, hydrostatic pressure distribution can be assumed. The Wadden Sea with its relatively small depth compared to the wavelength of the tidal wave, this condition is also met. The flow below a free surface in a fluid in shallow water can be described by the shallow water equations.

3.1.1 1D shallow water equations

Considering a prismatic channel, the shallow water can mathematically be described by the Saint-Venant equations or the cross-sectionally integrated shallow water equations:

Equation 4 - Continuity equation

$$\underset{(1)}{\frac{\partial \zeta}{\partial t}} + \underset{(2)}{\frac{\partial hu}{\partial x}} = 0$$

Equation 5 - Momentum equation

$$\underset{(3)}{\frac{\partial u}{\partial t}} + \underset{(4)}{u\frac{\partial u}{\partial x}} + \underset{(5)}{g\frac{\partial \zeta}{\partial x}} + \underset{(6)}{c_f\frac{u|u|}{h}} = 0$$

In which:

ζ	=	water level,	[m]
h	=	channel depth,	[m]
u	=	current velocity,	[m/s]
Q	=	discharge,	[m^3/s]
W	=	channel width,	[m]
A	=	cross-sectional area,	[m^2]
g	=	acceleration due to gravity,	[m/s]
c_f	=	dimensionless friction coefficient,	[-]
R	=	hydraulic radius = A/P in which P is the perimeter.	[m]

With the terms of the shallow water equations indicated by a number representing:

(1) the storage term,
(2) discharge gradient term,

(3) the local inertia term: rate of change of momentum in the channel with time,
(4) the advection term: rate of change of momentum flux due to velocity,
(5) the slope term,
(6) the bottom friction term.

The shallow water equations apply, provided that, by fair approximation (Speer & Aubrey, 1984):

- the pressure distribution is hydrostatic,
- the surface level elevation doesn't vary across the channel,
- the depth h is relatively small compared to the width W of the channel: h/W<<1,
- the length of the channel $L_{channel}$ is large compared to the width W of the channel: $W/L_{channel}<<1$.

These two equations form a set of partial differential equations. Together with boundary and initial conditions, they represent a boundary value problem. The number of boundary conditions is determined by the number of characteristics entering the domain. Considering subcritical flow ($Fr = \frac{|u|}{\sqrt{gh}} < 1$), there are two ingoing characteristics propagating in opposite direction. Therefore, at each side of the domain one boundary condition is needed, i.e. x = 0 and x = L. Also, there are two initial conditions required, one for the water level ζ and one for the discharge Q (Zijlema, 2015).

The solution to these equations comprise of a homogeneous and a particular part. The homogeneous part depends on the initial conditions and the particular part on the boundary conditions. To start a time-dependent simulation, the initial conditions are needed.

The homogeneous part of the solution asymptotically decays as result of the presence of bottom friction, indicated with (6) in Equation 5.The homogeneous solution vanishes after the spin-up time is exceeded. The remaining solution is the particular solution. The particular part of the solution depends on the boundary conditions, also called periodic state solution. The solution is in a state of equilibrium only depends on the boundary conditions (Zijlema, 2015). The initial conditions can therefore be chosen arbitrarily. The boundary conditions are described in section 4.2.2.

The periodic state solution is the result of the periodic forced boundary conditions. One representing the tidal wave at the seaward side of the model and the other the interaction of the channel and the basin. The combined boundary conditions give the response of the system (the periodic solution) comprised of the channel and basin. This is the solution that is used to determine the tide-residual transport.

3.1.2 Non-linearity

Long waves can be distorted (change its shape) as result of the geometry of the channel. Whether these changes occur, depends on the non-linearity of the long waves. A measure for the non-linearity of the long wave is given by the ratio u/c. For long waves u/c = a/h, which is known as the Non-dimensional wave amplitude. To situations are possible:

- When a/h is small, large changes of the channel geometry (width) have no effect on the non-linear development of the tidal wave.
- When a/h is large, changes of the channel geometry will influence the non-linear development of the tidal wave.

For the area of interest, for the study on the effect of a flushing basin, the non-linearity is also of importance. The next describes the various change of the as result of the non-linear effects.

3.2 Tidal asymmetry

To predict tidal waves the method of harmonic analysis is used. By use of this method for each location in a tidal area, the water level variation of the tidal waves can be expressed in the formula:

Equation 6 - water levels by harmonic analysis

$$\zeta(t) = a_0 + \sum_{n=1}^{N} a_n \cos(\omega_n t - \alpha_n)$$

With:

$\zeta(t)$	=	tidal water level with reference	[m]
a_0	=	mean level	[m]
a_n	=	amplitude of component number n	[m]
ω_n	=	angular velocity of component number n	[1/hr]
α_n	=	phase angle of component number n	[-]
t	=	time	[hr]
N	=	Number of harmonic components	[-]

The tidal wave is described by its tidal components or constituents. These tidal constituents represent the influence of the sun and declinational effects of the sun and the moon. However, at most places in the world including the Wadden Sea the tide is predominantly semi-diurnal and indicated by M_2 (Bosboom & Stive, 2015). The 2 in M_2 refers to the two high waters and two waters each day and the M refers to the influence of the moon. In the North Sea the other constituents have a minor contribution.

For comprehension of the analysis in this study a semi-diurnal (M_2) tide is assumed, without the presence of other constituents. The mean level a_0 is defined by NAP, the fixed reference level in the Netherlands.

There are also constituents that are generated by the non-linear effects of the bottom friction: the advection of inertia and the geometry of the tidal basin. These non-linear effects introduce the asymmetry, which is the cause of the tide-residual transport. The reason for this tide-residual transport is that the transport is proportional to the current velocities u to the order n (n = 3…5). When u is composed of a linear combination of sinusoidal components, u^n might not be equal to zero and a tide-residual transport is present. An indication of the direction of the tide-residual transport as result of asymmetry can be given by looking to the higher harmonics in the velocity signal. From research is known (Speer & Aubrey, 1984) that the combination phases and amplitudes of the M_2 and M_4 gives a good representation of the asymmetry. Different types of asymmetries can be determined and may affect the sediment transport:

- Time asymmetry
- Peak velocity asymmetry
- Internal asymmetry

After a description of the generation of the asymmetry, the different types of asymmetries are elaborated upon in the subsequent sections.

3.2.1 Generation

The generation of the asymmetry can be described by the combination and interaction of two tidal components. The linear combination of two components results in an amplitude modulation called subharmonic tides (e.g. spring-neap cycle). The non-linear interactions of tidal components lead to both subharmonic and superharmonic tides (e.g. M_4, M_6, M_8, etc. as a result of the interaction of M_2 with itself or as a result of the interaction with various components) (Wang et al., 1999). With the shallow water equations, the generation of the higher harmonics can be mathematically described as they include the non-linear phenomena advection and bottom friction.

The higher harmonics are the result of the following **non-linear effects**:

- Quadratic friction
- Advection of momentum
- Interaction of the tide with the geometry, e.g. tidal flats

The effect of the geometry of a channel and the presence of tidal flats has been presented in (Speer & Aubrey, 1984). In this research, it is stated that: ‘In general, more time-variable geometry and stronger friction produce larger M4 /M2 ratios. The increase in this ratio is dominated by growth in M4 as opposed to decrease in M2.’

In the subsequent sections the generation of the superharmonic tides as result of the non-linear interaction of the semi-diurnal component by the non-linear advective inertia term (4) and friction term (6) of momentum equation, is described. For the analysis, the shallow water equations for a prismatic channel are considered. Although tidal flats are present in a tidal basin, these are excluded for the description of the generation of the higher harmonics. For the situation with the tidal flats a combined effect of non-linearity is present and makes the analysis opaque.

3.2.1.1 Higher harmonics by friction term

The friction term in the momentum equation, indicated by (6) in Equation 5, comprises a multiplication of the current velocity, resulting in a non-linear effect.

Considering the tidal component, defined by:

Equation 7 - tidal component

$$u(x,t) = u_a(x)\cos(\omega t)$$

In which:

u(x,t)	=	local and time depend current velocity
$u_a(x)$	=	velocity amplitude
ω	=	tidal frequency

Considering the product of the current velocity after using the Galerkin method and extensive algebra, Le Provost 1991 defined that:

Equation 8 - higher harmonic by friction

$$u|u| = u^2 \sum_{n=0,1,2,\ldots} (-1)^{n+1} \frac{8}{(2n-1)(2n+1)(2n+3)\pi} \cos(2n+1)\,\omega\, t$$

The non-linear product of the velocity results in the development of the odd superharmonic tides (the odd numbers 3, 5 times the basic frequency) such as M_6 (Wang et al., 1999).

3.2.1.2 Higher harmonics by advection term

Another non-linear term in the shallow water equations is the advective inertia term indicated by (4) in Equation 5. As for the previous case, a semi-diurnal tidal component M_2 is considered. The velocity is defined by:

Equation 9 - tidal velocity of M_2

$$u(x,t) = u_a(x)\cos(\omega t - kx)$$

Substitution into the advective inertia term results in:

Equation 10 - higher harmonic for advective inertia

$$u\frac{\partial u}{\partial x} = u_a \frac{\partial u_a}{\partial x} cos^2(\omega t - kx) + k\, u_a^2\, \sin(\omega t - kx)\, \cos(\omega t - kx)$$

$$= \frac{1}{2}\, u_a \frac{\partial u_a}{\partial x} + \frac{1}{2}\, u_a \frac{\partial u_a}{\partial x} \cos 2(\omega t - kx) + \frac{1}{2}\, k\, u_a^2 \sin 2(\omega t - kx)$$

This Equation 10 has a time-independent or non-periodic term also called M_0 and two terms that represent superharmonic M_4 which has a frequency that is twice that of the M_2.

3.2.1.3 Higher harmonics by continuity equation

Considering the continuity equation for a prismatic channel:

Equation 11 - continuity equation

$$\frac{\partial \zeta}{\partial t} + \frac{\partial hu}{\partial x} = 0$$

With

Equation 12 - water depth

$$h = d + \zeta(t)$$

and

$$\zeta(t) = a_{M2} \cos(\omega_{M2} t)$$

The above equation is also non-linear, as the water depth h is dependent on the tidal water level variation $\zeta(t)$. Higher harmonics are therefore caused as result as a non-linear effect. This effect is also called Stokes' drift.

3.2.1.4 Higher harmonics by variable geometry (incl. tidal flats)

The hypsometry of an area is another cause of the generation of higher harmonics as studied by (Speer & Aubrey, 1984). When taking the flow over the tidal flats into account the one-dimensional shallow water equations must be extended. This can be done by defining a variable width W that is dependent on the water level. Considering the Equation 11 and a variable width $W(\zeta, x)$ the continuity equation changes into the next equation:

Equation 13 - continuity equation with variable width

$$\frac{\partial \zeta}{\partial t} + \frac{1}{W(\zeta, x)} \frac{\partial Q}{\partial x} = 0$$

The water level dependent cross-sectional area is another cause of non-linearity for the current velocity, see

Equation 14 - Velocity non-linear related to the discharge

$$u(t) = \frac{Q(t)}{A\big(\zeta(t)\big)}$$

In case of the presence of hypsometry the geometry of the wet surface of the tidal channel varies with time. As a result, the relation between the discharge Q and the time depend water level ζ is therefore not linear. Consequently, higher harmonics are generated.

There are various causes of the generation of the higher harmonics that lead to the asymmetry. The generation of higher harmonics is the result of the combination of the above described effects. In the situation with tidal flats, it is difficult to pinpoint the cause of the occurring asymmetry. In the next sections the different types of asymmetries are discussed. They can give an indication for the direction of the tide-residual transport.

3.2.2 Time asymmetry

When the availability of fines (fine sediment particles) is limited, the timing of mobilization of the sediments is of importance. Limited availability is referred to as starved bed conditions. There is a delay between the current velocities and the sediments that are in suspension. This delay in time is defined by the slack water periods; High water slack and Low water slack, HWS and LWS respectively.

There are two descriptions possible: Lagrangean and Eulerian. The Lagrangean description describes the decreasing velocities towards up-estuary or basins. This results in flood dominant net transport (van Straaten & Kuenen, 1958) and (Postma, 1961). The Eulerian description describes the inequality between the slack water periods due to slack water asymmetry. This asymmetry results in a shorter LWS and longer HWS.

Consequently, the particles remain longer on the bed during HWS than during LWS and therefore have a net transport in flood-direction.

Whether this asymmetry takes place, can be determined with the relative phase difference between the semi-diurnal tide; M_2 and the first higher harmonic; M_4 (Speer & Aubrey, 1984). Dependent on the value of the relative phase difference there are two extreme situations possible, see Figure 11 and Figure 12.

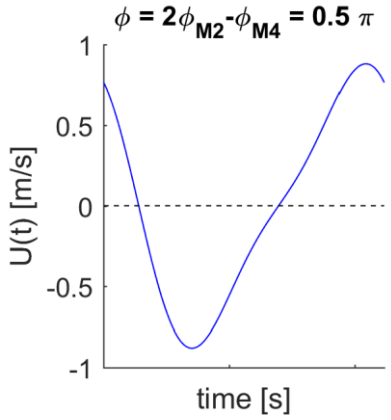

Figure 11 - Time asymmetry; ebb dominant

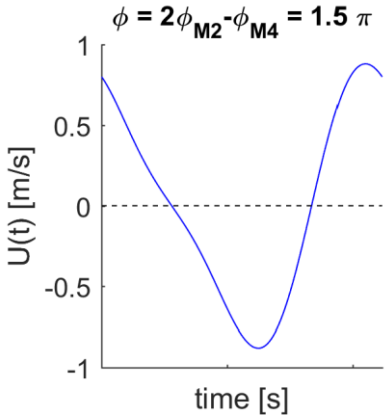

Figure 12 - Time asymmetry; flood dominant

For maximal time asymmetry, the values for relative phase difference (ϕ) between M_2 and M_4 tidal components can be used as a measure. As the above graphs illustrate, there are two extreme distortions in time:

- $\phi = 2\,\phi_{M2} - \phi_{M4} = 0.5\,\pi$ $t_{HWS} < t_{LWS}$ **Ebb-dominance of the fine sediments**

  Consequently; the fine sediments have more time to settle after ebb, than after flood. Therefore, a net export of sediments can be expected.

- $\phi = 2\,\phi_{M2} - \phi_{M4} = 1.5\,\pi$ $t_{HWS} > t_{LWS}$ **Flood-dominance of the fine sediments**

  Consequently; the fine sediments have more time to settle after flood, than after ebb. A net import of sediments can be expected.

3.2.3 Peak velocity asymmetry

The peak velocity asymmetry is the asymmetry around the horizontal axis. This represents uneven magnitudes of the flood and ebb velocities. This asymmetry is dominant for alluvial bed conditions. Alluvial bed conditions are considered when the sediment availability is unlimited and therefore in equilibrium at all time.

The peak velocity asymmetry resulting from the higher harmonics with its extremes at the relative phase difference $\phi = 0$ and $\phi = \pi$, is illustrated by Figure 13 and Figure 14.

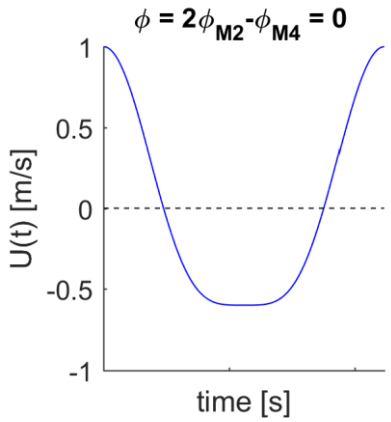

Figure 13 - Velocity asymmetry; flood dominant

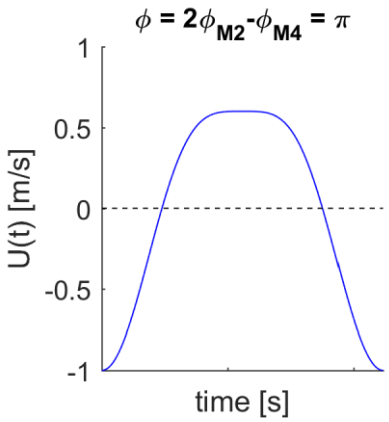

Figure 14 - Velocity asymmetry; ebb dominant

The above situations result in:

- $\phi = 2\,\phi_{M2} - \phi_{M4} = 0$ $u_{flood} > u_{ebb}$ **Flood-dominance of the fine sediments**
- $\phi = 2\,\phi_{M2} - \phi_{M4} = \pi$ $u_{flood} < u_{ebb}$ **Ebb-dominance of the fine sediments**

In Figure 13, the peaks of the positive current velocities (flood) are enforced. The peaks of the negative velocities (ebb) are diminished. For larger maximum ebb current velocities, the net residual transport is in the ebb direction and called ebb-dominant. Flood dominance is the other way around. The slack water periods LWS and HWS for the situations in Figure 13 and Figure 14 are the same. For relative phase difference of $\phi = 0.5\,\pi$ and $\phi = 1.5\,\pi$ there is no difference in peak current velocities.

The next section describes how this asymmetry affects the net transport load.

3.3 Tidal asymmetry and sediment transport

The above time asymmetries assume a limited amount of availability of sediment, described by 'starved bed'. In this situation the scouring-, settling- and space-lag, can be defined to determine the transport rate.

Another approach is that of an 'alluvial bed'. This approach assumes an unlimited amount of sediment. This situation occurs in hyper- sediment concentrated water columns. For the alluvial conditions the transport quantities can be approximated by the relation of the current velocities. This is described next.

For starved bed conditions there are no formulae that quantify the transport as result of the cross-sectional area integrated velocity. However, the above described time asymmetry is can give an indication for the direction of the tide-residual transport.

Starved bed conditions are considered for fine cohesive sediments. For fine sediments the instantaneous conditions together with the flow conditions upstream and the flow conditions in the past determine their transport (Bosboom & Stive, 2015). The sediment transport quantity in case of fine sediments is a product of the actual concentration and the velocity. For an exact formulation of the distribution of the sediment transport over the channel length and over time, the sediment balance must be solved.

In the next section, the sediment transport is described by considering an alluvial bed and therefore uses the asymmetry of the peak velocity.

3.3.1 Peak velocity asymmetry and sediment transport

There is a direct response between the current velocities and the particles, when considering alluvial bed conditions and coarse sediments. Bagnold formulated a relation between the velocities and the transport quantities.

Equation 15 - Sediment transport by Bagnold

$$S \approx cu|u|^{n-1}$$

With:

u = current velocity
c = concentration of $10^{-7} - 10^{-4}\ [m^{2-n}s^{n-1}]$
n = coefficient, n = 3 for coarse bed load transport, n = 4 - 5 for suspended transport.

The sediment transport rate is proportional with the velocity to the order n, with n depending on the kind of transport. For a linear wave (that is a perfectly sinusoidal and symmetric wave) the flood transport equals the ebb transport. Therefore, there is no net transport of sediment. When there is an asymmetry in peak velocities of ebb and flood. For n > 1, a net transport is present.

The amount of suspended sediment transport (f) at capacity conditions is scaled with u^5; $f \sim u^5$. For one tidal period, the tide-residual transport S_{net} is defined as follows:

Equation 16 - tide residual transport

$$S_{\mathrm{net}}(\mathrm{x}) \sim \int_0^T u(x,t)\,|u(x,t)|^{n-1}\,dt$$

In general sediment transport can occur in different modes. Close to the bottom as bed load transport and over the water column as suspended load when the particles are in suspension. Close to the landward end of the back-barrier basins of the Wadden Sea, the fine suspended sediment quantities are regarded as the predominant transport modes and therefore used for the tide-residual transport in this study. By varying the geometric parameters, the effect on the tide-residual transport is determined. These parameters determine the optimal function of the flushing basin system. In the next chapter the methodology of this study is described and discussed.

4 MODEL - METHODOLOGY

The generation of higher harmonics causes asymmetry of the peak velocities which results in a tide-residual transport. The geometry of the channel has a large contribution in generating asymmetry. Moreover, the addition of the flushing basin might affect the generation of higher harmonics and therefore on the tide-residual transport.

To determine the effect of the geometry of a flushing basin system the reference location of Noordpolderzijl is used, as described in section 4.1. The harbour channel of Noordpolderzijl is located in one of the tidal basins in the Wadden Sea. The assumption of predominantly channel directed tidal flow enables a simplification from the horizontal two-dimensional description to a one-dimensional description. This one-dimensional description moreover enables a unidirectional analysis of the generation of the higher harmonics.

Depending on the dimensions of the flushing basin system, the response of the system can be determined. For various dimensions of the flushing basin system the generation of higher harmonics and the tide-residual transport can be determined. As result of the dimensions, a tide-residual transport in seaward direction is strived for, for the total length of the channel.

The shallow water equations are used to determine the tide-residual transport for a schematic representation of the actual tidal harbour channel of the reference location Noordpolderzijl. This is done by using the hypsometry to determine a representative cross-sectional area of the tidal channel including the tidal flats. The schematization of the reference location is described in 4.2.

In this study, the tide-residual transport is determined for various scenarios of the dimension of a flushing basin system. This is done by varying the design parameters. The design parameters are elaborated on in section 4.2.1.

The shallow water equations form a set of partial differential equations. Initial and associated conditions are needed to determine a well posed problem. The model area is the channel and therefore, the boundary conditions must be defined at each side of the channel. At the seaward side the imposed boundary represents the forced tidal water level variation. The landward end represents the interaction with the flushing basin. The periodic response of the flushing basin system to the forced tide is used to determine the tide-residual transport along the channel. As the periodic solution of the shallow water equations is used, the initial conditions can be chosen arbitrarily. These boundary conditions are discussed in section 4.2.2. The numerical procedure to solve the shallow water is discussed in the proceeding section 4.2.3.

To check the validity of the results, a simplified situation is used, see section 4.5. This is done by determining the generation of higher harmonics considering a deep channel. Due to the almost total absence of higher harmonics, a linear solution is expected. I.e. the tidal forced semi-diurnal water level variation at the seaward side must be remained along the channel. A single wave with a constant amplitude must be present.

4.1 Reference location

A representative harbour channel in the Dutch Wadden Sea with a net siltation problem had to be chosen for this study. The criteria for the reference location with a harbour channel were:

- located close to the primary dike.
- aligned perpendicular to the primary dike
- surrounded by tidal flats
- a minimum amount of bends in the channel

The harbour channel of Noordpolderzijl located in the north of the Netherlands, illustrated in Figure 15, satisfies the above criteria and is used as reference for the model study. The area of Noordpolderzijl comprises of several, at hydraulic point of view, interesting elements:

- shallow channel, that is connected to a deeper tidal channel and the shore
- tidal flats
- salt marshes
- primary dike

These elements are used to schematize the situation, see Figure 16. In the deeper tidal channel, no problems concerning navigational depth are present. However, in the smaller side channel that is connected to the landward boundary situated harbour, large siltation occurs. See Appendix A for the siltation locations in the Wadden Sea. The flushing basin can be added behind the shallow channel, see Figure 16 for the schematization of the area of Noordpolderzijl.

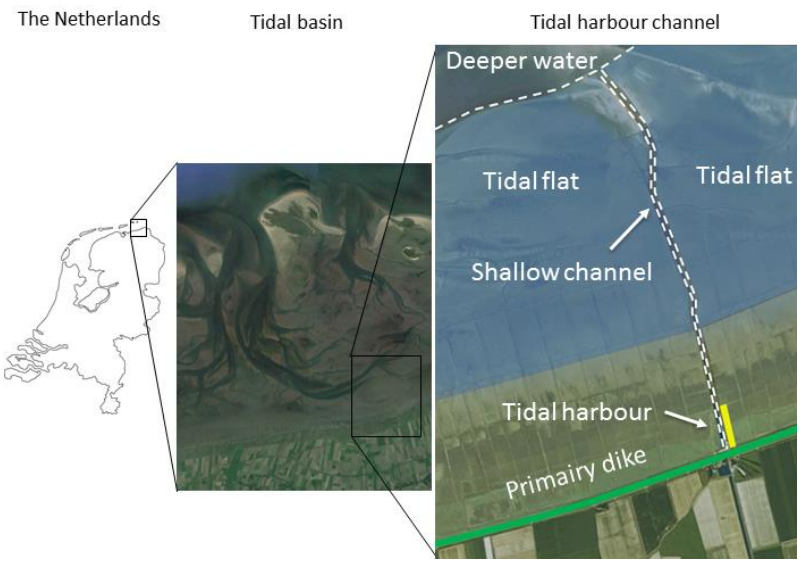

Figure 15 - Areal overview of reference location Noordpolderzijl

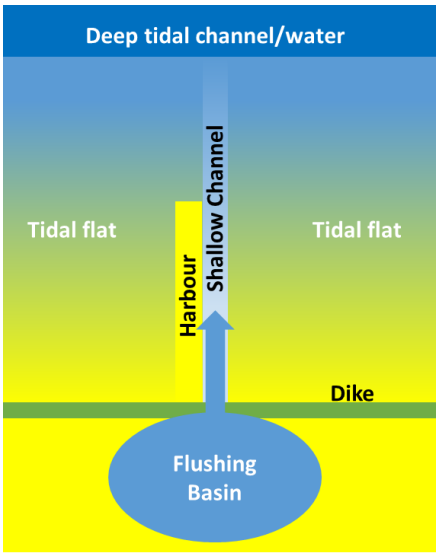

Figure 16 - Schematization of the reference location

To be able to represent the above illustrated reference location as well as possible, the following relevant quantities are defined:

- tidal range ≈ 2 m
- hypsometry of the area; which is used for a depth - width relation, see appendix C.
- length of the navigational channel ≈ 3000 m
- roughness coefficient; C ≈ 57. For the Wadden Sea this is a common used value.

In the next section, this schematization is used to determine the model set-up.

4.2 Model set-up

The shallow water equations are used to determine the response of the flushing basin system as result of the semi-diurnal forced tidal wave signal. For a prismatic channel, the one-dimensional shallow water equations can be used to describe the current velocities and water level variations along this channel. For the generation of the asymmetry it is however important to include the tidal flats into the analysis. In the next section the equations describe the physics of the tidal wave within the shallow area of a tidal basin which is located close to the shore. In this section, the criteria that determine the geometry are elaborated.

4.2.1 Geometry

The flushing basin system comprises of the tidal channel that is surrounded by tidal flats and connected by a sluice with the flushing basin. The dimensions of these various parts together with the boundary conditions determine the period response. A depth dependent width is defined to represent the tidal channel and the tidal flats properly. This is done by using the bathymetry of the area of Noordpolderzijl.

4.2.1.1 Bathymetry

For modelling the flow in a tidal basin, the tidal flats are important features (Speer & Aubrey, 1984). They are, for a large part, responsible for a variable flow dependent on the depth. For the smaller values of the water level, the flow takes part within the boundaries of the channels. For the higher water levels, the flow of water also takes part over the tidal flats.

To take this part of the flow into account, the hypsometry is defined. With the bathymetry, the inundated area as function of the height is determined; the hypsometric curve. In Figure 17 the bathymetry is illustrated for the area of Noordpolderzijl. The black dashed box marks the area for which a hypsometric curve is made. This hypsometric curve is converted to a depth - width relation by taking the squared root of the area.

In Figure 18, the hypsometric curve is illustrated in blue. The deeper parts, the left side of the blue line is the deeper area. This area represents the deeper tidal channel at the northern side of the dashed marked area. The middle part represents the tidal flats. At the right side, from 1200 m., the tidal marshes are visible.

This hypsometric curve that is converted into the depth-width curve of Figure 18, forms a basis for the definition of a representative cross-section for the one-dimensional model. For the longitudinal direction, there are no changes in the cross-section for modelling and physical comprehension.

The salt marshes and the deeper tidal channel are excluded in the defined representative cross-section, see Figure 18 depicted in red. Therefore, the red line deviates from the blue line at the left and the right side. The presence of the salt marshes generates higher harmonics as result of the change in the geometry and this can result in extra asymmetry. By excluding the salt marshes, this effect is not considered. Furthermore, the transition of the tidal flats to the tidal channel is relatively smooth. This transition is arbitrarily chosen, as the width is determined by using a tangent hyperbolic function. Both sides of the channel are included in the representative width that is illustrated in Figure 18 in red.

In general, when the channels in a tidal basin are shallow and the area of the tidal flats is relatively small, the tide-residual transport is in the flood direction. For deep channels and large wide tidal flats, the tide-residual transport is in the ebb direction. The determined bathymetry can be expected to be in ebb-direction.

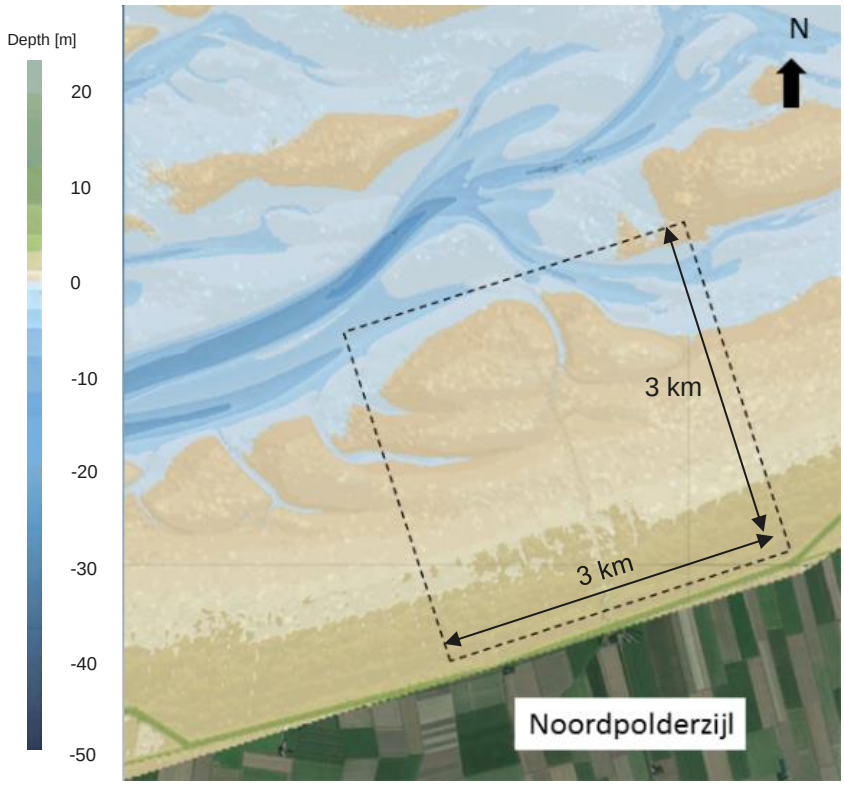

Figure 17 - Bathymetry of the area around Noordpolderzijl in various colours. Area of the hypsometric curve in black dashed line

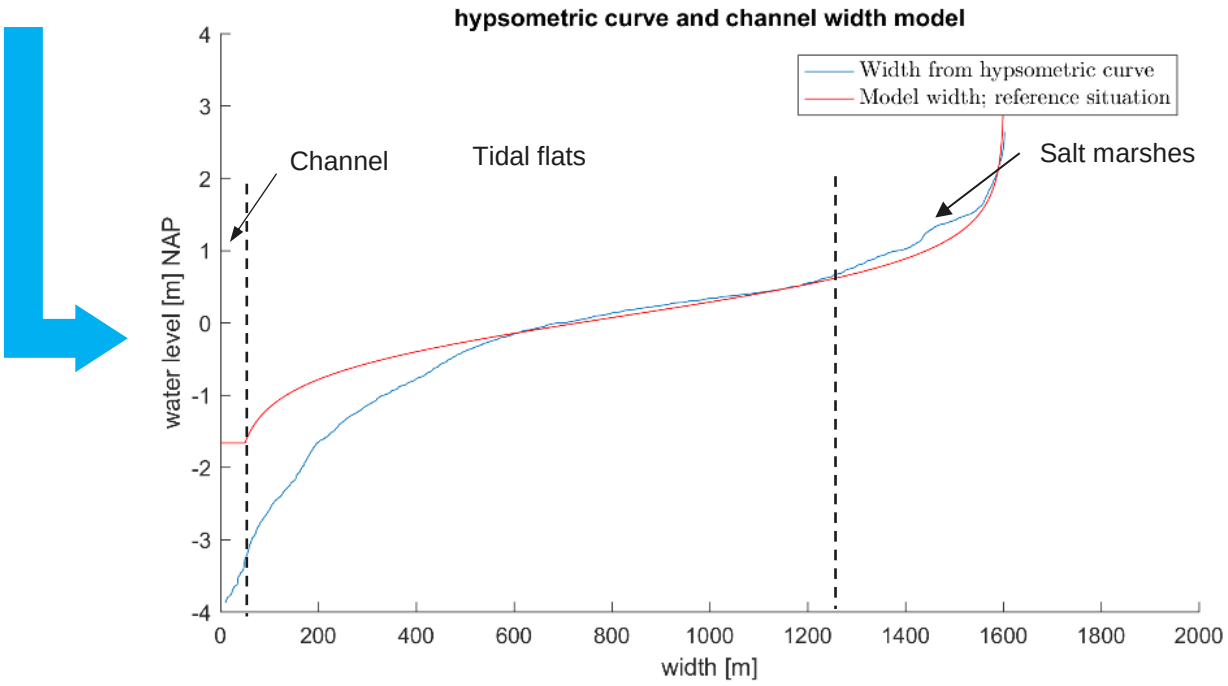

Figure 18 - Depth dependent width; determined from the hypsometric curve (b) and reference width curve of the model

4.2.1.2 Overview; Tidal channel with flushing basin and tidal flats

An overview of the reference situation, which is the situation of a tidal channel without the presence of a flushing basin, is given in Figure 19. In this figure the proportions are exaggerated, as the width of the tidal flats is much larger than the channel and the depth much smaller than the width. This channel has the width and depth of the reference location for the tidal channel of Noordpolderzijl.

The left side of Figure 19 is a top view of the geometry of the model. At the left side, the deeper channel is located, depicted with 'tide' as this is the seaward boundary. The right side represents the channel-end and is also the boundary between land and water, therefore depicted with 'Hinterland'. The sluice which connects the flushing basin with the channel is located here. In between the sea and the hinterland, the shallow channel is located. This is the domain of the model. The physics at the boundaries are represented by the boundary conditions. These are elaborated in section 4.2.2.

At the left side of Figure 19 the channel cross-section is depicted. The water level is such, that for the lower water levels of the tide, the discharge take place only in the channel section. Whereas for the higher water levels the tidal flow also take part on the tidal flats.

The width of the sluice, which connects the channel with the flushing basin, is chosen smaller than the channel width.

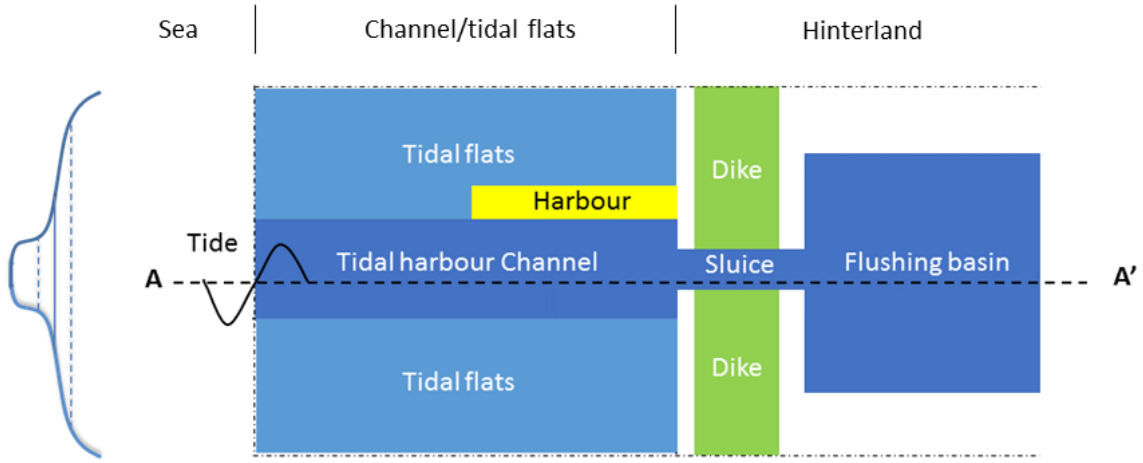

Figure 19 - Cross-section of the channel, with the presence of the flushing basin.

4.2.1.3 Geometric parameters

The used parameters in the model can be divided into geometric and physical parameters. Both parameters influence the behaviour of the water levels and current velocities of the flushing basin system. The geometric parameters that are of importance are depicted in Figure 20 and summarized in Table 2.

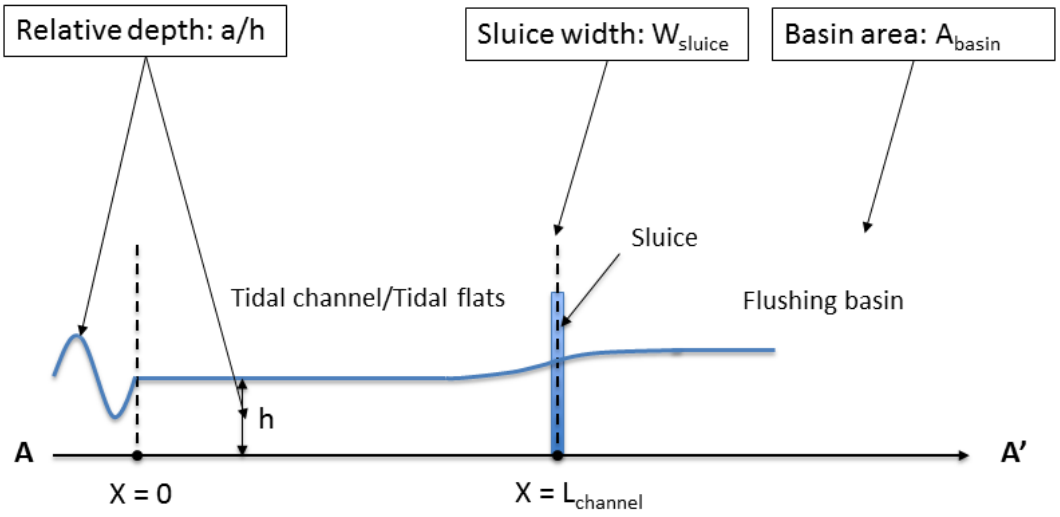

Figure 20 - design parameters: relative depth, sluice width and basin area

In the third column: value(s), either a constant value is given or depicted with 'variable'. In case of a constant value the value is used in this thesis and does not change. The parameters indicated with 'variable', are changed to determine the effect of this change on the tide-residual transport in chapter 0.

Table 2 - Geometric parameters

parameters	description(s)	value(s)	dimension(s)
h	mean depth	variable	[m]
A_{basin}	flushing basin area	variable	[ha]
$W_{channel}$	channel width	50	[m]
W_{sluice}	sluice width	variable	[m]
W_{flats}	tidal flat width	1500 (water level dependent)	[m]
$L_{channel}$	channel length	3000	[m]

The prescribed values are deduced from the reference location of Noordpolderzijl. This location is used as a reference, for this study the following is considered:

- The width of the channel; $W_{channel}$, has one representative value. The harbour channel of Noordpolderzijl is chosen as a reference. This channel has a width of about 10 – 50 m. Considering the navigational purpose, a width of 50 m is used as the reference width.
- The width of the tidal flats is determined by fitting the converted hypsometric curve of the storage area of the navigational channel of Noordpolderzijl as previously described.
- The channel length; $L_{channel}$ could be a changing variable. However, for this study the reference location with its hypsometric area is considered. Therefore, the channel length is not varied.

4.2.1.4 Physical parameters

The physical parameters are the characteristics of the tide: tidal period; T and amplitude; a. In the Wadden Sea the main component of the tide is semi-diurnal, depicted with the subscript in Table 3 with M_2.

The Chezy coefficient C is the parameter that represents the smoothness of the bed. This parameter can be determined by the formula of White-Colebrook:

Equation 17 – White-Colebrook

$$C = 18 \log \frac{12h}{k_s}$$

In which:

h = water depth,
k_s = equivalent geometrical roughness of Nikuradse,

For the Wadden Sea values of about 55 to 60 are commonly used.

Table 3 - Overview of the physical parameters

parameters	description(s)	value(s)	dimension(s)
T_{M2}	Tidal period, semi-diurnal	44712	[s]
a_{M2}	tidal amplitude	1	[m]
C	Chézy coefficient	57	[$m^{1/2}s^{-1}$]

The tidal amplitude; a_{M2}, is considered as a constant. Together with the depth; h, the relative depth; a/h can be used as an indication for the shallowness of the model. This relative depth has a strong influence on the importance of the non-linear terms in the momentum equation, (Speer & Aubrey, 1984).

4.2.2 Boundary conditions

Considering the one-dimension shallow water equations which form a set of partial differential equations, there are two boundary conditions. For subcritical flow one at each end of the line. These conditions simulate the behaviour at the boundary. On the one hand, these conditions are representative for information that can move from outside of the domain to the inside domain. For a tidal basin, one of the boundary conditions represents the tidal motion of the water level variation. The other side represents the landward boundary. These can be modelled by chosen zero velocities at the end of the domain for all times. $U(L_{channel},t) = 0$. For this study however, a flushing basin is added at the landward end of the channel. Both boundaries conditions are elaborated in the next section.

4.2.2.1 Seaward boundary; Weakly reflective boundary

To simulate the propagation of a tidal wave into a tidal channel, the boundary conditions at two sides of the channel-end must be defined properly. In this study a semi-diurnal tidal water level variation is chosen. This tidal water level variation at x = 0, is defined by:

Equation 18 –Tidal variation

$$z_{tide}(x,t) = z_{tide}(0,t) = a_{M2} \sin(\frac{2\pi}{T_{M2}} t)$$

This forced tidal wave reflects at the landward boundary. This reflected wave must be able to pass freely out of the domain. This is done by choosing the boundary conditions such, that the reflected wave is extinguished. Total extinguishing is not possible and therefore these boundaries are called: ‘weakly reflective’. By using the Riemann invariant, this weakly reflective boundary is defined by:

Equation 19 - Seaward boundary

$$Q(x,t) = Q(0,t) = \sqrt{\frac{g}{h + \zeta_m^t}} \, (z_{tide} - \zeta_m^{n+1}) \, A$$

In which ζ_m^t is the water level variation of the previous timestep and ζ_m^{n+1} that of the new timestep.

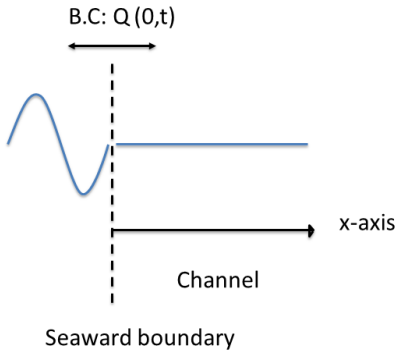

Figure 21 - Seaward boundary condition; sea

4.2.2.2 Landward boundary; flushing basin boundary

At the landward boundary interaction of a channel with a flushing basin is described by two conditions. Along the channel, the water levels and current velocities are described by the momentum - and continuity equation. As the flushing basin is relatively large compared to the cross-sectional area of the channel, the current velocities are reduced in the flushing basin. Therefore, not the momentum equation is used, however the storage capacity of the flushing basin. The discharge $Q_{sluice}(t)$, is the result of water level variations $\zeta_{basin}(t)$ over time at this boundary and is represented by:

Equation 20 - Storage equation for flushing basin

$$\frac{d\zeta_{basin}(t)}{dt} = \frac{Q_{sluice}(t)}{A_{flbasin}}$$

The momentum equation is substituted by the discharge equation as result of water level differences by:

Equation 21 - Discharge sluice

$$Q_{sluice}(t) = m\, A_{sluice}(t) \sqrt{2g\zeta_{basin}(t) - \zeta_{channel-end}(t)}$$

With:

$$A_{sluice}(t) = W_{sluice}\left(h + \zeta_{sluice}(t)\right)$$

The coefficient ‘m’ is commonly used for the reduction of the discharge as result of the energy dissipation which is occurs because of the constriction in the cross-sectional area. An optimal design of the sluice results in values which are close to 1. As sluice design is not part of this study and to exclude the influence of this factor, m = 1 is assumed.

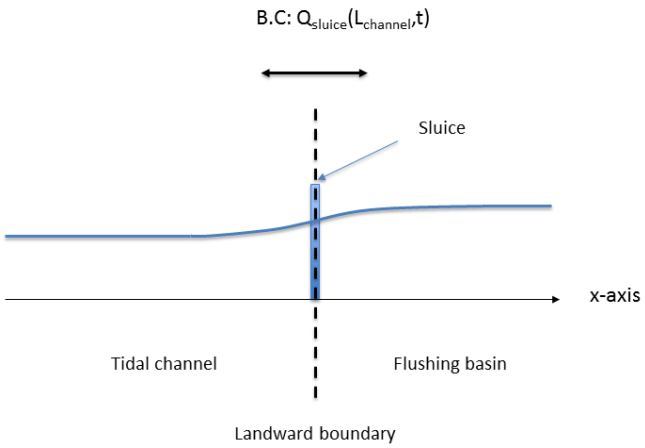

Figure 22 - Landward boundary condition; sluice

4.2.3 Model scheme

Shallow water equations are used to give a proper description of the water levels and current velocities in the spatial domain of the back-barrier basin. The shallow water equations are partial differential equations, which only can be solved when the following points are known: (Zijlema, 2015):

- the solution itself
- spatial domain
- boundary conditions
- initial conditions, in case of time stepping.

The above described boundary conditions combined with the geometry, are used to define a well posed problem.

An explicit time-stepping method is used to discretize the shallow water equation. This is done by using finite differences. For the derivatives in time, forward differences are used. For spatial derivatives, central differences are used.

The shallow water equations for a prismatic channel have been described in 3.1.1. However, because of the presence and influence of the tidal flats on the asymmetry of the tidal current velocities along the channel, a prismatic channel can't be used. Instead a variable width as function of the water level must be considered to include these asymmetry effect as result of the tidal flats. The one-dimensional shallow water equations, therefore must be adjusted to the next two equations:

Equation 22 - Continuity equation

$$\frac{\partial \zeta}{\partial t} + \frac{1}{W(t)} \frac{\partial Q}{\partial x} = 0$$

Equation 23 - Momentum equation

$$\frac{\partial Q}{\partial t} + \frac{\partial}{\partial x} \frac{Q^2}{A} + gA \frac{\partial \zeta}{\partial x} + g \frac{Q|Q|}{C^2 A R} = 0$$

The water level; $\zeta(x,t)$ is the variation with the initial depth; h as reference, see Figure 23 for these definitions.

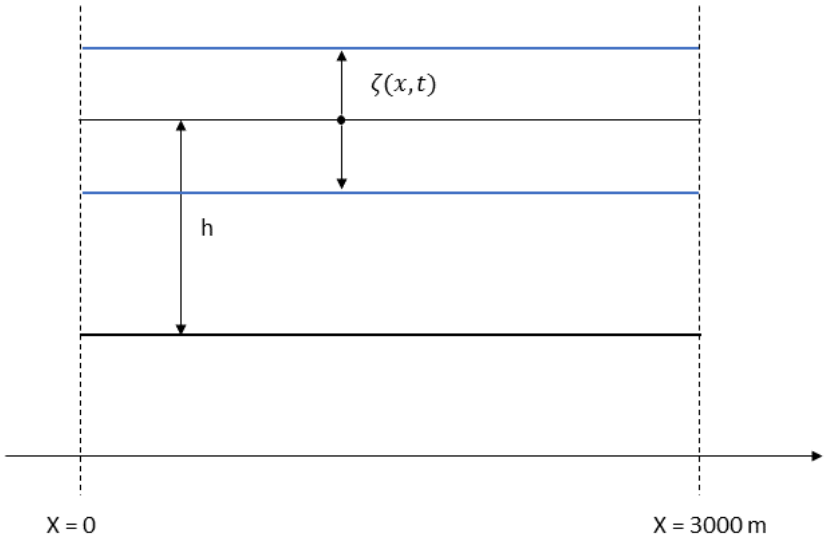

Figure 23 - Definition model set-up

These equations are discretized as follows:

- Interpolation of the depth dependent width of the channel defines the geometric parameters A and R. This depth dependent width is defined by considering the hypsometry of the reference location around

Noordpolderzijl. The water level of the previous timestep for each location is used to determine these parameters.

- The above continuity equations are replaced by its discrete analogue for all grid points excluding the boundaries. The spatial domain is defined from x = 0, the seaward boundary to x = $L_{channel}$ = 3000 m the channel-end at the landward side. This domain is divided into a spatial grid point, with equidistance $\Delta x = \frac{L_{channel}}{M}$. Each location is now defined by $x_m = \Delta x\ m$, with m = 0… M. The time is also discretized $\zeta(x,t)$ now is defined by Z_m^n. The discrete analogue of the continuity Equation 22 and momentum Equation 23 are:

Equation 24 - Discrete analogue of Equation 22

$$W_m \frac{Z_m^{n+1} - Z_m^n}{\Delta t} + \frac{Q_{m+1}^{n+1} + Q_{m-1}^{n+1}}{2\,\Delta x} = 0$$

and

Equation 25 - Discrete analogue of Equation 23

$$\frac{Q_m^{n+1} - Q_m^n}{\Delta t} + \frac{Q_{m+1}^{n+1}\frac{Q_{m+1}^n}{A_{m+1}^n} - Q_{m+1}^{n+1}\frac{Q_{m-1}^n}{A_{m-1}^n}}{2\Delta x} + g\,A_m^n \frac{Z_{m+1}^{n+1} - Z_{m-1}^{n+1}}{2\Delta x} + g\,\frac{|Q_m^n|}{C^2 A_m^n R_m^n} Q_m^{n+1} = 0$$

- At the seaward boundary, a weakly reflective condition is defined:

Equation 26 - Discrete analogue of Equation 19

$$Q_m^{n+1} = \sqrt{\frac{g}{h_m + Z_m^n}}\,(X^n - Z_m^{n+1})A_m^n$$

With:

$$X^n = a_{M2} \sin\left(\frac{2\pi}{T_{M2}} t\right)$$

- At the landward side, a discharge equation as result of the flushing basin is defined:

Equation 27 - Discrete analogue of Equation 21

$$Q_m^{n+1} = W_{sluice} \cdot (h_m + Z_m^n)\sqrt{2\,g}\,|Z_m^n - Z_{m+1}^n|^{-0.5}\,(Z_m^n - Z_{m+1}^n)$$

And

Equation 28 – Discrete analogue of Equation 22

$$\frac{Z_{m+1}^{n+1} - Z_{m+1}^n}{\Delta t} = \frac{Q_m^{n+1}}{A_{basin}}$$

These equations are constructed into a matrix- vector notation and solved numerically by using matrix inversion operations. The new values for the quantities are determined by using values of the previous timestep. This process is called time stepping. After enough time, the solution is converted to a periodic state. I.e. the spin up time has been exceeded.

4.3 Assumptions

To describe the function of a flushing basin in an intertidal area accurately and without unnecessary details, assumptions are made. On the one hand, assumptions decrease the complexity of the description, but on the other hand they also increase the applicability. By considering these assumptions, wrong conclusions can be avoided. The assumptions are subdivided into model and process based assumption.

4.3.1 Model assumptions

The choice to describe the tidal flow through the tidal channel by a one-dimensional cross-sectional integrated velocity with a water level dependent width has direct consequences for the applicability of the model. These assumptions are:

- Hydrostatic pressure:

Hydrostatic pressure cannot be assumed if there are large changes in velocities caused by strong geometric changes as: strong bends and changes in bathymetry. For one dimensional description these changes are excluded.

Another aspect is that the shallow water equations is valid in a subcritical regime. When the current velocities become too high in relation to the wave celerity, the flow changes from subcritical into a super-critical regime. When the flow is super-critical, the boundary conditions must be defined both at the upstream side. The transition from sub-critical to super-critical flow occurs with large energy dissipation due to turbulences. These are difficult to be quantified and subcritical flow is therefore assumed. The transition from subcritical flow to supercritical flow is given by the Froude number and defined by $Fr = \frac{u}{c}$ and for shallow water $c = \sqrt{gh}$. For $Fr = \frac{u}{\sqrt{gh}} < 1$ the flow is subcritical.

- No bathymetry induced circulations

The tidal flow in the back-barrier basin of the Wadden Sea, predominately takes place within the channels and or in channel direction. A relatively small area is used for this model study. As the tidal wave predominantly takes place in longitudinal channel direction and the bathymetry changes along the channel are small, the bathymetry induced currents will be small. In addition, a one-dimensional model only can describe the variations in longitudinal direction, these circulations cannot be implemented in the model.

- No estuarine circulations

The salinity of the water is constant; $\rho_{water} = 1025\ kg/m^3$. The estuarine circulations affected by salinity differences are excluded.

- Small horizontal aspect ratio h/W<<1

The averaged depth in the Wadden Sea in relation to the average width of the watershed is large. Moreover, the average tidal range is in the same range as the depth.

- Long channel; W/L<<1

As the propagation of the wave is modelled by a one-dimensional shallow water equations, the flow is in the longitudinal direction of the channel. Therefore, the length must be much larger than the width of the channel.

- Quadratic friction

The non-linear effect by bottom friction is introduced by the quadratic friction. The formulation is only dependent on the changing discharge parameter Q, cross-sectional area A and a Chezy coefficient C. An overestimation of the odd harmonics can be a result of this assumption.

4.3.2 Process based assumptions

- No wave induced transport

Waves have an important impact on the sediment transport in shallow water. Especially during storm conditions, waves are dominant for inducing sediment transport. However, for the long-term net sediment transport wave induced transport is excluded.

- No roughness variations: one Chezy-value

Although this is an important variable for the propagation of a tidal wave in shallow water, the variability in a tidal barrier basin is low.

- Horizontal bottom: $i_b = 0$

The bottom slope in back barrier basins is in general slightly increasing. As the current velocities in basin-end direction are decreasing, a general decreasing depth can be observed. The slope of the bottom in slightly increasing. However, these slopes are very small. The effect on the water levels and current velocities is therefore in relation the other term in the momentum equation relatively small.

- Alluvial bed

Whether starved bed or alluvial bed conditions can be assumed is not straightforward for the Wadden Sea. The seabed in the Wadden Sea is partly alluvial, and partly of Holocene origin (van Duren, Winterwerp, van Prooijen, Ridderinkhof, & Oost, 2001). Considering high concentration mud suspension, observed at Holwerd (van Kessel, 2016), the assumption of alluvial bed conditions is legitimate. The composition of the bed has implications for the processes of erosion and deposition. By considering an alluvial bed, the availability of sediment is not limited.

- Semi-diurnal tide

The predominant tidal water variation in the Wadden Sea is semi-diurnal. Water level variation at specific locations differ from a semi-diurnal tide, however there is large resemblance. The advantage of a semi-diurnal tide is that it is symmetric. By using the semi-diurnal tide for the seaward boundary condition, the asymmetry of the current velocities of the periodic state, is the result of the generation of higher harmonics and can be determined.

4.4 Scenarios

As described before, the effect of the geometric design parameters on the tide-residual transport is determined in this study. For various scenarios of the design parameters of the flushing basin system the tide-residual transport is determined.

The number of parameters of the flushing basin system is large. For this generic approach, the geometric parameters are varied as these parameters/quantities have the largest influence on the hydrodynamics of the flushing basin system. In Table 4 and Table 5, an overview of the experiments is given. The experiments have been done by varying one variable at a time. The key parameters are:

- The relative depth parameter; a/h is changed only due to the change of the depth; h. The tidal amplitude of the semi-diurnal tide is kept constant; a_{M2} = 1 m. The varying parameters are bounded by the numerical instability and the occurrence of super-critical flow.
- The sluice width: W_{sluice}. The sluice width together with the initial depth (h) and water level variation ($d(x,t) = \mathrm{h} + \zeta(\mathrm{x},\mathrm{t})$) determine the cross-section $A_{sluice}(t)$.
- The flushing basin area; A_{basin}. The basin area is varied to create a substantial effect on water levels and current velocities. As the transport flux can be determined by the fifth order of the current velocities: u^5, a substantial tide-residual transport can be expected.

Table 4 - Overview varying parameters

Parameter(s)	Varying values	Dimension(s)
a/h	0.2 – 0.6	[-]
W_{sluice}	5 – 50	[m]
A_{basin}	30 - 300	[ha]

Table 5 - Overview constant parameters

Parameter(s)	Constant values	Dimension(s)
T_{M2}	44712	[s]
$W_{channel}$	50	[m]
$L_{channel}$	3000	[m]
C	55	[-]
g	9.81	[m/s^2]

The solution of the shallow water equations, define the water levels and the current velocities as function of location and time. For each location, the determined quantities are:

- water level: $\zeta(x,t)$
- current velocity: $u(x,t)$
- relative phase difference: ϕ of the Fourier components; M_4, M_6 and M_8
- amplitude ratio: i.e. a_{M2}/a_{M4} of the Fourier components; M_4, M_6 and M_8

The current velocities are used to determine the tide-residual suspended sediment transport flux and capacity for each location (grid point) as described in 3.3.

4.5 Check; linear solution

Before using the model, the model must be checked. A common method to check the model validity, is by using available measurement. These are not available for this situation. Therefore, a simplified situation is used to check the model. This is done by using the scenario of a relatively large depth. For this scenario the generations of higher harmonics should not occur. This can be checked by determining the amplitudes of the higher harmonics; M_4, M_6 and M_8

The linear solution occurs in case of:

- very large relative depths,
- a rectangular narrow channel (without tidal flats),
- a relatively short basin.

As a result, the tidal water level variations do not vary over the total length of the channel. A single propagating wave with constant amplitude is present. The water level varies as a standing linear wave. This theory is used as a check for the proper working of the model. The values for the ideal situation are given in Table 6.

Table 6 - Idealized situation for a standing wave

parameters	value(s)	dimension
A_{basin}	0	[ha]
a/h	0.05	[-]
W_{sluice}	0 and 25	[m]
$W_{channel}$	50	[m]
$L_{channel}$	3000	[m]

4.5.1 Results

The model results of the linear situation, for the water level and current velocity variation at the two channel-ends, are depicted in Figure 24. It can be observed that the current velocity reaches its maximum or minimum (maximum flood flow or maximum ebb flow) exactly at that time when the water level is zero. On the other hand, when the current velocity is zero again (slack water), the water levels are at its maximum or minimum (high water or low water). This occurs because the water level has a phase difference of exactly a quarter tidal period; -½ π. The situation is called a standing wave.

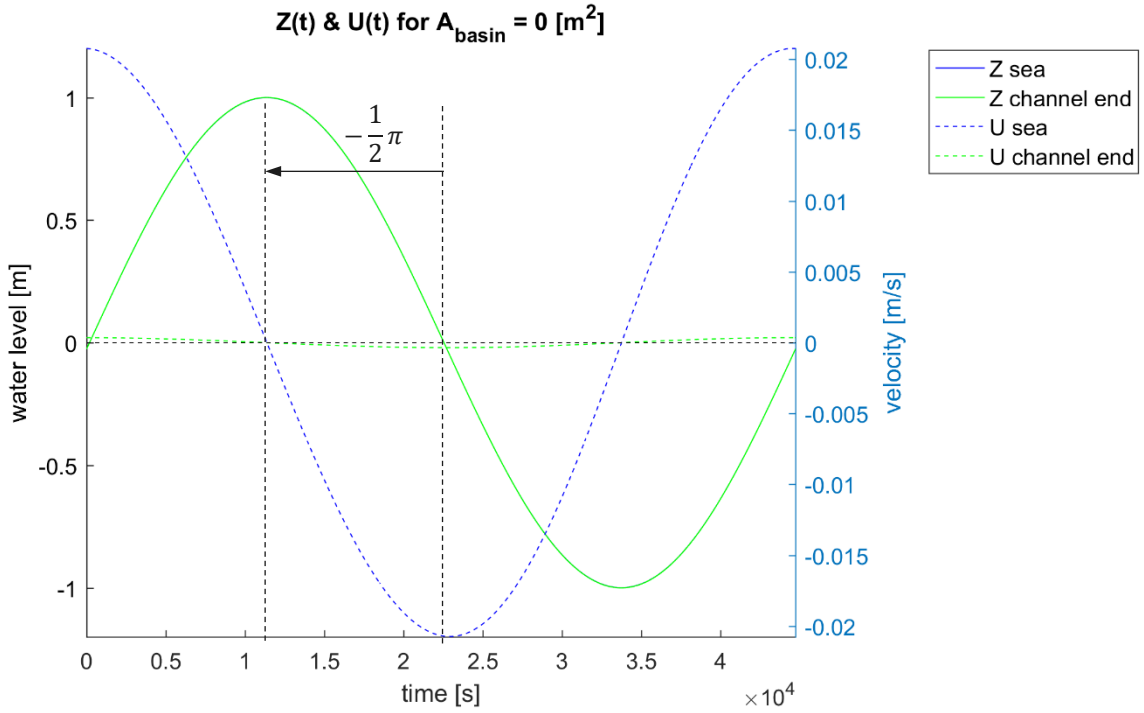

Figure 24 - Water level and current velocity for rectangular channel

To describe the shape of the velocity, the velocity is harmonically decomposed using Fourier analysis. The first three higher harmonics of the semi-diurnal tidal wave are used; M_4, M_6 and M_8. These higher harmonics are introduced by the non-linearity and are responsible for the distortion of the current velocities.

The result of the harmonic decomposition is visualized in Figure 25 and Figure 26. In Figure 25, the tidal forced semi-diurnal tide is the only harmonic present. In absolute sense, the values of the higher harmonics are very small. The phase of the semi-diurnal tide; ϕ_{M2} to its third higher harmonic; ϕ_{M8} are constant along the channel axis, see Figure 25 the right graph.

The relative dominance of each harmonic can be seen in Figure 26 at the left side. It can be observed that the only contributing harmonic beside M_2, is the M_4 tidal component. With a relative amplitude of M_4 that is twenty times as small; $a_{M4} = 0.05\ a_{M2}$. From the right graph of Figure 26, it can be observed that the relative phase difference is $\frac{3}{2}\ \pi$ or $-\frac{1}{2}\pi$; which is not of any relevance because of the low ratio of $a_{M4}/a_{M2} = 0.05$.

From the above it can be concluded that with the configuration for the linear solution, the wave maintains its perfectly forced sinusoidal shape due to the absence of the higher harmonics. Therefore, the wave is not only a standing wave due to the phase shift of -½ pi, but also a linear wave. This is as expected and is the first check of the validity of the model for the case without a flushing basin.

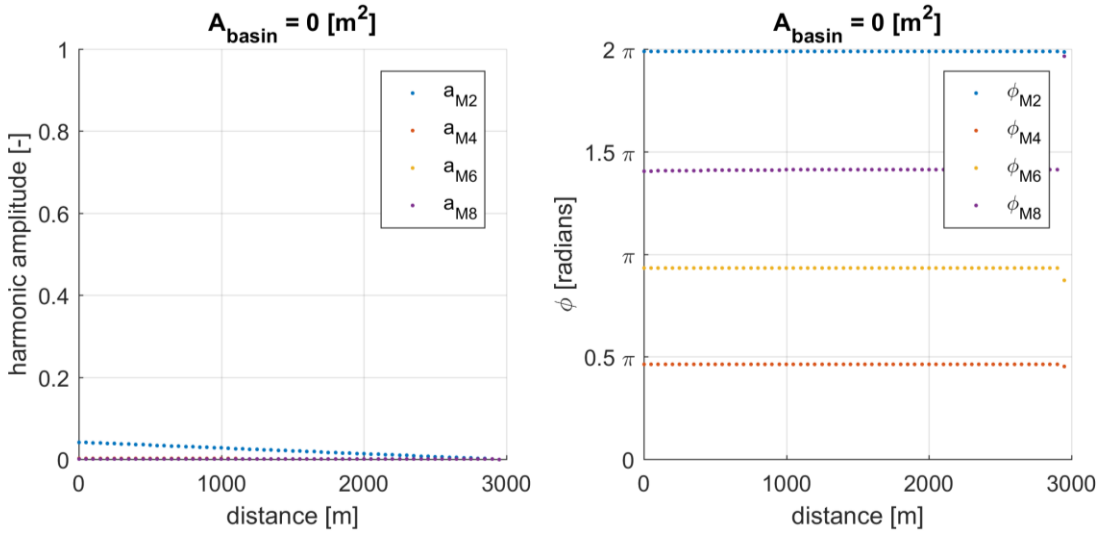

Figure 25 - Harmonics amplitudes and phases

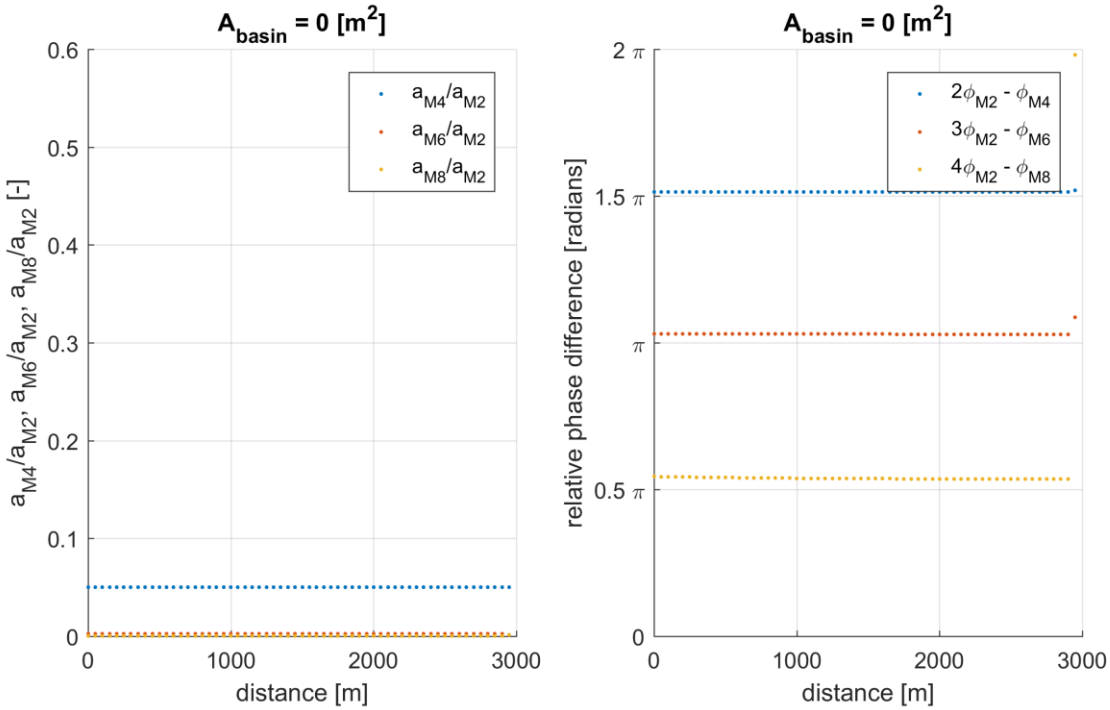

Figure 26 - Harmonic decomposition for a channel without a flushing basin.

4.6 Equilibrium cross-sectional area of the channel

For tidal channels there are equilibrium relationships between the cross-sectional area of the channel and their tidal prism. For the tidal channel that fills and drains the flushing basin the equilibrium relationship gives insight in the equilibrium dimensions. Comparison of the actual channel size with the calculated equilibrium size is used to indicate whether the channel tend to erode or to fill in. The relationship between the tidal prism P of the flushing basin and the cross-sectional area A_c of the channel (below mean sea level) is used. The tidal prism represents the total volume that during half a tidal period is flushed. Most of the relationships have the following form:

Equation 29 - equilibrium channel area relation

$$A_c \propto P^{n(n-1)}$$

With:

A_c = cross-sectional area of the channel of the inlet.
P = tidal prism of the basin.
n = coefficient

For the basins in the Wadden Sea, the relationship of (Eysink, 1979) is often used:

$$A_c = C\,P$$

With:

C = empiric coefficient: $70 \cdot 10^{-6}$

For the depth various scenarios are chosen. For each chosen scenario of the depth the cross-sectional area is determined. The tidal prism for the equilibrium situation is then calculated by using the inversed relation P = A_c/C, see Table 7. With the tidal amplitude of 1 m and a depth independent basin area, the basin area is then determined.

Table 7 - cross-sectional channel and prism relation

a/h	h [m]	A_c [m^2]	Prism [m^3]	A_{basin} [m^2]
0.2	5.0	536	$7.7 \cdot 10^6$	$3.8 \cdot 10^6$ (380 ha)
0.4	2.5	410	$5.9 \cdot 10^6$	$2.9 \cdot 10^6$ (290 ha)
0.6	1.67	366	$5.2 \cdot 10^6$	$2.6 \cdot 10^6$ (260 ha)

The channel width at depth h is 50 m. The cross-sectional area of the channel is much larger than 50 m x h, because the gentle slopes of the channel are part of the cross-section as well. The reason for this is the relatively smooth transition of the channel to the tidal flats as is discussed in 4.2.1.

The required basin areas to create equilibrium conditions for the given channel areas are presented in the last column of Table 7. Because the channel is relatively wide is relation to the depth, the channel depth has a large influence on the channel area and thus the basin area. Therefore, the variability in the basin area is relatively large. The values for the basin area are a good indication for the required size of the flushing basin, to maintain the channel geometry on the long term.

5 SCENARIO RESULTS

This chapter presents and discusses the results of the various scenarios for the dimensions of a flushing basin system. The results comprise four main parts. In each part one key design parameter of the model is varied. Before the key parameters are varied, the reference situation is investigated.

In the first section 5.1, the initial situation without flushing basin is presented. In the second section 5.2, a flushing basin of 100 ha is added to the system and the effect of a flushing basin is observed. In the subsequent sections, the various key design parameters are discussed individually. For various values of the various key design parameters, the effect on the tide-residual transport is investigated. After the discussion of parameters individually, a combined variation of the key design parameters is given in 5.6. An optimum combination is searched after. Overall conclusions of the various variations are given in the concluding section 5.7.

The key design parameters are discussed in section 4.2.1. The key design parameters that are varied in the various scenarios, are:

- $\mathbf{W_{sluice}}$: the width of the sluice,
- **a/h** : the relative tidal amplitude,
- $\mathbf{A_{basin}}$: area of the flushing basin.

For the various scenarios of these parameters, the following output is compared in this chapter:

- Water level differences (Z(x,t)): the water level differences (vertical tide) change so that the duration of rising water differs from the duration of falling water. The water levels change as a result of the effect of a flushing basin.
- horizontal tide; the current velocities (U(x,t). For the current velocity signal two properties are important that can change:
    - the maximum amplitudes of the velocity
    - the duration of slack water after flood and ebb.

  Assuming an alluvial bed, the focus is on the maximum current velocities: peak current velocities.

The effect on the current velocities is determined under the assumption that the amount of sediment transport can be defined by the fifth order of the current velocities. Integration over one tidal period for each location gives the tide-residual transport.

In addition, the peak flow asymmetry and time asymmetry are known indicators to determine the dominant direction of the tide-residual transport for alluvial and starved bed conditions. These asymmetries are determined by the phase difference between the semi-diurnal tide M_2 and its first higher harmonic M_4 combined with the ratio between these two harmonics. A Fourier decomposition is used to determine the phases and amplitudes of the higher harmonics. This gives an indication for the dominant tide residual transport direction along the channel. This is compared with the tide-residual transport direction by use of integration of the current velocity with the fifth order as described in section 3.3.

5.1 Reference situation without flushing basin

As the name implies, the reference situation is presented to give a reference with which the various scenarios are compared. Actually, two reference situations are presented. The first is the situation without the presence of a flushing basin. In the second part, a flushing basin of 100 ha has been added at the end of the tidal channel. In the section that follow the reference situation the variation of the key parameters is presented and the effect of each parameter on the sediment transport is determined.

The implementation of a flushing basin behind a tidal channel might influence the current velocity distribution as function of time and place. To determine this effect, a reference situation is chosen.

5.1.1 Bathymetry

The bathymetry is chosen so that it matches the hypsometric curve near Noordpolderzijl, see Figure 18. In blue, the present hypsometric curve diverted to the quantity width of the area of Noordpolderzijl is illustrated. For the model calculations, this depth as function of width is approximated by a tangent hyperbolic function. As the hypsometric curve also includes the deeper parts of the primary channel, the hypsometric curve and the approximated tangent hyperbolic deviate. The middle part of the tangent hyperbolic represents the tidal flats. On the left side of the curve the tidal harbour channel with a width of 50 m and depth of -2 m NAP.

The present tidal harbour channel (the last 3 km to the harbour) has a variable width. For the reference case, the tidal channel width is set at 50 m. The initial depth is chosen such that it is large enough to accommodate the tidal range. This is done by determining the parameter a/h, the relative depth with the tidal amplitude a in relation to the channel depth h. The initial value of a/h = 0.5 [-] is used. With the a/h = 0.5 [-] the depth is two times larger than the amplitude of the tidal variation. The situation simulates an intermediate deep channel in a tidal environment, without the addition of a flushing basin. The parameters and their values of the reference situation are summarized in Table 8.

Table 8 – Defined values for the parameters for the reference situation scenario

parameters	value(s)	dimension
A_{basin}	(not present)	[ha]
a/h	0.5	[-]
W_{sluice}	(not present)	[m]
$W_{channel}$	50	[m]
$L_{channel}$	3000	[m]

5.1.2 Water levels & velocities

At the seaward boundary, a semi-diurnal tide is forced. In case of a rectangular cross-section the distortion of the tidal wave is minimum as the width is not dependent on the depth. However, in this reference situation there is a strong dependency between channel depth and width. Therefore, strong distortion of both the water level and velocity curves is expected.

In Figure 27 left side, the water levels at the two boundaries are depicted. In blue, the seaward boundary and in green the landward boundary/channel-end. What can be observed is that the rising tide results in a smaller shift between the water levels than the falling tide. Therefore, the water level difference between these two boundaries is larger in the case of falling tide.

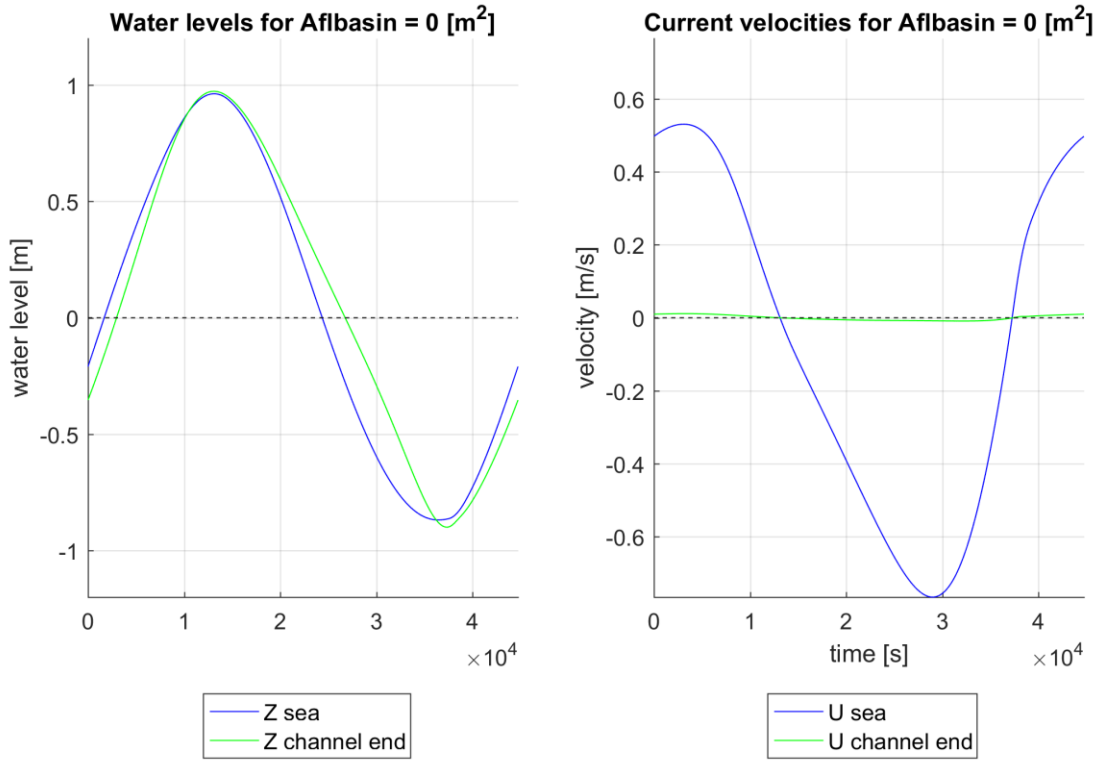

Figure 27 - Water levels and velocities for reference situation

The current velocities are visualized in Figure 27, at the right side. The current velocities at the seaward side are large. At the landward side, the current velocities are zero. The landward boundary is simulated by defining u = 0 [m/s] at x = 3000 [m]; u(3000,t) = 0. In Figure 28 the graphs of Figure 27 are combined. Water level is depicted in the solid blue and green lines, on the left axis. The velocities are visualized with blue and green dashed lines, on the right axis, the phase shift between the water levels and the velocities differs from $-0.5\,\pi$. Therefore, the wave within the channel is not a standing wave anymore, but a propagating wave.

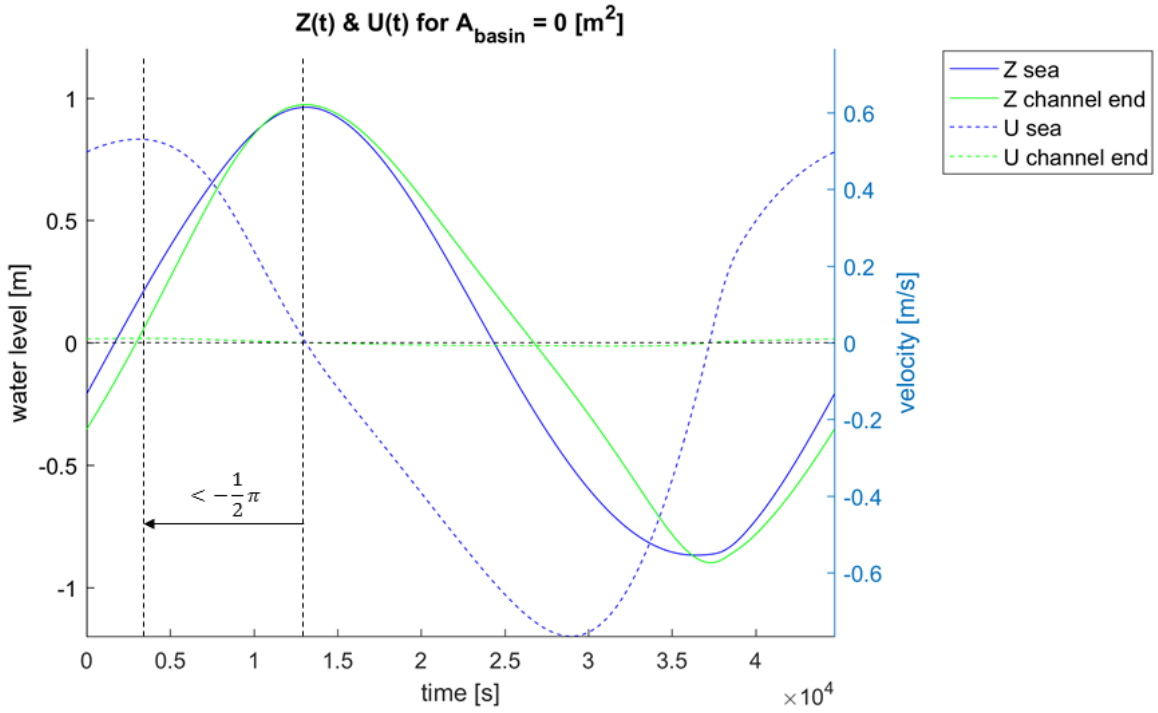

Figure 28 - Velocities and water levels combined for the situation without a flushing basin.

The above graph visualizes only the situation at the two ends of the channel. For an overall overview of the velocities in the channel Figure 29 is presented. In this figure, the current velocities are depicted as function of time and location within the channel. The time, on the vertical axis, represents exactly one tidal period. The horizontal axis comprises the total length of the channel; $L_{channel}$ = 3000 m. In yellow the flood current velocities and in blue the ebb current velocities are shown. The white lines visualize the time and location at which the current velocities are zero. The locations of the maximum current velocities are depicted with the plus sign '+', whereas maximum ebb current velocities are depicted with a black dot '·'.

Along the channel the current velocities are maximum at the same time, indicated by '+'. There is no shift in time between the occurring current velocities and this is also the case for zero current velocities. However, for the maximum ebb current velocities there is a shift in time between the occurring maximum ebb current velocities along the channel. This implies the deformation of the current velocity along the channel.

The velocity amplitudes, which are indicated by a colour in Figure 29, also change along the channel. In general a decrease in the amplitude of the current velocities occurs in longitudinal channel direction and this is visible in Figure 30. Furthermore, the maximum velocities for ebb are higher than for flood at the seaward side and thus an export of sediments can be expected.

The average depth that includes the tidal flats is relatively large for lower water levels whereas for higher water levels it is relatively low. Furthermore, the width during high water levels is high. The dominance of the friction term in the shallow water equations results in relatively high current velocities during low water in comparison to high water.

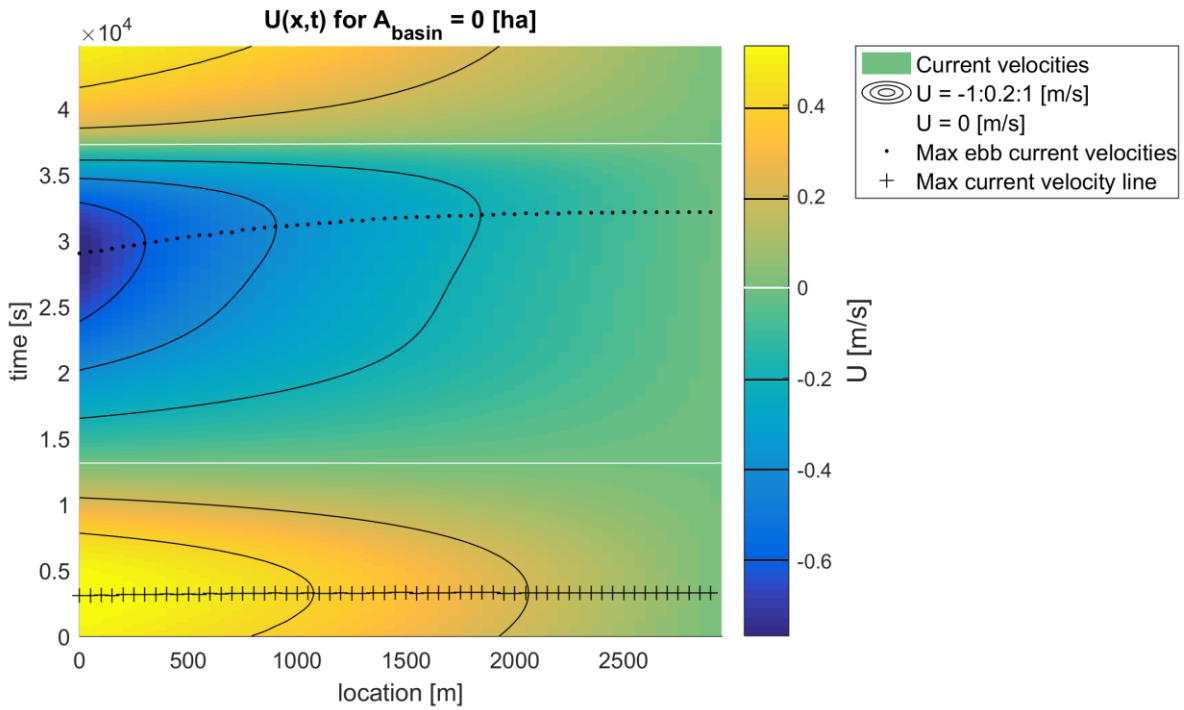

Figure 29 - Current velocities for the reference situation

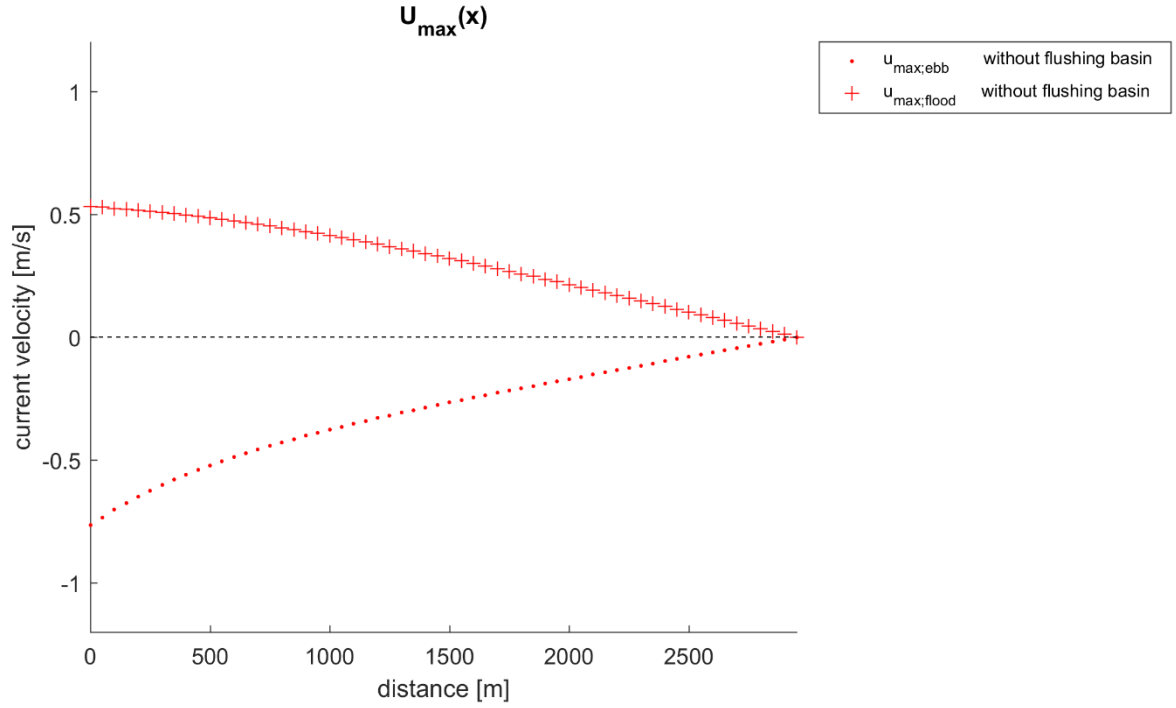

Figure 30 - Maximum and minimum current velocities along the channel axis.

5.1.3 Sediment transport

The transport as function of distance and time for the reference situation without a flushing basin is visualized in Figure 31. The sediment transport is the fifth order of the current velocity. The sediment transport takes predominantly place at the seaward boundaries, where the current velocities are highest. As the current velocities decrease over the channel length, the transport capacity decreases. Despite the ebb dominance of the seaward side of the tidal channel, deposition is expected in the middle part of channel end, due to the strong decreasing in transport capacity.

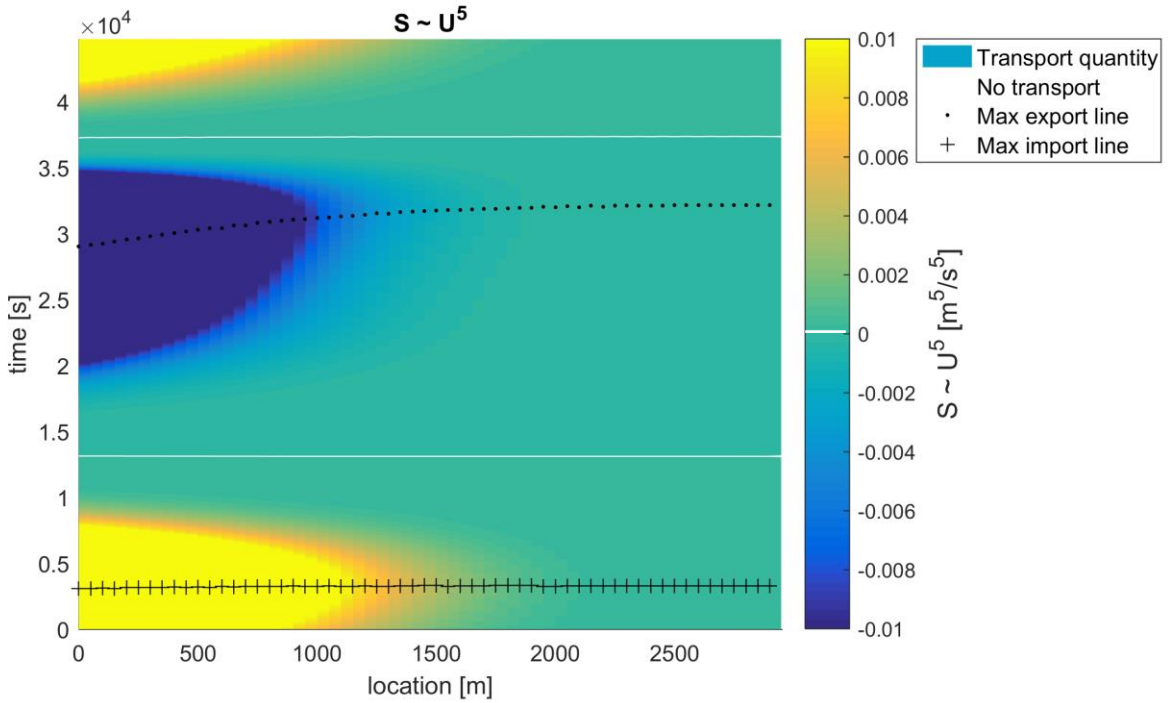

Figure 31 - Transport as function of time and space for the reference situation without flushing basin.

To confirm the deposition in the middle part of the channel its tide-residual transport is determined. For one location, halfway the channel the transport flux over time is depicted in Figure 32. The transport quantities during the flood tidal period are larger than during ebb. This can be observed by comparing the integrated area of the transport flux line for the flood part the positive fluxes and for the ebb part the negative fluxes. A positive net tide-residual transport quantity of S_{net} = 11.78 [m^5/s^4] is the result. This situation is therefore flood dominant. In the next section, the tide residual transport is determined and compared with the case with a flushing basin.

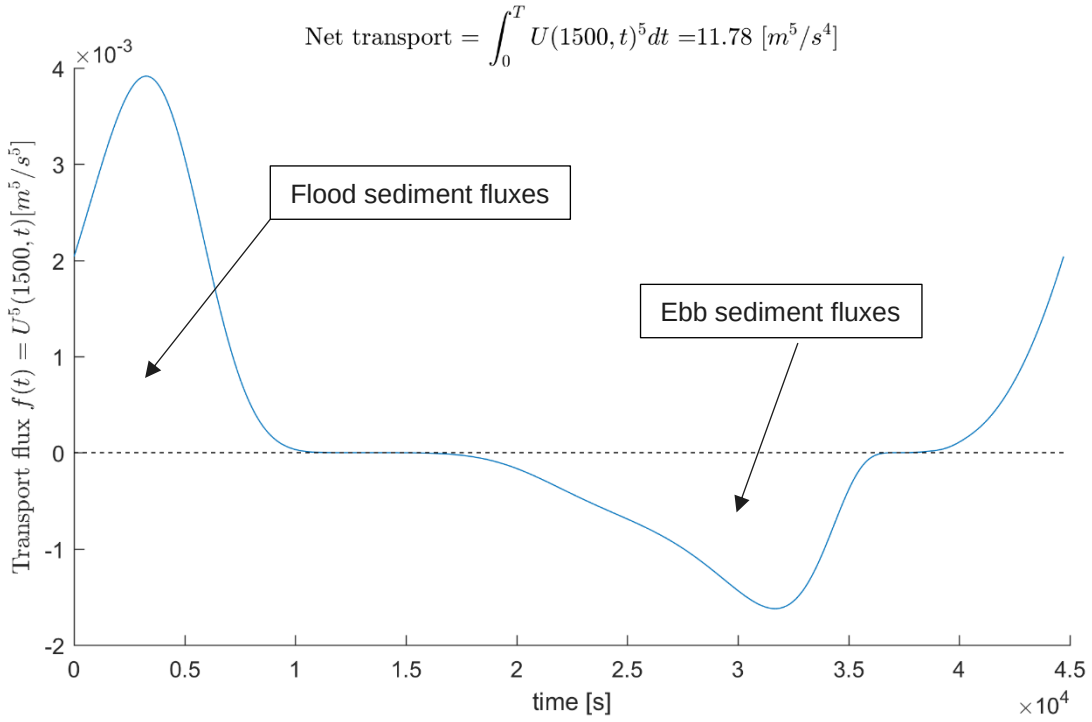

Figure 32 - Net transport halfway channel; S(1500,t) for reference situation without flushing basin

5.2 Reference situation with flushing basin

The above chapter described the present situation of tidal channel. In this part the effect of the addition of a flushing basin at the landward boundary is described. The flushing basin is modelled by using the continuity equation and discharge formulation of Torricelli, see section 4.2.2. The sluice width has a value of half the channel width. This is arbitrarily chosen, in the middle of the variations of the sluice width. The influence of the sluice upon the velocity distribution is determined in section 5.3. In Table 9, the values of the parameters are given for the reference situation with the addition of a flushing basin and sluice width.

Table 9 – Defined value for the reference situation with flushing basin.

parameters	value(s)	Dimension
A_{basin}	100	[ha]
a/h	0.5	[-]
W_{sluice}	25	[m]
$W_{channel}$	50	[m]
$L_{channel}$	3000	[m]

The addition of a flushing basin behind a channel results in a change in the velocity distribution over the channel length. In the situation without flushing basin, the current velocities are reduced at the channel-end to zero for all times. The addition of a flushing basin results in a flow in and out of the basin and therefore the current velocities do not drop to zero at the end of the channel. In the basin no current velocities are calculated. The flushing basin is in practice an area of sedimentation, because the current velocities will be very low. This study focusses on the change in current velocities in the channel only. Although ultimately the use of a flushing basin results in a strong decrease of dredging operation within the tidal channel, a new sedimentation problem in the basin can be created. Nevertheless, this results in less dredging operations within the channel and is therefore preferable.

5.2.1 Water levels & velocities

Changes in the water level variations in the channel are observed, when comparing these with the situation without a flushing basin, see Figure 33. Small differences in water levels between the channel end and the basin are introduced by the flushing basin in time. The amplitudes of the water level variation in the channel and basin are the same. There are two reasons for this effect:

- The basin area is small enough to follow the water level variations of the channel.
- The sluice does not hinder the in- and outflow in this configuration. When the sluice would be much narrower in relation to the channel width, the water level variation decreases in amplitude and is delayed in time.

The water level variation at the seaward side of the channel differs from that of the channel-end and basin. The water level variations are the result of the velocity boundary conditions, which can be described as weakly reflective. In systems with low distortion due to propagation through the system the water level variations are the same as semi diurnal water level variation with an amplitude of 1 m. This situation is used as a verification of the model and described in 4.5. For the situation with variable width as function of the depth; in which tidal flats are considered, the water level variation is distorted from a sinusoidal one.

The velocities at the channel-end and sluice are the same for the situation with a flushing basin. A slight difference between maximum and minimum velocities (velocity asymmetry) can be observed.

Around the horizontal axis (time), there is a stronger asymmetry. The time between slack water and maximum ebb current velocities is much longer than the time between slack water and maximum flood current velocity. This slack water asymmetry is the result of the strong influence of channel width at these periods of slack water. During high water slack (HWS), the average depth changes marginal and is relatively low compared to that of low water slack (LWS). For low water levels, the width of the channel remains (almost) the same, with changing water level. The small width at this stage, results in a smaller contribution of the friction term.

At the seaward boundary, there is asymmetry of the velocity amplitudes (velocity asymmetry). The ebb currents are much stronger than the flood currents velocities.

In Figure 34, the water levels and current velocities within the channel are combined. In the left panel, the situation without a flushing basin is visualized and in the left panel the situation with a flushing basin of 100 ha. What can be seen in Figure 34 is that there is an increased phase shift between the seaward side and channel-end of the water levels and current velocities for the lower values only. Generally, the current velocities increase in magnitude by the addition of the flushing basin.

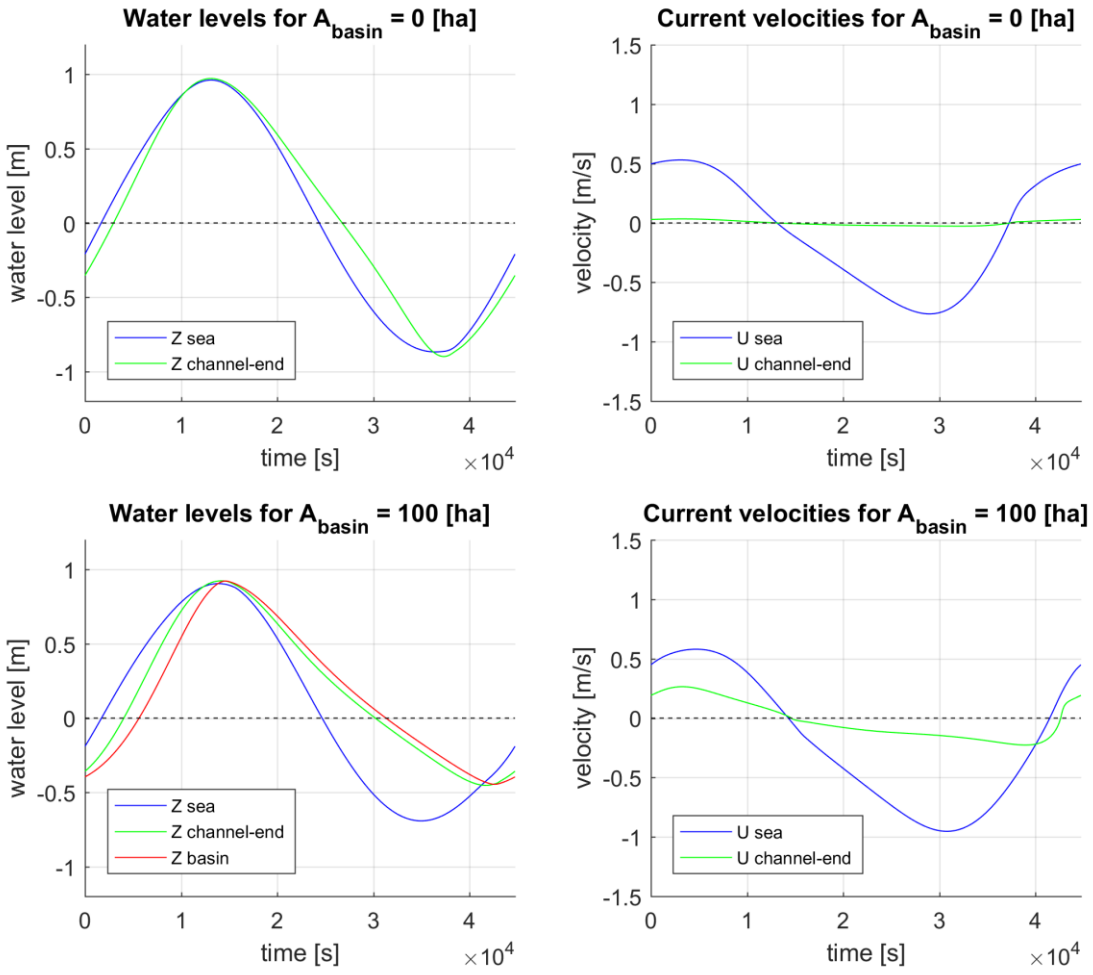

Figure 33 - Water levels and velocities for reference situation with the addition of a flushing basin.

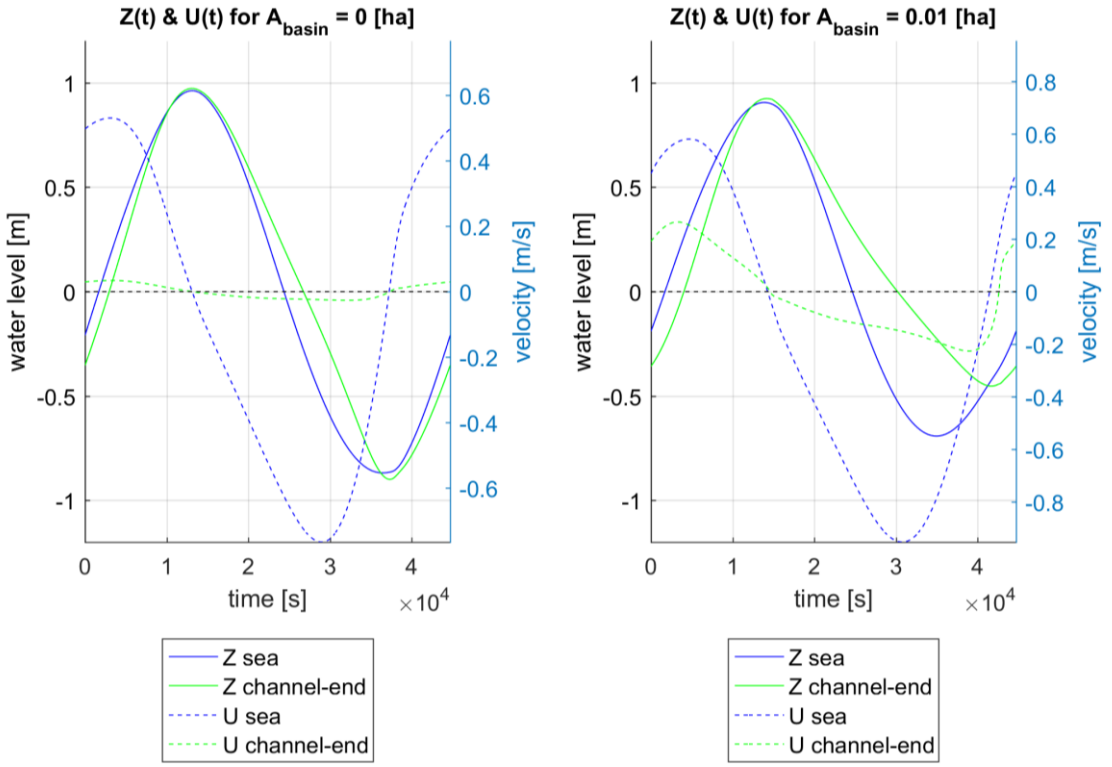

Figure 34 - Velocities and water levels combined with and without a flushing basin.

The variability over the length of the channel can be observed in Figure 35 and Figure 36. In Figure 35 the cases with and without a flushing basin are shown. These differences can be observed:

1. For the case with the flushing basin the duration of ebb flow is longer.
2. Overall magnitudes of the velocities are larger for the case including the flushing basin (see also Figure 36). At the landward boundary the differences are the largest.
3. The times at which the maximum flood current velocities occur ('+') changed slightly.
4. The times at which the maximum ebb current velocities occur ('·') changed as well. The variability along the channel is much larger with the flushing basin. For the case with a flushing basin of 100 ha, there is an increased phase lag in channel-end direction.
5. In both cases there is no variability in time at which slack water occurs.
6. For both cases the maximum and minimum current velocities have a non-linear decrease, see Figure 36.
7. For the flushing basin case the variability of maximum velocities is smaller, as the velocities at the channel-end are not zero, see Figure 36 depicted in red.

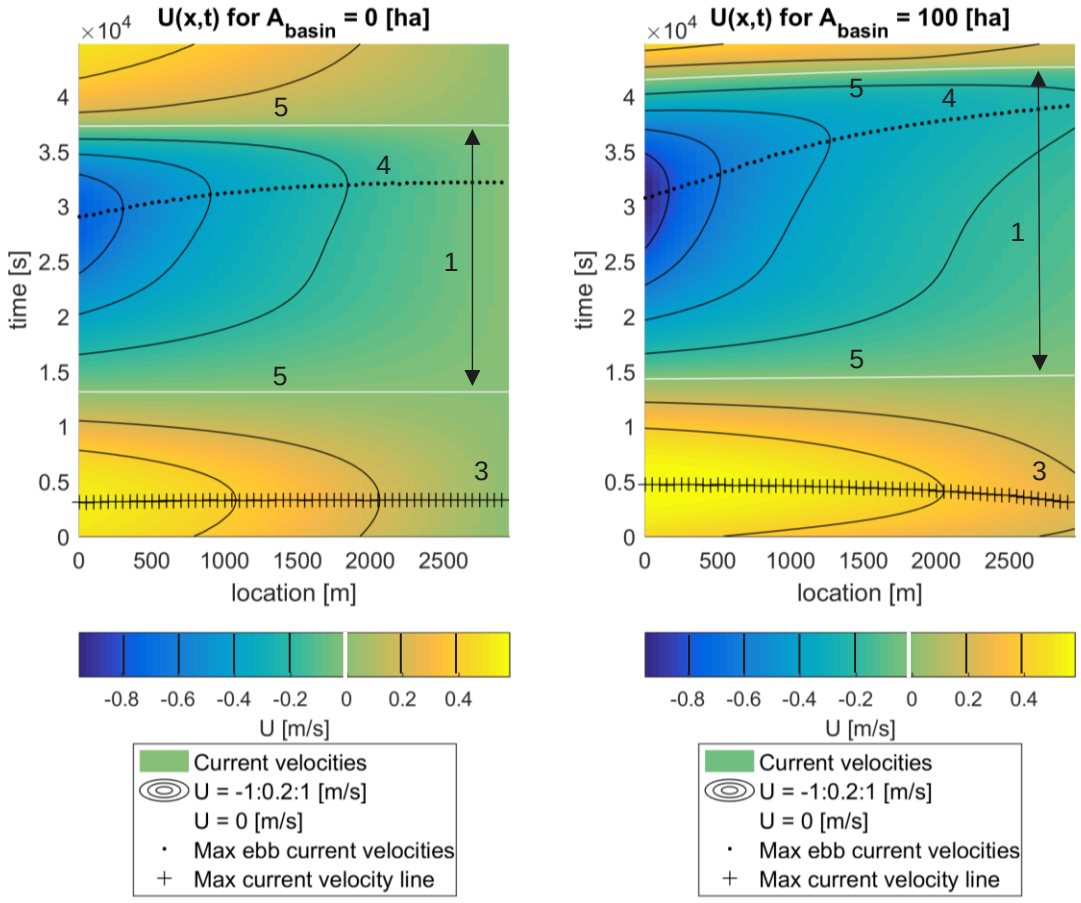

Figure 35 - Velocity distribution over space and time; U(x,t) for the case without and with a flushing basin.

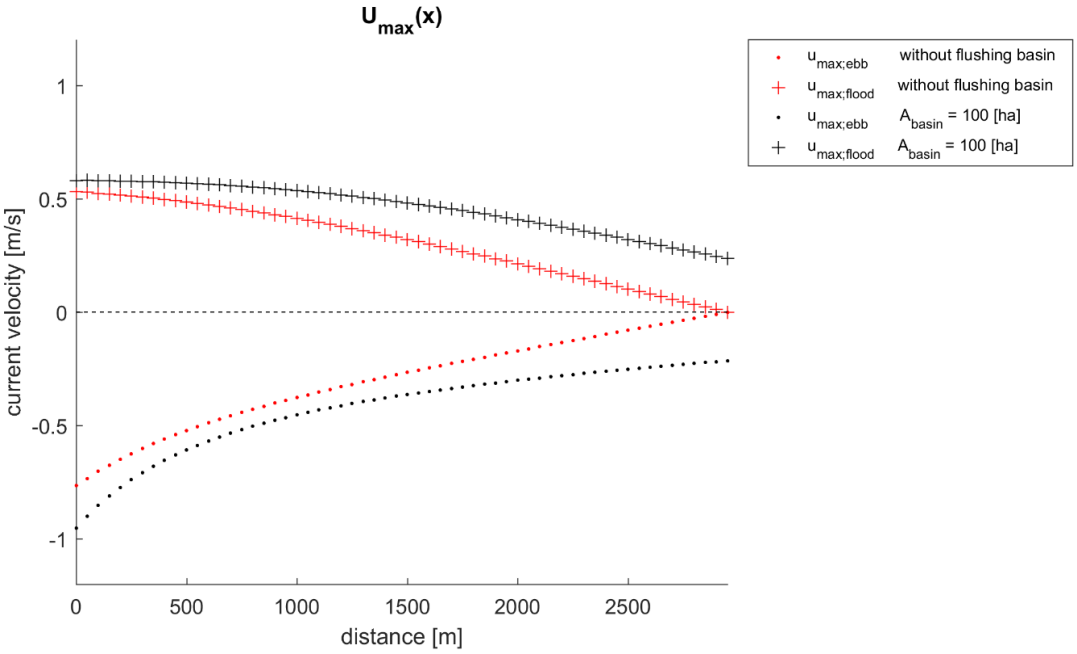

Figure 36 - Maximum velocities along the channel for the case without flushing basin and with flushing basin

5.2.2 Sediment transport

The distribution of the transport quantity is illustrated in Figure 37 for the situation without and with a flushing basin. The shape of the blue area that represent the ebb phase is comparable for both situations. However, the duration and distance over which the same sediment transports are present in the channel are larger for negative and positive transport fluxes. The current velocities are higher for the case with flushing basin (see Figure 36) and therefore, the sediment fluxes are higher too.

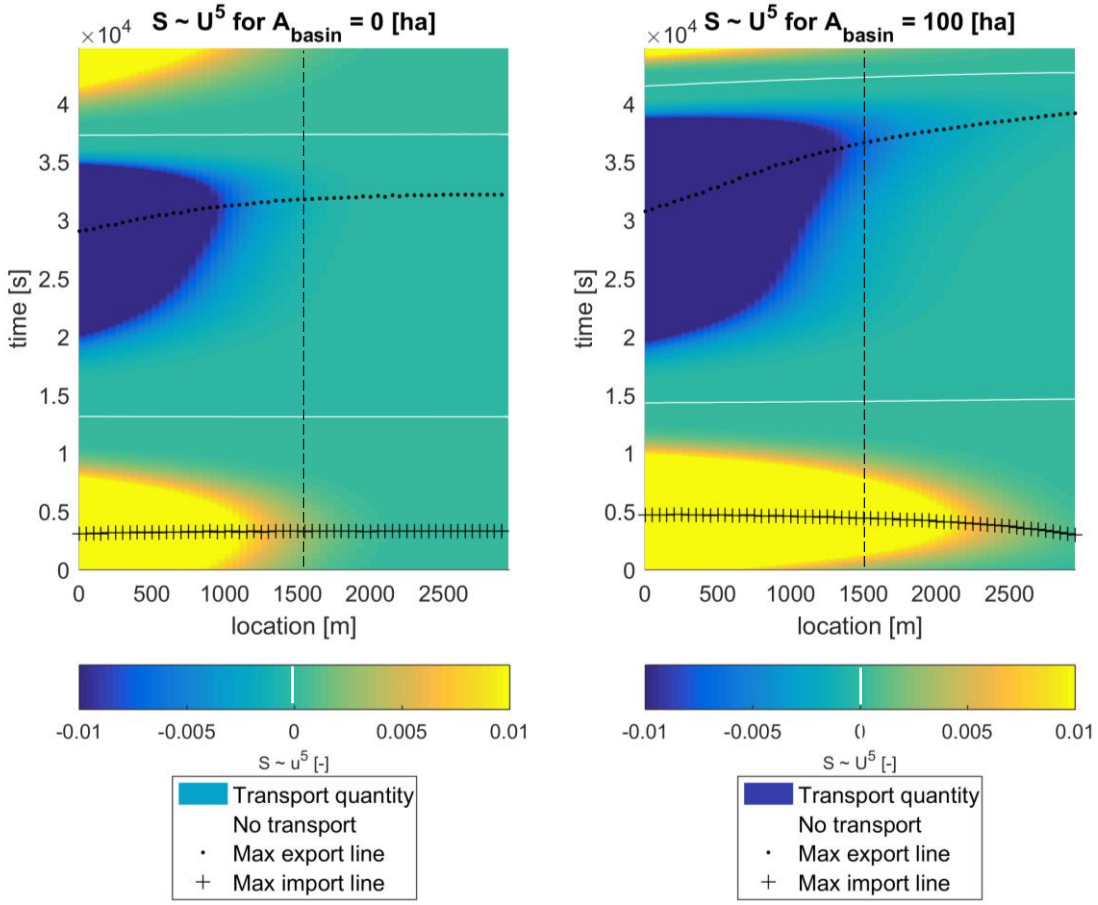

Figure 37 - Transport distribution for both with and without flushing basin

For one location; x =1500 m, indicated with a black dashed line in Figure 37, the transport fluxes are illustrated over time in Figure 38. What can be observed is that that the transport quantities during flood are larger than during ebb. Integration of the transport curves of Figure 38 gives the net transport quantity due to one tidal cycle and this represents the tide-residual transport can be determined at this location. For both cases the tide-residual transport S_{net} has a positive value thus in flood direction.

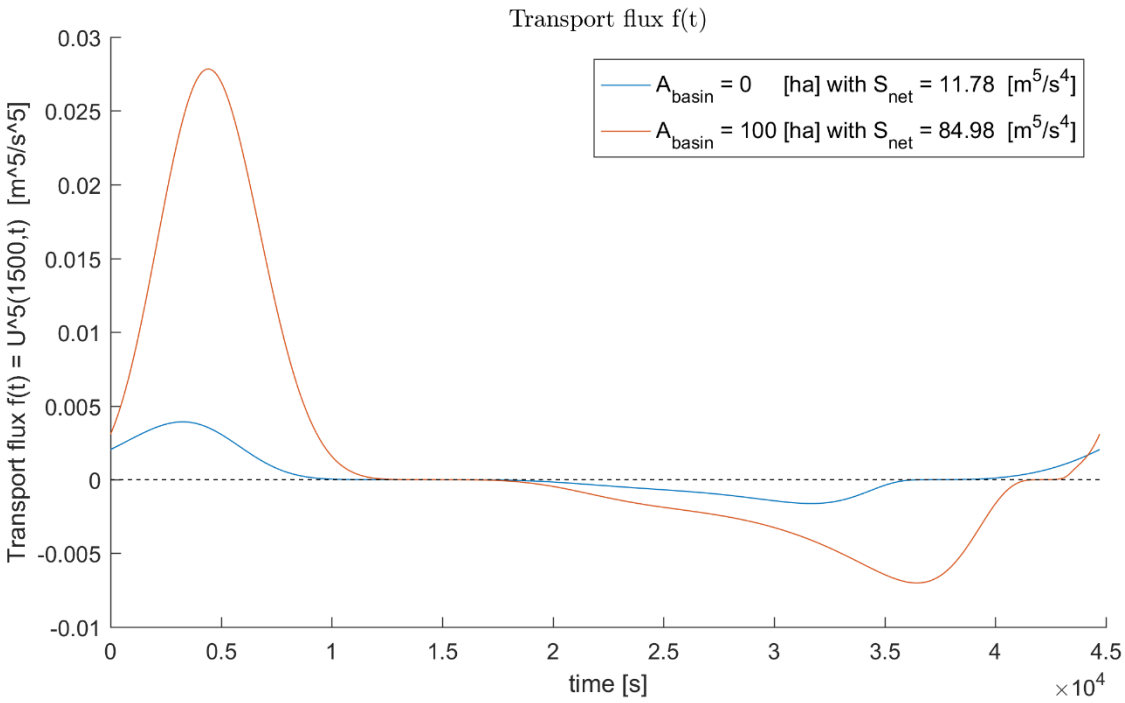

Figure 38 – Transport flux as function of time; f(t) for halfway the channel (x = 1500 [m])

When integrating over time for each location along the channel an overview of the net transport along the channel can be determined ($S_{net}(x)$). This is illustrated in Figure 39 for the situations with and without a flushing basin. A large difference in transport quantity between the first couple of hundred meters and the rest of the spatial domain can be observed. Furthermore, there is a change around x = 800 m from ebb dominant to flood dominant transport for both cases. Whereas for the situation without a flushing basin the transport quantities are low, for the situation with a flushing basin of 100 ha, transport quantities are larger for the second half of the channel.

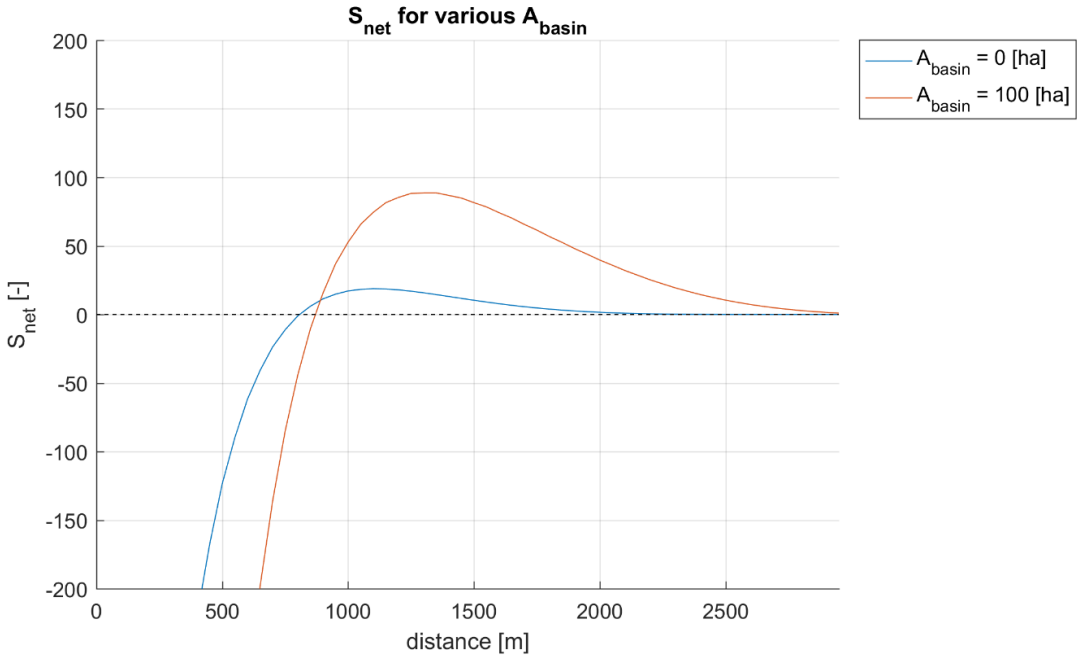

Figure 39 - Net transport quantity for all locations for A_{basin} = 0 and A_{basin} = 100 ha.

Both situations illustrate that at the seaward side the ebb transport quantities are exceptional large compared to the quantities at the rest of the domain. Both cases also have net flood dominancy in the second half of the channel. For practical purposes the siltation at the landward boundary, at which harbours are located, aimed

to be minimal. However, the situation with the flushing basin results in an increase of the net import of sediment for the second half of the channel. For management purposes this is an undesirable effect.

The switch in the sediment transport from ebb direction to flood direction results in divergence of the sediment transport. Divergence in the transport will result in erosion (Figure 40). The strong local erosion would result in a large pit in the channel.

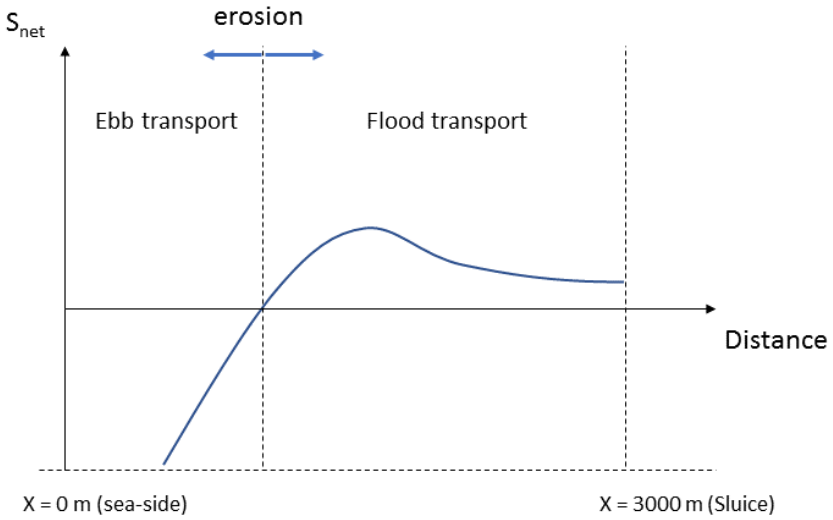

Figure 40 - Behaviour; situation 1: flood dominance at the landward second part and ebb dominance in the seaward of the channel.

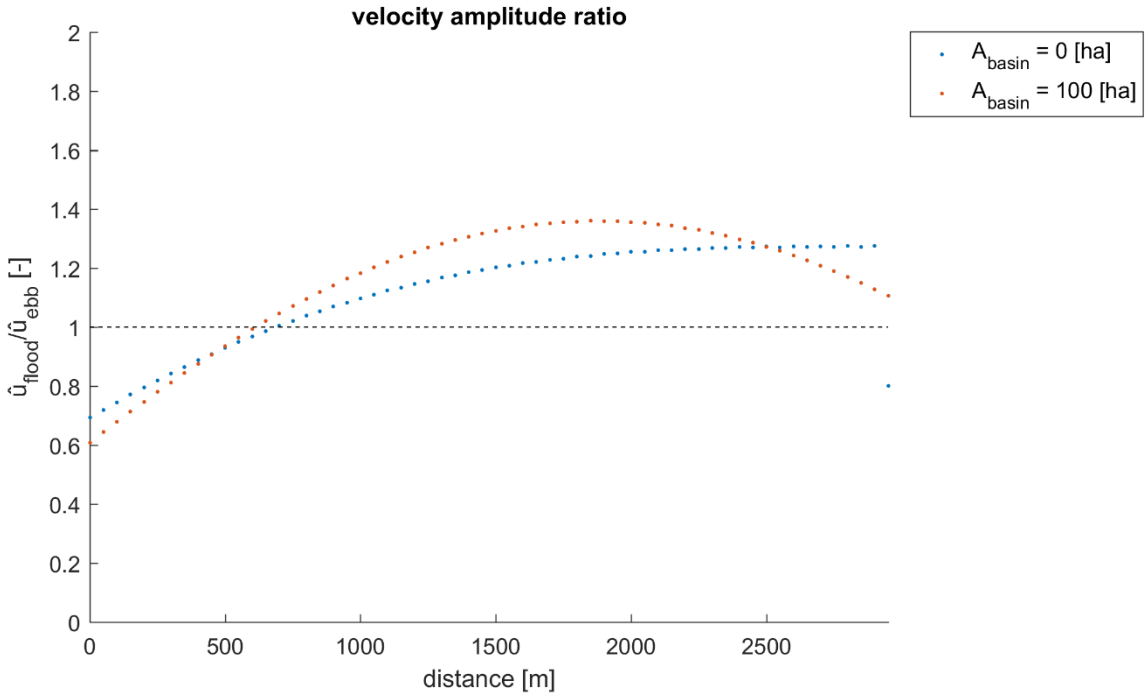

Figure 41 - Velocity amplitudes for the reference situation with and without flushing basin

5.2.3 Transport indicators – harmonic decomposition

The harmonic decomposition of the current velocities along the channel allows to quantify higher harmonics that are generated in the channel. For the two situations with and without flushing basin, the decomposition is visualized in Figure 42. An indication for the transport direction can be given by the semi-diurnal tide and the first higher harmonic M_4

For both situations, the predominant harmonic is the tidal forced water level variation M_2, see Figure 42 in blue in both left graphs. For the situation without a flushing basin, the other terms have small contributions. The illustrated phases on the right are highly variable for the situation without a flushing basin.

In 3.2 the tidal asymmetry is described using the first higher harmonic M_4. This is done by defining the relative phase difference between the semi-diurnal tide M_2 and the first higher harmonic M_4 given by $\phi = 2\phi_{M2} - \phi_{M4}$. The shape of the original current velocity U(t) can be reconstructed by use of the relative phase, see the right panels of Figure 43 for the relative phases. Depending on the relative phase two asymmetries can be described: the peak velocity asymmetry and time asymmetry.

- For peak velocity asymmetry the tide-residual transport has a maximum transport in flood direction when: $\phi = 2\phi_{M2} - \phi_{M4} = 2\pi$
- For time asymmetry the tide-residual transport has a maximum transport in ebb direction when:
  $$\phi = 2\phi_{M2} - \phi_{M4} = \frac{3}{2}\pi$$

For the total length of the channel flood dominance occurs when $\frac{3}{2}\pi \leq \phi \leq 2\pi$.

In Figure 42 a strong decrease of the velocity amplitudes is observed over the length of the channel, which was already presented in Figure 36. This is the case with and without a flushing basin. The relative amplitude of the higher harmonics $a_{M4}/a_{M2} \approx 0.2$ is larger for the situation without a flushing basin than for the linear situation; $a_{M4}/a_{M2} \approx 0.05$. This is due to a smaller relative depth of a/h = 0.5 and the presence of the tidal flats.

For the situation without a flushing basin, the relative phase difference in the upper-right panel of Figure 43, increases from 1.5π to 1.75π in the first part of the channel and becomes constant in the last part of the channel. A distortion to a larger flood dominance in the first part of the channel can be observed.

For the situation with a flushing basin, there is a decrease of the relative phase at the end of the channel, see the lower-right panel of Figure 43, which resembles a decrease of flood dominance. This is not the case for the situation without a flushing basin as the phases remain constant at the end of the channel, see Figure 43, right panels. The increasing relative amplitudes in the situation with a flushing basin, are the result of a stronger decrease of the M_2 amplitude than the higher harmonics, see Figure 43 left lower panel.

There is a difference between the dominant direction of the sediment transport by using the decomposition of the semi-diurnal tide and its first higher harmonics on the one hand and using the sediment formulation $S_{net} = \int u|u|^{(n-1)}dt$ with n = 5, on the other. The sediment formulation allows the observation of a transition between net ebb and flood transport with and without a flushing basin, see Figure 39. The transport indicators from the harmonic decomposition display only a flood dominant tide-residual transport. An approximation of the dominant direction by use of these transport indicators is therefore not recommended.

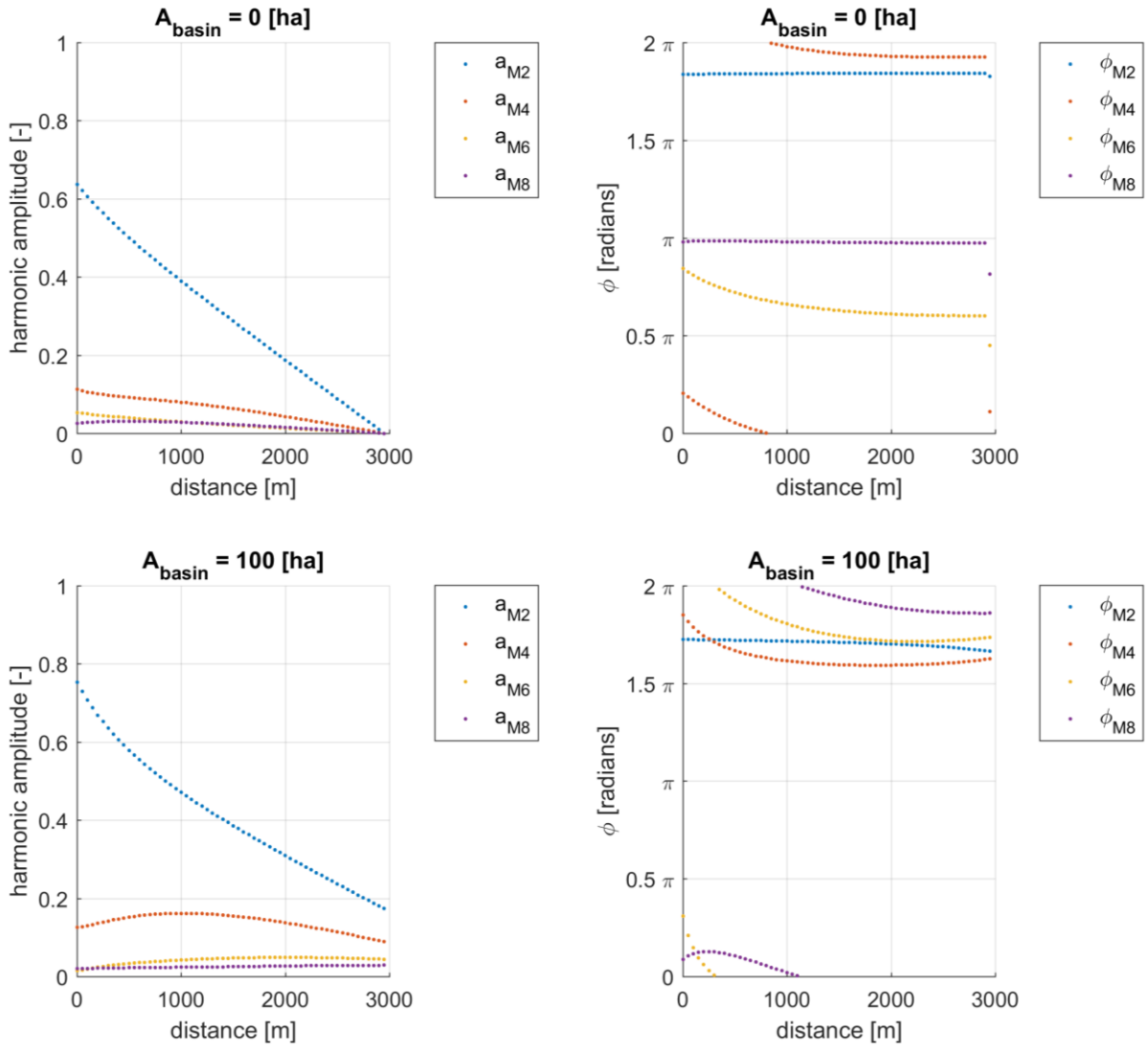

Figure 42 - Harmonic decomposition of the reference situation

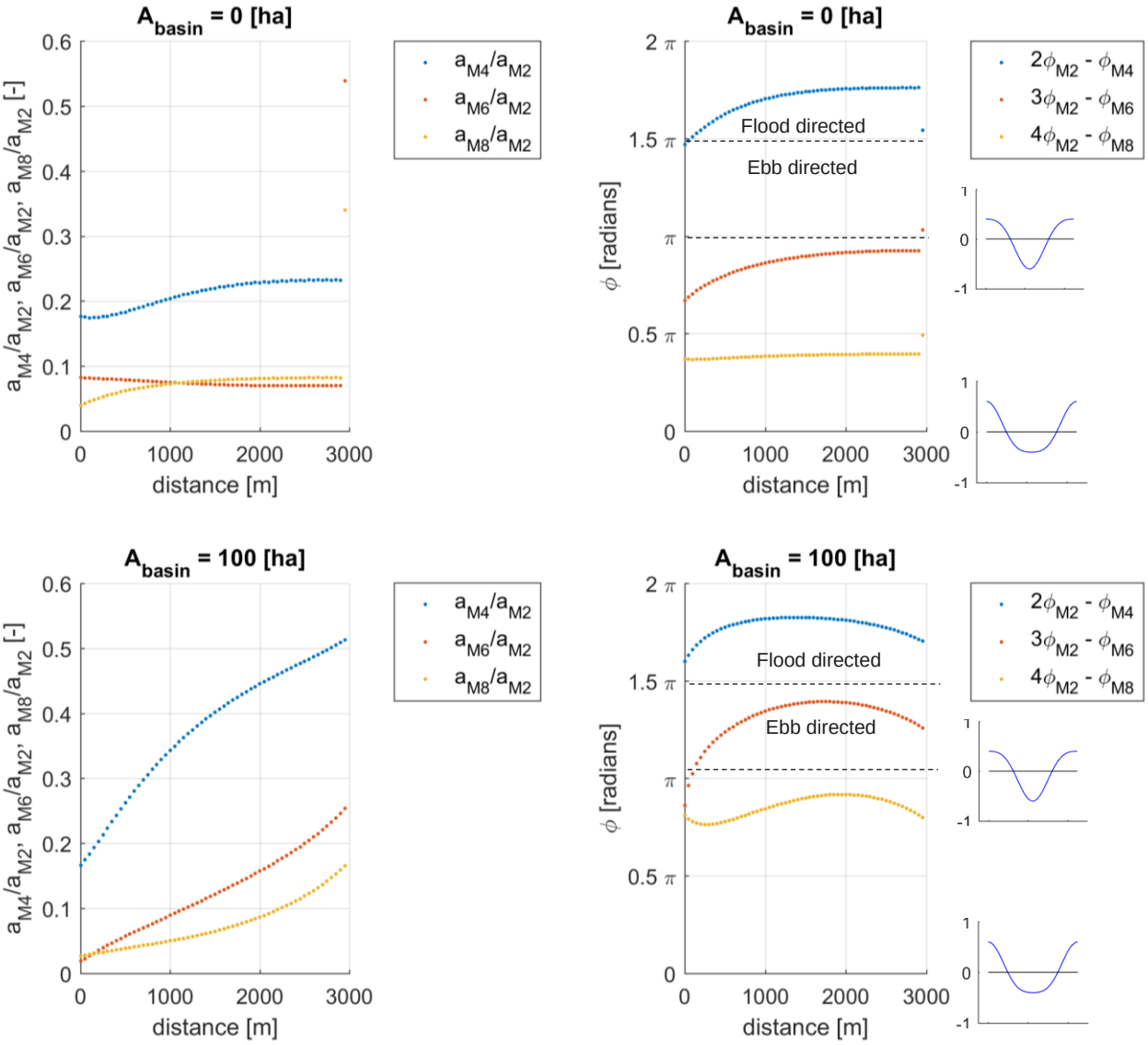

Figure 43 - Relative amplitudes and phase differences

5.2.4 Equilibrium cross-section

For each tidal channel in a tidal basin an equilibrium channel cross-section can be determined by Equation 29 described in section 4.6. In this section, the required basin area is determined for the defined cross-section of the channel for the reference situation. For a/h = 0.5 the required basin area is about 280 ha.

For a basin area of 100 ha the current velocities are not sufficient to be able to create a tide-residual transport that is about zero. I.e. the cross-sectional area of the channel is too large for the relatively small basin area. Various scenarios for the basin area have been executed section 5.5, illustrates and confirm this effect.

5.2.5 Conclusion

Without the addition of a flushing basin, the maximum and minimum current velocities decrease to zero at the landward boundary. The sediment transport quantity spatially varies over the channel. At the seaward side, the net sediment transport is in ebb direction, whereas at the landward side this is in flood direction.

With a flushing basin, the maximum current velocities in the channel do not decrease to zero at the landward boundary. The storage capacity of the basin results in exchange of water between channel and the flushing basin. This exchange during flood has a smaller variability of the maximum flood current velocities than for the case without the flushing basin. At the seaward boundary, the maximum ebb current velocities are much smaller in the situation without a flushing basin. The overall variability of the maximum current velocities is much larger for the case with a flushing basin than in case without a flushing basin.

Considering the total spatial domain in landward direction, for both cases there is a transition of the transport direction from an ebb dominance to a flood dominance. The larger current velocities in case of a flushing basin not only result in larger transports quantities, but also the ratio between flood and ebb transport increases, to a stronger ebb dominance at the seaward side and a stronger flood dominance at the landward side. The net transport quantities are larger at the second half of the channel; landward side, there is also a larger decrease of the net sediment transport. A stronger deposition in this area can be expected. At the channel-end for both cases the net transport decreases to almost zero.

By determining the tide-residual transport quantity for all locations, an overview of the transport along the channel for one tidal cycle and one configuration can be made. For various scenarios (values) of the key design parameters, the tide-residual transport is compared.

Summarizing:

- In both cases, with and without a flushing basin, strong ebb dominance occurs at the seaward side and flood dominance at the landward side.
- The variability of the current velocities increases because of the flushing basin. This results in larger gross and net transport quantities for the case with a flushing basin.
- Despite the presence of a flushing basin, the net transport quantities decrease to zero near to the channel end/sluice.
- The approximation of the dominant transport direction by using harmonic decomposition is not recommended as the difference with the results from the sediment transport formula is too large. A transition of the net transport direction is not determined by using harmonic decomposition.

5.3 Scenarios for W_{sluice}

At the seaward boundary of the model, the boundary condition is chosen such that it represents the in- and outflow quantities resulting from the presence of a tidal basin. The tidal basin stores a quantity of water and subsequently releases it. The sluice acts as a confinement. The exchange of water is influenced by narrowing or widening the sluice width. The discharge through the sluice is both dependent on Equation 30 - storage equation and Equation 31 - discharge equation, as result of water level differences.

Equation 30 - Storage equation

$$\frac{dZ_{basin}}{dt} = \frac{Q_{sluice}(t)}{A_{basin}}$$

With:

Equation 31 - Sluice discharge equation

$$Q_{sluice}(t) = A_{sluice}(t)\sqrt{2g\left(Z_{basin}(t) - Z_{channel-end}(t)\right)}$$

With:

$$A_{sluice}(t) = W_{sluice}\left(h + Z_{sluice}(t)\right)$$

For a semi-diurnal tide and with no variations along the channel, the water-levels at the channel-end and the basin are given by:

Equation 32 - water level channel-end

$$Z_{channel-end}(t) = cos(\omega_{M2}t)$$

Equation 33 – basin water level

$$Z_{basin}(t) = cos(\phi)cos(\omega_{M2}t - \phi)$$

With:

ω_{M2} = semi-diurnal wave frequency
ϕ = phase difference, with $0 < \phi < \frac{\pi}{2}$

For large phase differences the variation of the water level of the basin decreases. Larger differences between the basin and the channel-end occur. The phase difference can be influenced by the width of the sluice. The width of the sluice determines for a large part the cross-sectional area of the sluice (A_{sluice}). This area simulates the tidal discharge into the basin through a sluice. When the flow cannot enter freely into the tidal basin with small values of $A_{sluice}(t)$ a delay is introduced in the water level of the basin compared to that of the channel end. The water level difference between the basin and the channel end results in a discharge through the sluice.

Two extreme situations are described to demonstrate the effect of the sluice:

- Free flow: almost no water level differences occur. The water level in the basin follows almost directly the water level at the end of the channel. This is depicted in Figure 44 for the case of W_{sluice} = 50 m. The water levels at the end of the channel are equal to the basin water levels. This occurs when $W_{sluice} \approx W_{channel}$.
- Restricted flow: the water level in the basin cannot follow the water level in the channel. In the most extreme situation, the water level in the basin does not change at all, whereas in the channel variations with the amplitude of the tide occur (1 m).

In addition to the extreme situations, the results of intermediate situations are shown in the next section. In this chapter various scenarios for the width of the sluice are elaborated. The values of the design parameters of the scenarios are summarized in Table 10.

Table 10 - Defined values for the parameters for various scenarios for W_{sluice}.

Parameters	value(s)	dimension
W_{sluice}	5 : 50	[m]
a/h	0.5	[-]
A_{basin}	100	[ha]
$W_{channel}$	50	[m]
$L_{channel}$	3000	[m]

5.3.1 Water levels & velocities

Two scenarios are elaborated on in this chapter as these two scenarios are both the most extreme scenarios. For W_{sluice} = 5 m and for various locations the water levels are visualized in Figure 44 in the upper-left panel and W_{sluice} = 50 m in the lower-left panel. The current velocities for the two sides of the channel are illustrated at the right-hand side of the figure.

Due to the partly restricted flow, for W_{sluice} = 5 m, the water level in the basin (Figure 44 in red) follows the water level at the end of the channel with a large delay in time. Consequently, the water level cannot reach the level of the channel water level.

The delayed water level in the basin results in different velocities at the end of the channel. Variations of the sluice width therefore result in different distributions of the discharge over time, as can be seen in Figure 44, on the two right graphs. For the functioning of the tidal basin it is important to note that the delayed water level variations result in a reduction of the total tidal variation in the basin, see Figure 46. The average water level of the flushing basin is not equal to the original water level (Z = 0), but is increased to about 0.25 m.

For the situation of W_{sluice} = 5 m. the current velocities at the end of the channel are smaller than for the situation W_{sluice} = 50 m. Especially the flood current velocities are enlarged for W_{sluice} = 50 m. For the W_{sluice} = 5 m the tidal range is due to the reduced sluice width decreased.

The change of the tidal levels in the basin as function the sluice widths is illustrated in Figure 46. With increasing widths of the sluice, the high water level increase and the low water level decreases. For the increase of sluice width from 5 to 15 meters the change is largest and with each additional 10 m of sluice width less change occurs. As the prism is the product of the water level variation and the area of the flushing basin, each increase in sluice width of 10 results in less additional tidal prism. The effect of the width of the sluice on the water levels in the basin is substantial when W_{sluice} = 15 m and for smaller values. For higher values, the water levels in the basin are the same. Intuitively this response is expected: to use the full potential of the basin a wide sluice is needed. Whether the maximum water height coincides with the maximum effect in terms of sediment transport is elaborated below.

Figure 47 allows to compare the current velocities during rising water for W_{sluice} = 5 m (left panel) with W_{sluice} = 50 m (right panel). For W_{sluice} = 50 m the water level differences between the seaward boundary and the channel-end are larger than for W_{sluice} = 5 m. At the same time, the flood current velocities at the channel-end are larger for the scenario with W_{sluice} = 50. At the channel-end the flood current velocities are larger than the ebb current velocities when W_{sluice} = 50. Whereas for W_{sluice} = 5 m the opposite is the case.

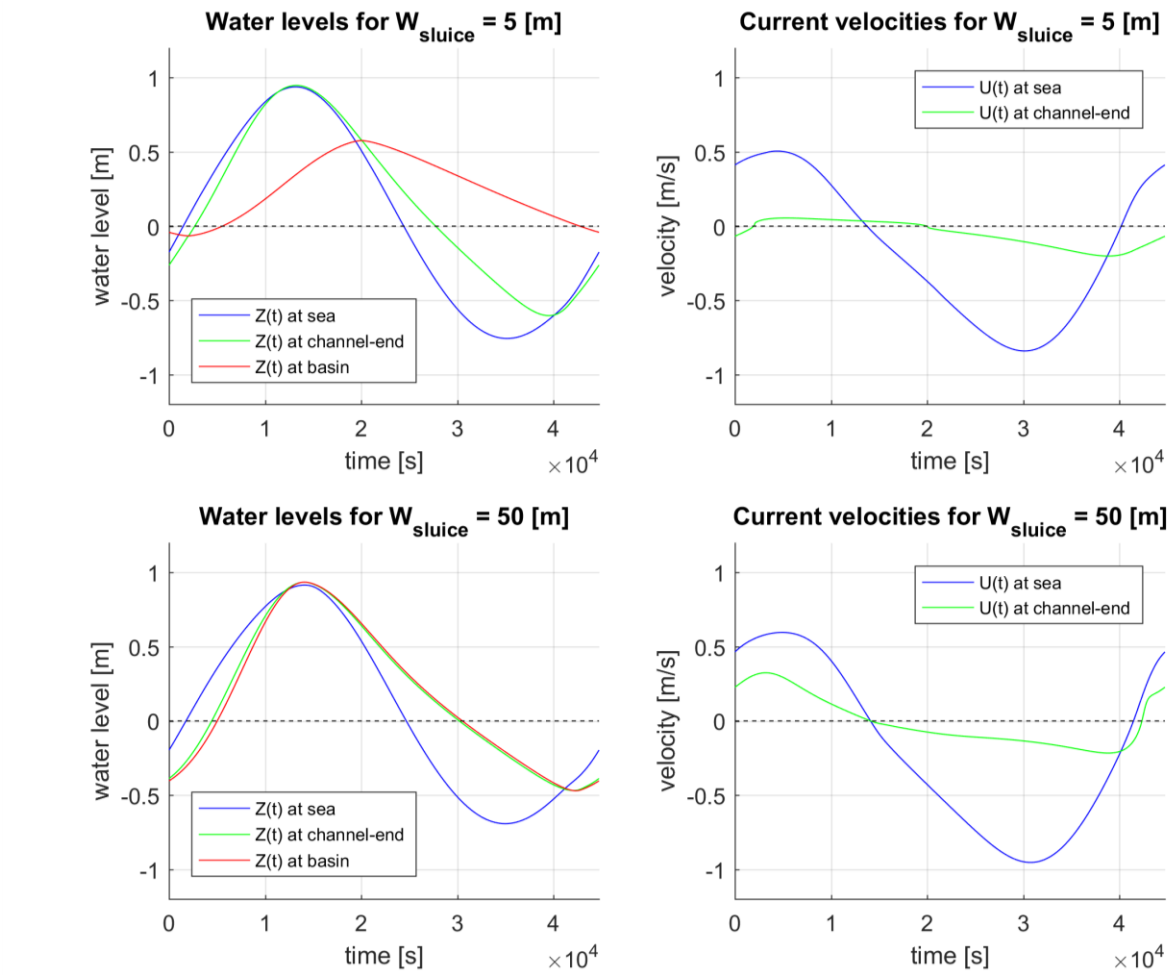

Figure 44 - Water levels (left axis) and velocities (right axis)

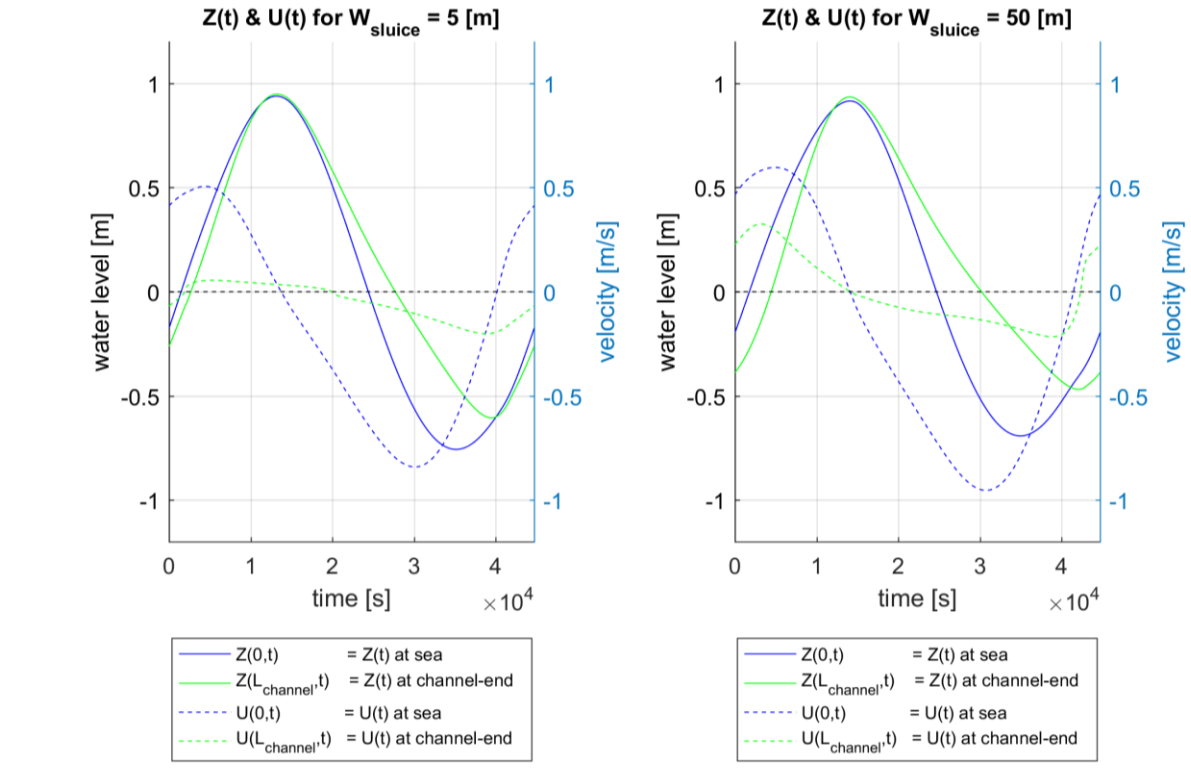

Figure 45 - Water levels and velocities for W_{sluice} = 5 and 50 m

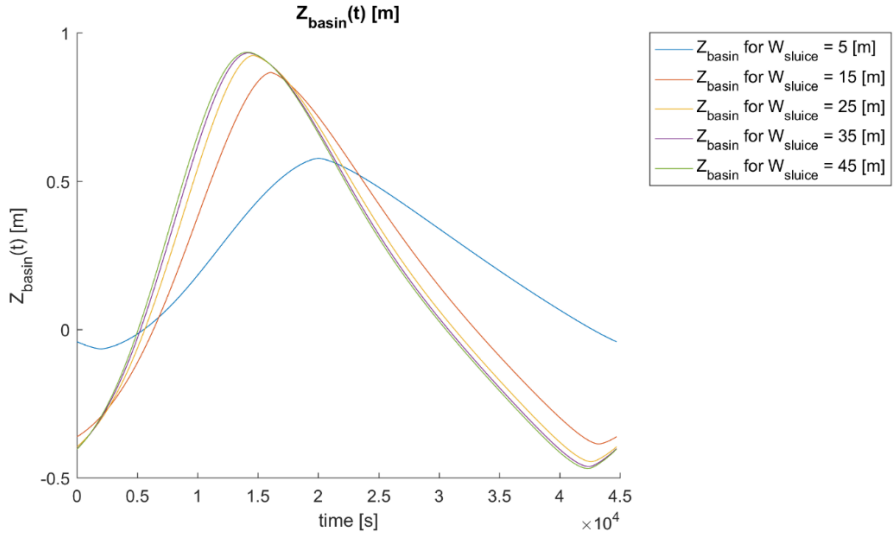

Figure 46 - Variations of $Z_{basin}(t)$ for varying width of the sluice

In Figure 44 and Figure 45 the variations over time are visualized for only 3 locations. In Figure 47 an overview of the current velocities for all locations along the channel is illustrated. For the two sluice widths, the following differences can be observed:

- Local differences are present at the seaward side and near the sluice. At the seaward side, for W_{sluice} = 50 m both the ebb as well as flood current velocities are larger than for W_{sluice} = 5 m. Near the sluice, there is an increased delay of velocities in the last kilometre, both for high water slack and for low water slack.
- For W_{sluice} = 50 m the current velocities are larger for all locations. Especially the flood current velocities are enlarged compared to the ebb current velocities. This same effect can be observed in Figure 48.

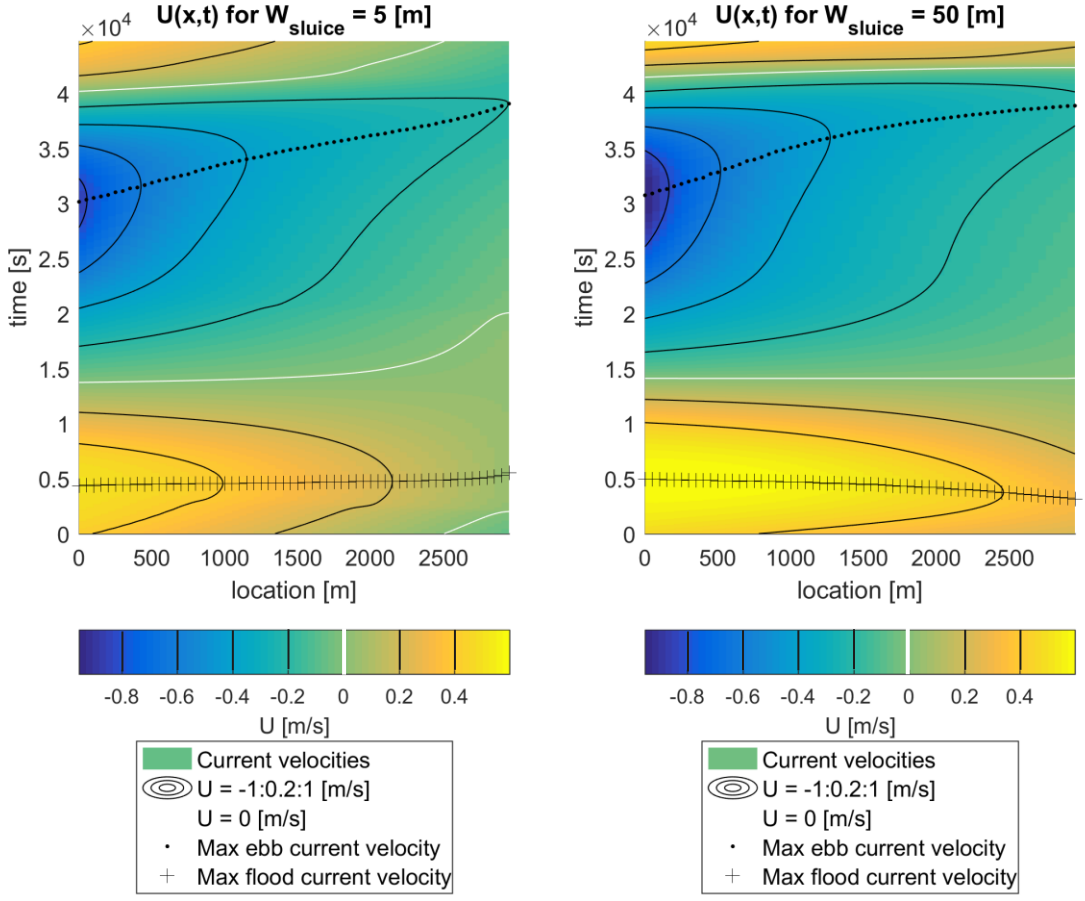

Figure 47 - Current velocities for W_{sluice} = 5 m and W_{sluice} = 50 m

In Figure 48 the differences in maximum velocities are presented. The maximum ebb tidal currents are roughly the same for W_{sluice} = 5 m and 50 m. For the maximum flood tidal currents there is a larger difference. A strong peak velocity asymmetry is visible. This can be observed by comparing these maximum current velocities. At the seaward boundary for all scenarios with varying width of the sluice, the tidal ebb currents are larger in magnitude than the flood currents: $\frac{\hat{u}_{flood}}{\hat{u}_{ebb}} < 1$. In Figure 49 the ratios are given along the channel. Near the channel-end for most scenarios, the asymmetry is the other way around: $\frac{\hat{u}_{flood}}{\hat{u}_{ebb}} > 1$, meaning that larger flood current velocities occur than ebb current velocities. But only for the scenario with W_{sluice} = 5 m $\frac{\hat{u}_{flood}}{\hat{u}_{ebb}} < 1$ for the total length of the channel. In the next section, the conversion to transport quantities is made.

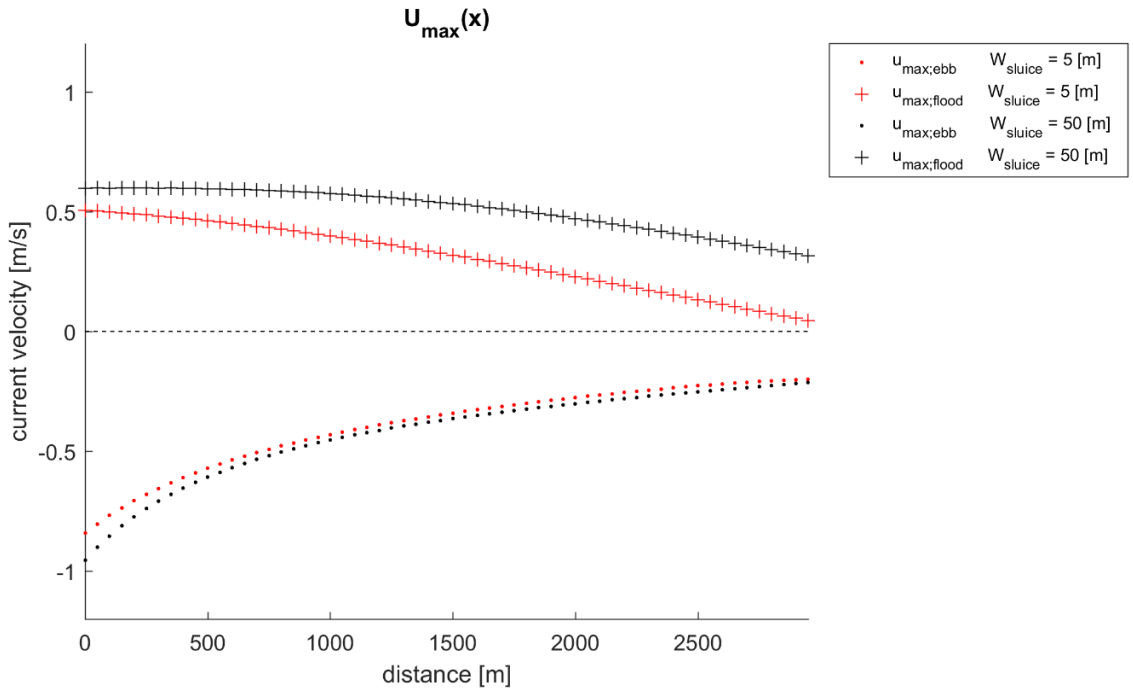

Figure 48 - Maximum and minimum current velocities along the channel, for W_{sluice} = 5 m and W_{sluice} = 50 m

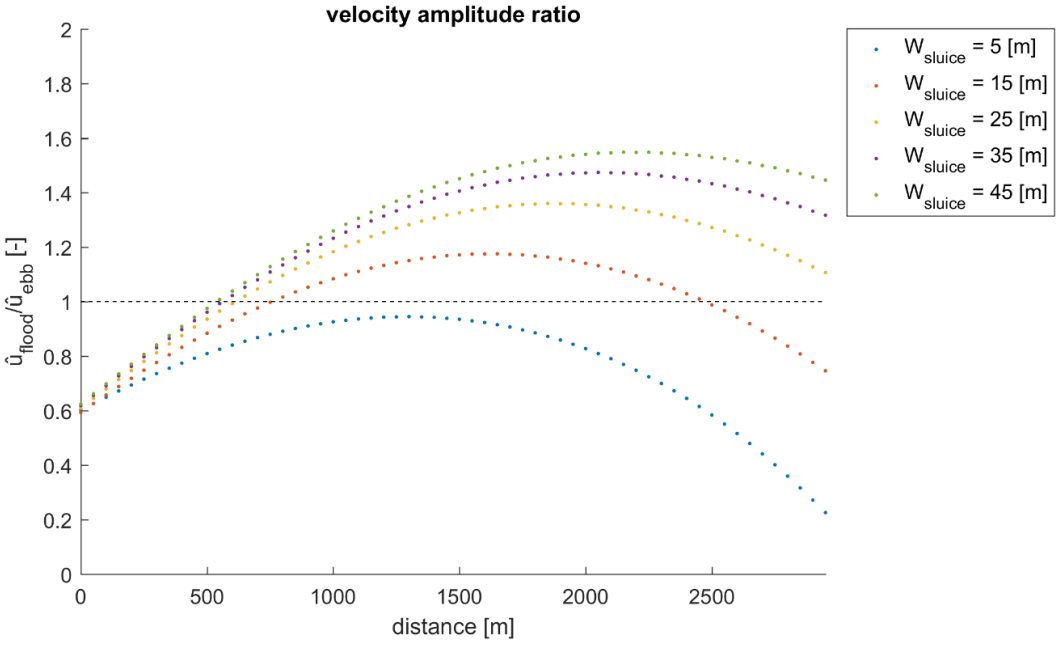

Figure 49 - Velocity amplitude ratio for varying W_{sluice}

5.3.2 Sediment Transport

In the previous sections the water level and current velocity variations are described for the two most extreme scenarios of the sluice width. To determine the effect of the various scenarios we are more interested in the tide-residual transport and direction, that dictate the import or export of sediments.

In the Figure 50 for the channel-end the transport as function of time is depicted for various scenarios. The integration of these lines results in a tide-residual transport quantity S_{net} which is given in the upper-right legend. A negative value implies an ebb-directed tide-residual transport. For higher values of W_{sluice} larger quantities result from the increased flood current velocities, as observed in Figure 45. Although the ratio of the maximum current velocities for W_{sluice} = 5 m is larger than for W_{sluice} = 45 m depicted in see Figure 49, the net quantities of S_{net} are much larger for W_{sluice} = 45 m. This is because of strong non-linearity between the current velocities and the sediment transport is introduced by n = 5 in section 3.3.

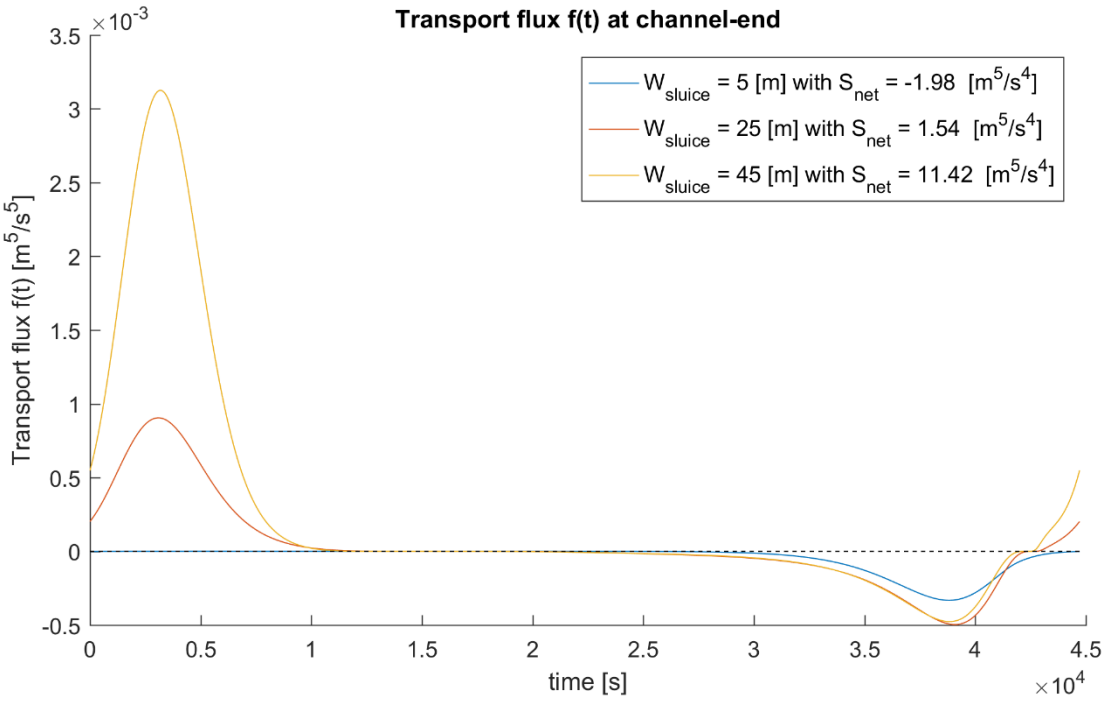

Figure 50 - Transport as function of time

The tide-residual transport is now determined for all locations along the channel and for all scenarios of the width of the sluice. The results are illustrated in Figure 51. On the left side of Figure 51, an overview is given of the sediment transport quantity for each variation of the sluice width (W_{sluice}) for all locations along the channel. At the vertical axis, the channel location is depicted. With x = 0 the seaward side and x = 3000 the sluice. At the horizontal axis, the various scenarios of W_{sluice} are given. The colours indicate the tide-residual sediment transport quantities: the net flood transport quantities are shown in yellow and net ebb quantities in blue. The white line depicts the situation of zero transport.

A couple of scenarios of W_{sluice} are illustrated at the right panel of Figure 51. In the right panel several lines illustrate the tide residual transports quantities. The tide-residual suspended transport is depicted on the vertical axis and the position along the channel on the horizontal axis.

In Figure 51 can be observed:

- For the smallest sluice widths; 5 – 10 m, the net transport is ebb dominant along the total length of the channel. For the W_{sluice} = 15 m and higher, part of the channel is flood-dominant and part of the channel is ebb-dominant. For values W_{sluice} > 15 m the flushing basin creates an undesirable effect. For the second half of the channel the net sedimentation quantities are larger for sluice width's.
- The effect of the increase or decrease of the sluice width of 10 m, can be observed at the right panel of Figure 51. For smaller sluice widths, a decrease of the flood dominant for the second half of the channel is visible. The decrease of flood dominance is also larger for lower values of sluice widths, but decreases again for $W_{sluice} \approx$ 15 m. The effect of the sluice width is largest for $W_{sluice} \approx 20\,m \approx 0.4\,W_{channel}$

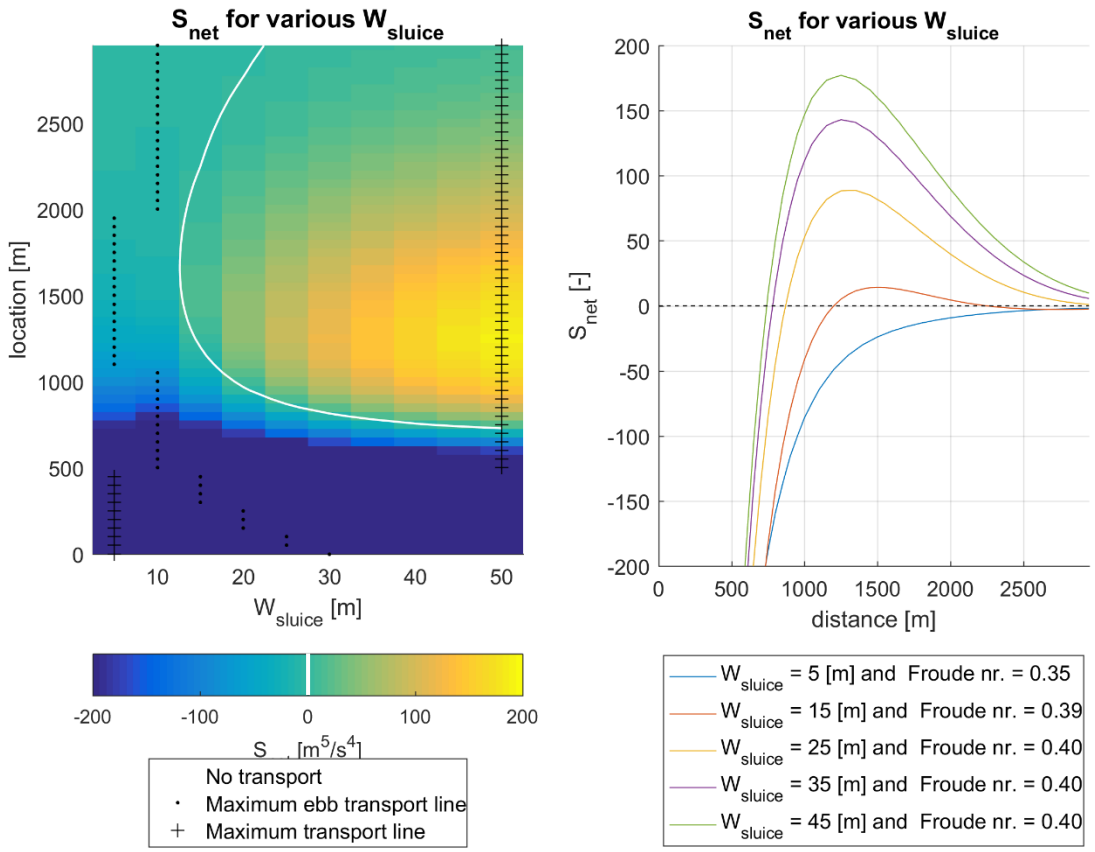

Figure 51 - Net transport along the channel length as function of width of the sluice.

Figure 51 shows that three situations for the tide-residual transport along the channel are possible. Which situation is present depends on the width of the sluice. These situations are depicted and elaborated on in Figure 52 - Figure 54.

Situation 1

Along the channel there are two transport areas. At the seaward side of the channel, net ebb transport is present and at the second half net flood transport.

What can be expected is that at the transition between these areas, erosion will take place.

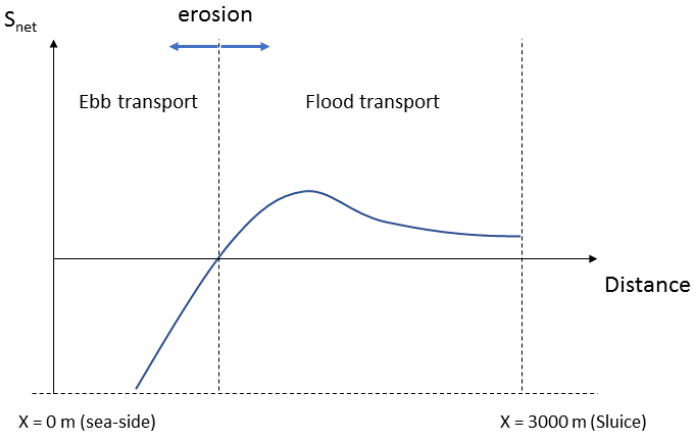

Figure 52 - Net effect of net sediment transport variation over the channel length; situation 1.

Situation 2

This situation comprises three transport areas. Two situations occur:

- Erosion at the transition from ebb to flood in the first half of the channel.
- Deposition at the second half of the channel. Although the net quantities at the landward side are marginal, there is an effect. However, the deposition is smaller than the erosion at the first half of the channel.

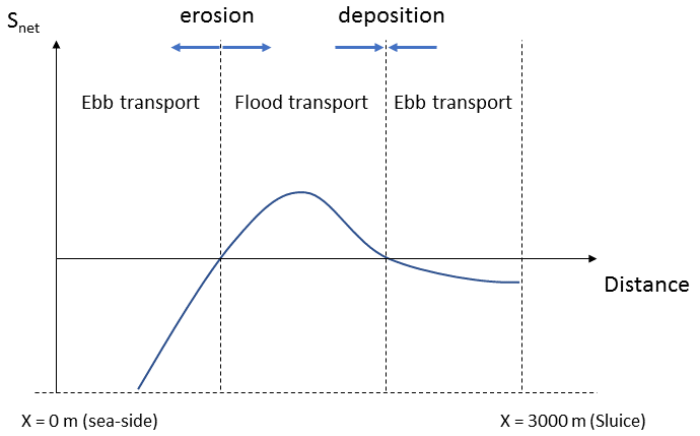

Figure 53 - Net effect of net sediment transport variation over the channel length; situation 2.

Situation 3

For the total length of the channel the tide-residual transport is in the ebb direction. Therefore no transitions are present in transport direction.

This is the preferred situation the tide-residual transport is in the ebb direction for the total length of the channel.

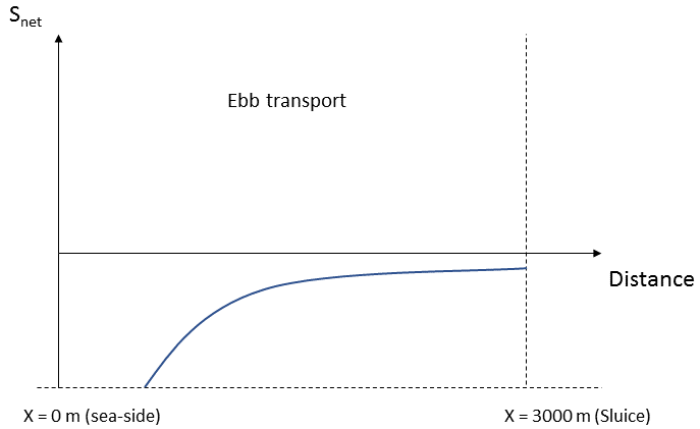

Figure 54 - Net effect of net sediment transport variation over the channel length; situation 3.

5.3.3 Equilibrium cross-section

The relation between the cross-sectional area and the tidal prism in section 4.6 is used to determine the required basin area. The described scenarios of the width of the sluice show that the water level variation in the basin (Z_{basin}) is affected by the width of the sluice (see Figure 46).

For the scenario $W_{sluice} = W_{channel}$ the basin area of 100 ha is not sufficient to create a tide-residual transport that is close to equilibrium along the channel.

However, for a narrow sluice (W_{sluice}= 5 m), the variation of Z_{basin} decreases, thus the tidal prism decreases. A phase lag between the water level in the channel and the basin is created. Although basin area is smaller than required for equilibrium, an equilibrium situation along the channel can be established by decreasing width of the sluice.

5.3.4 Conclusions

The effect of the variations in the width of the sluice is substantial. Especially over the second half of the channel the smaller widths of the sluice have a strong effect on water levels and current velocities. This results in larger variations in the tide-residual sediment transport along the channel. At the channel-end, the flood current velocities decrease with decreasing sluice width, whereas the ebb current velocities are marginally influenced.

For the situation of $W_{sluice} = W_{channel}$ = 50 m, the tide-residual transport for the second half of the channel is flood dominant, whereas the first part it is ebb dominant, see Figure 51.

For the situation of W_{sluice} = 5 m, the tide-residual transport is in ebb direction for the total length of the channel. At the channel-end/sluice the net transport is however marginal. For the last 500 m, there is e.g. no difference between W_{sluice} = 5 and W_{sluice} = 15 in the net transport quantities, see Figure 51 the right graph.

The transition between the presence of flood dominance and no flood dominance can be found at W_{sluice} = 10 m.

Summarizing:

- For larger sluice widths, a large tide-residual flood directed transport quantity is present at two third of the channel, at the landward.
- For smaller sluice widths, a tide-residual transport in ebb direction for the total length of the channel is established, although the nominal values are very small at the channel-end / sluice.
- The required basin area (A_{basin}) to create an equilibrium situation for the determined cross-section of the reference case can be smaller by decreasing width of the sluice (W_{sluice}).

5.4 Scenarios for a/h

The relative depth a/h is the second parameter for which the effect on the tide-residual transport is discussed is. It represents the depth (h) in relation to the tidal amplitude (a). For the lower values of a/h the channel is relatively deep. For the large values a/h, the channel is relatively shallow. All other parameters are remaining fixed. The parameter a/h has a large effect upon the celerity of the tidal wave, as it depends on the depth in the channel.

The width of the channel in red is depth depended, see Figure 55 and matches the hypsometric curve at the reference location Noordpolderzijl in blue. With varying values of a/h, the transition between flats and channel mildly changes.

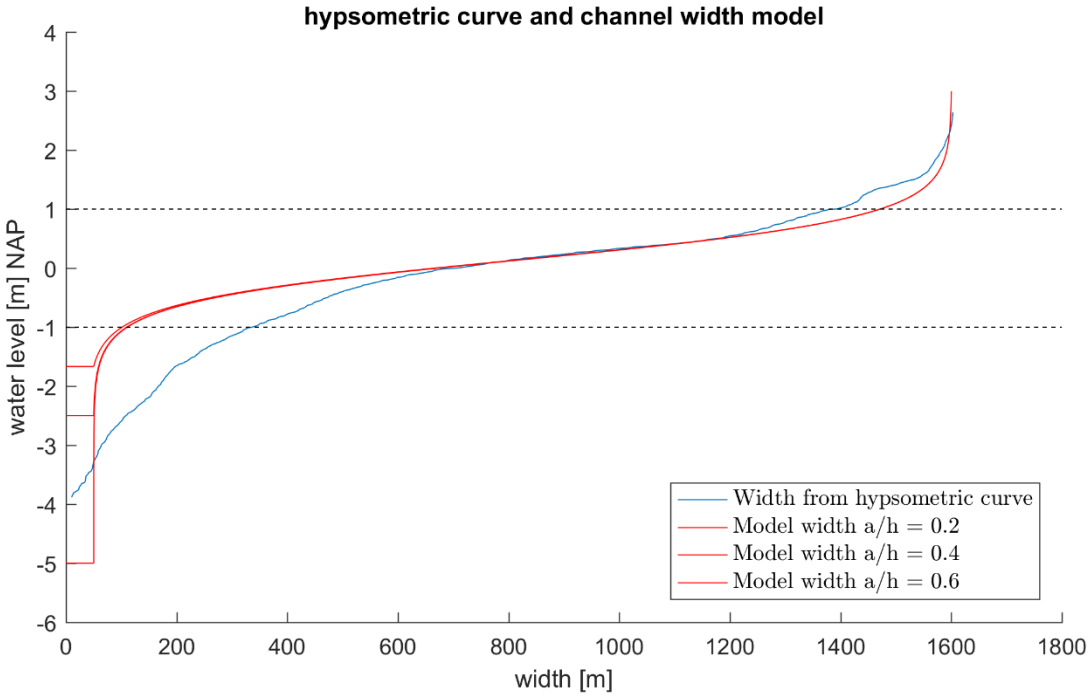

Figure 55 - Width as function of water level of the model for different values of a/h

In Table 11 the design parameters of the various scenarios for a/h are summarized. The only difference to the reference situation is that the relative depth is varied between 0.2 and 0.6. Values above 1 are not investigated, because these would result in dry situations during a tidal cycle. Even values for a/h < 0.1 are not recommended as supercritical flow regime can be present for values of a/h closer to one.

Table 11 - Defined values for the parameters for various scenarios of a/h.

parameters	value(s)	dimension
a/h	0.2 : 0.05 : 0.6	[-]
A_{basin}	100	[ha]
W_{sluice}	25	[m]
$W_{channel}$	50	[m]
$L_{channel}$	3000	[m]

5.4.1 Water levels & velocities

For the most extreme situation a/h = 0.6 the variability in velocities and water levels due to the tidal water level variation is shown in Figure 56. In this figure the two extreme scenarios for the relative depth are compared. Distortion of the water level signal due to the reduced current velocities for lower water levels can be observed at the channel-end in the situation of a/h = 0.6.

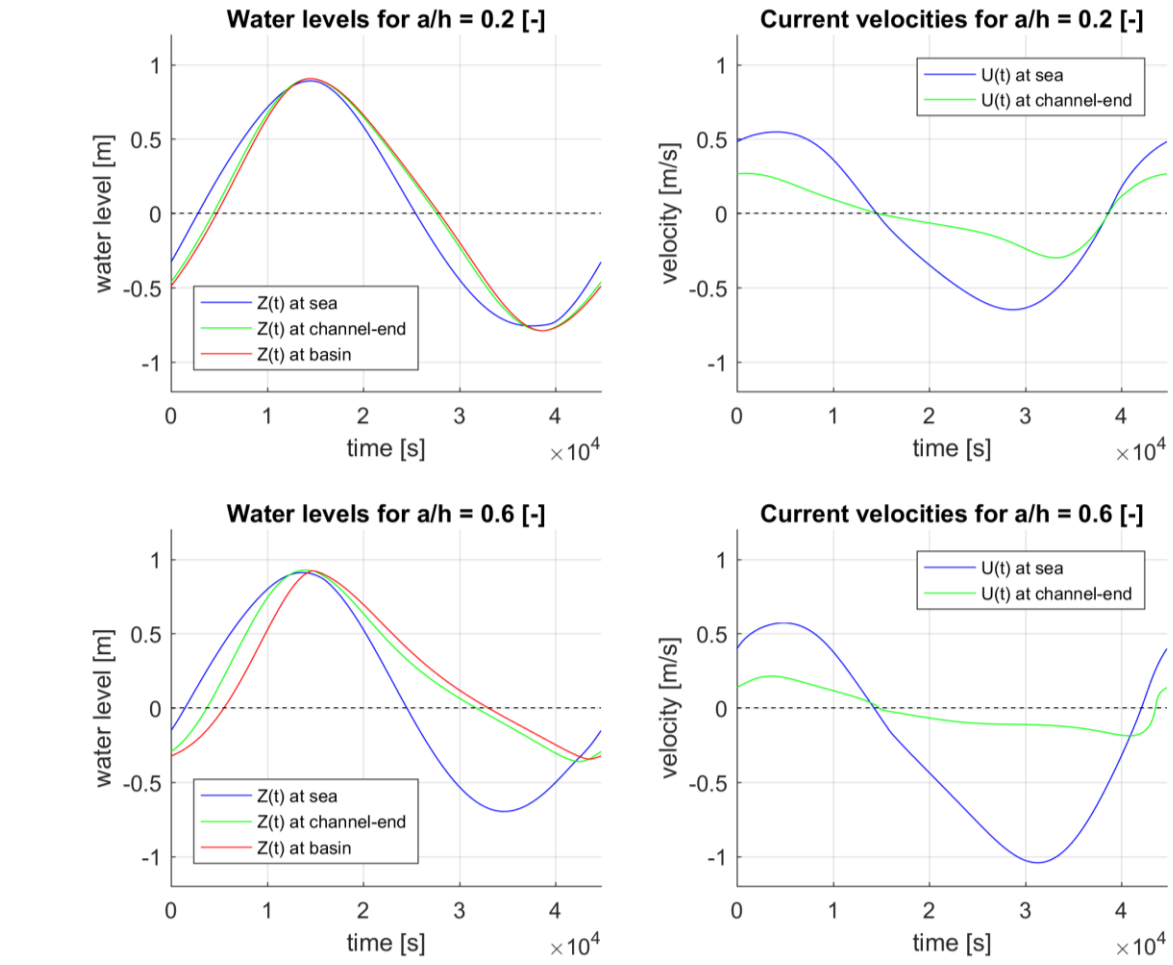

Figure 56 - Water levels and velocities for a/h = 0.2 and 0.6 [-]

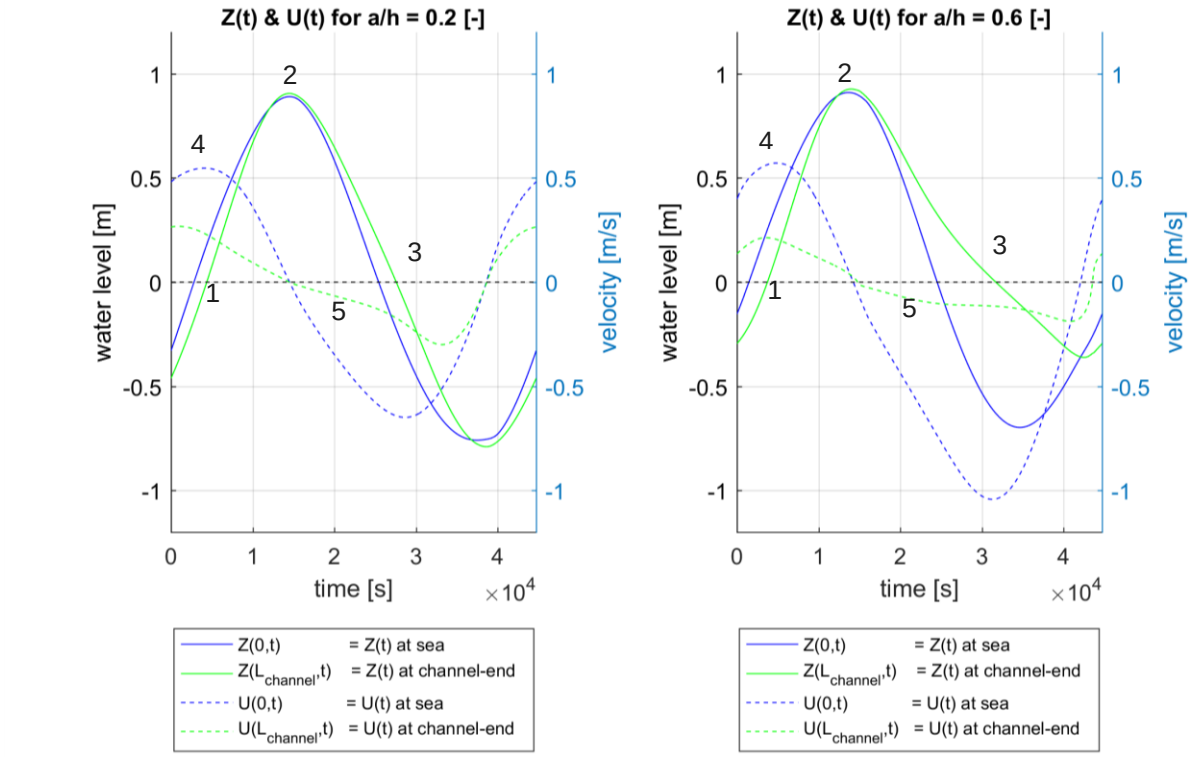

Figure 57 - Water levels and velocities combined for a/h = 0.2 and 0.6

The water levels and current velocities in Figure 56 and Figure 57 are indicated with numbers corresponding with the subsequent numbers. Some observations:

1. In the reference case the water levels mostly follow the seaward tidal forced signal with a/h = 0.6 there is a delay in between the locations for increasing water levels. A slope in the water level is present during rising tide between seaward boundary and the channel end.
2. At high water, the water levels at the seaward side and the channel-end are equal. Only the flushing basin has preserved its delay.
3. An increased shape shift between seaward side and channel-end is present for decreasing water levels. For the shallow situation; a/h = 0.6, the phase shift is increased. A large level difference is present for lower water levels.
4. Comparing the situations of a/h = 0.2 and a/h = 0.6, the velocity signal has changed dramatically. For a/h = 0.6, at seaward side, a strong velocity asymmetry to ebb dominant is present. The maximum ebb velocities are 2 times larger than the flood velocities. The time of ebb and flood flow also changed in ebb direction. Whereas for a/h = 0.2 the flood and ebb current velocities are almost equal, for a/h = 0.6 the flood current velocities are smaller than the ebb current velocities.
5. The velocities at the channel-end and sluice are also strongly deformed. The deformed behaviour is the effect of the flushing basin. There is an increased water level difference between the flushing basin and the seaward boundary.

Figure 58 gives an overview for the lowest and highest values of the velocities in the channel for two scenarios. All deformations described above can be seen. The intensities of the colours increase, which indicate larger current velocities. In general:

- The variability of the current velocities is much higher for shallower depths; a/h = 0.6.
- The much higher current velocities at the seaward side decrease faster over the channel for a/h = 0.6. Especially the ebb current velocities are influenced.
- The ebb period is increased for shallower depths; a/h = 0.6. This can be observed by looking at the time between the white lines.

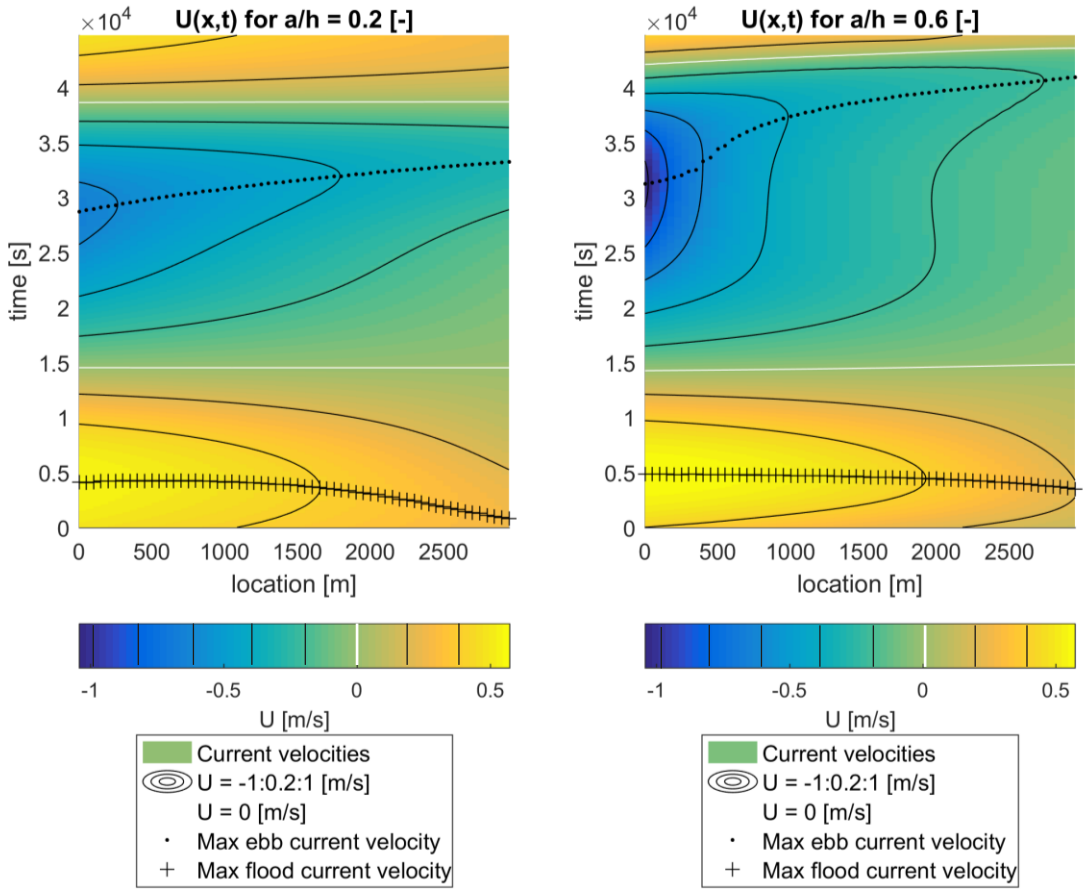

Figure 58 - Current velocities for a/h = 0.2 and 0.6 [-]

For each location, the maximum and minimum current velocities can be determined. These are indicated by a plus sign: '+' and a dot: '.' in Figure 58 and Figure 59. Comparing the situations of a/h = 0.2 with a/h = 0.6, the maximum velocity lines deviate from each other. The maximum velocities for the case of a/h = 0.6 are larger. For the ebb flow the difference is larger than for flood flow.

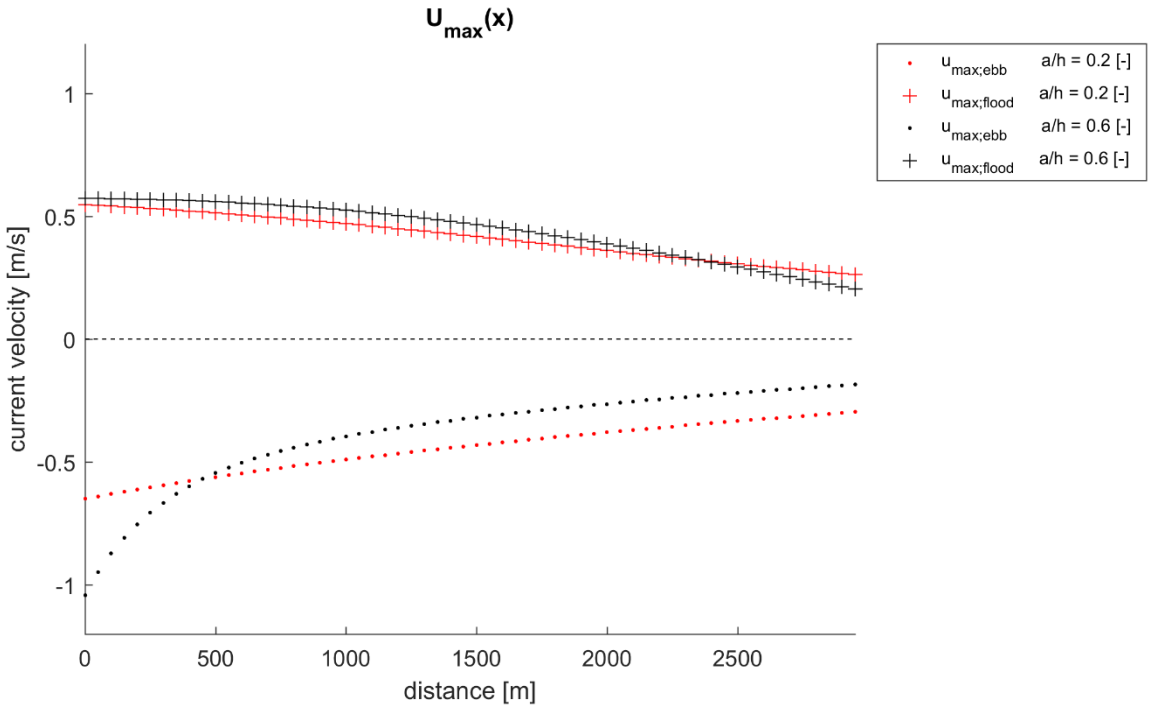

Figure 59 - Maximum and minimum current velocities for a/h = 0.2 and a/h = 0.6

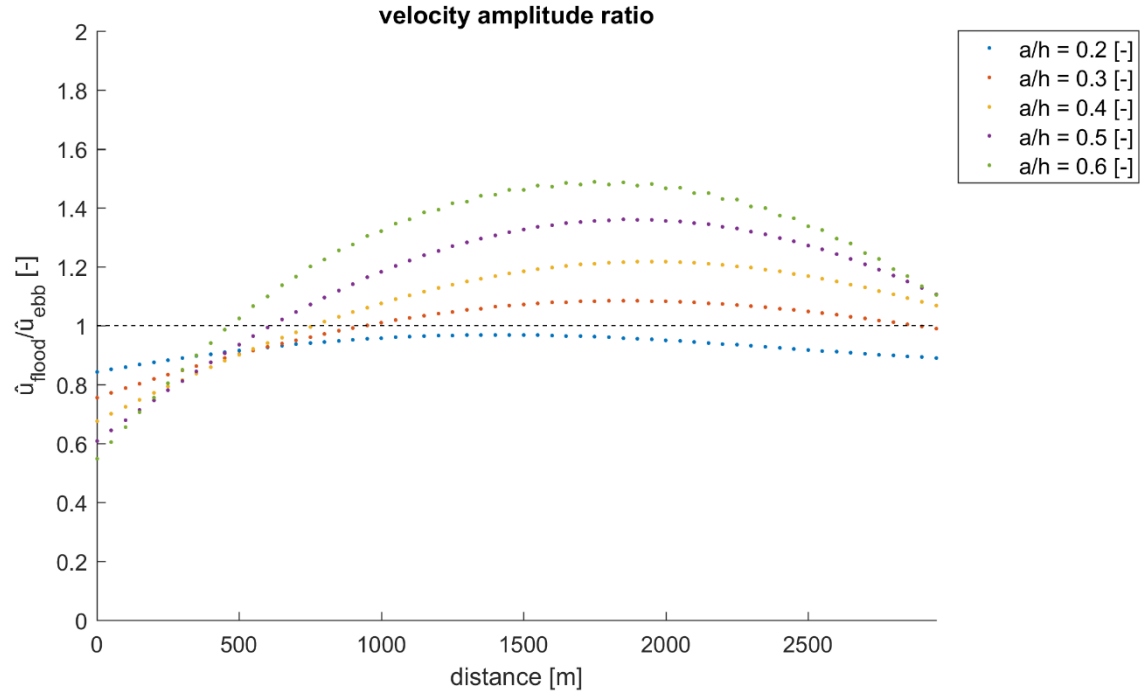

Figure 60 - Velocity amplitude ratio for varying a/h

Comparing the ebb and flood velocities a first indication for the dominant sediment direction can be made. In Figure 60 the velocity amplitude is visualized. For all values of the relative depth:

- the seaward side is ebb dominant. For decreasing depths, the ebb -dominance decreases. The variation of the maximum current velocities is large, because the current velocities depend on the relative depth.
- From the seaward-end to the channel-end the ratio increases first and thereafter decreases, for all scenarios.

For a shallow channel (large values of a/h) the variability of the ratio is large. For a deep channel (small values of a/h) the variability is low. An increase of depth results in an increase of flood dominance along the second half of the channel and an increase of ebb-dominance at the seaward side.

5.4.2 Sediment Transport

The sediment transport varies much more than the velocities, because the transport Is proportional to the fifth order to the velocity. In Figure 61 the two extreme scenarios for the relative depth are illustrated (a/h = 0.2 and a/h = 0.6). At the channel-end for both cases the transport fluxes are low because the velocities are low.

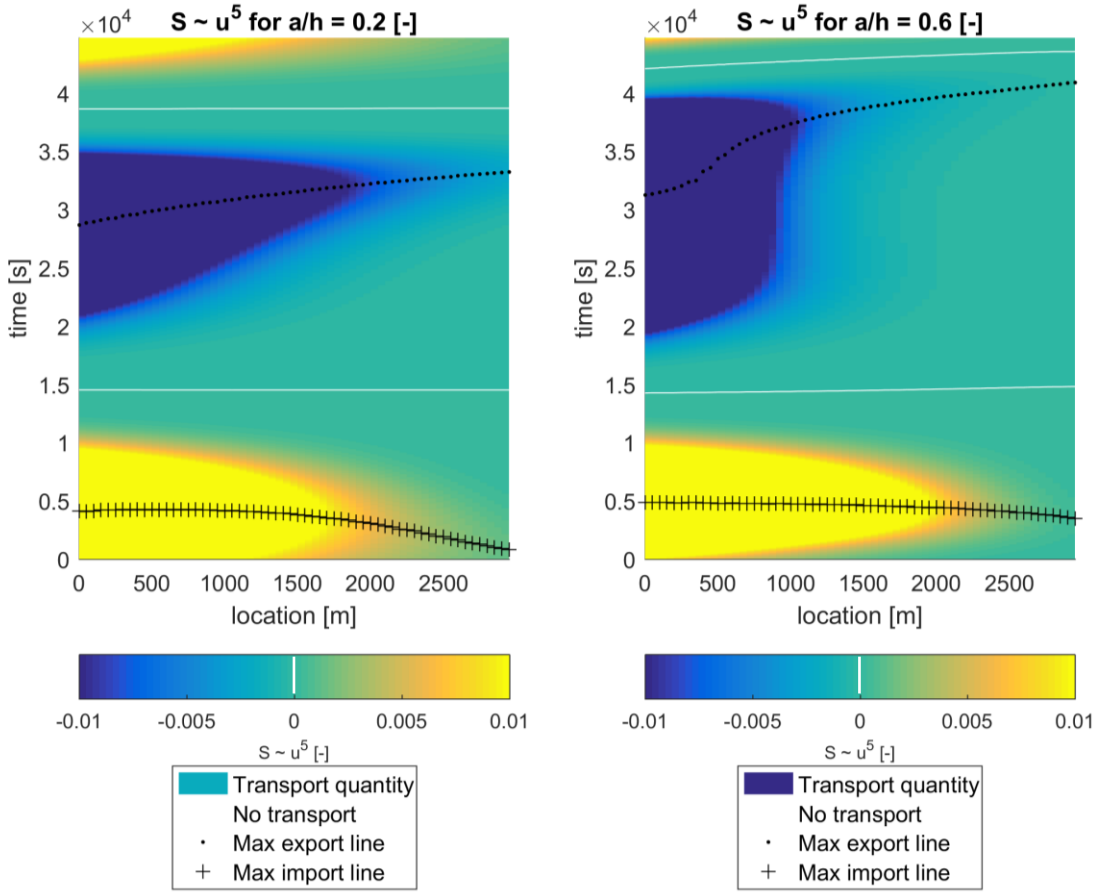

Figure 61 - Transport quantity as function of time

Figure 62 presents the sediment transport at the channel-end in one tidal period for three scenarios of the relative depth. The largest ebb directed flux is given by a large depth a/h = 0.2. For this situation the tide-residual transport is in ebb direction, whereas for the other values of a/h it is flood directed.

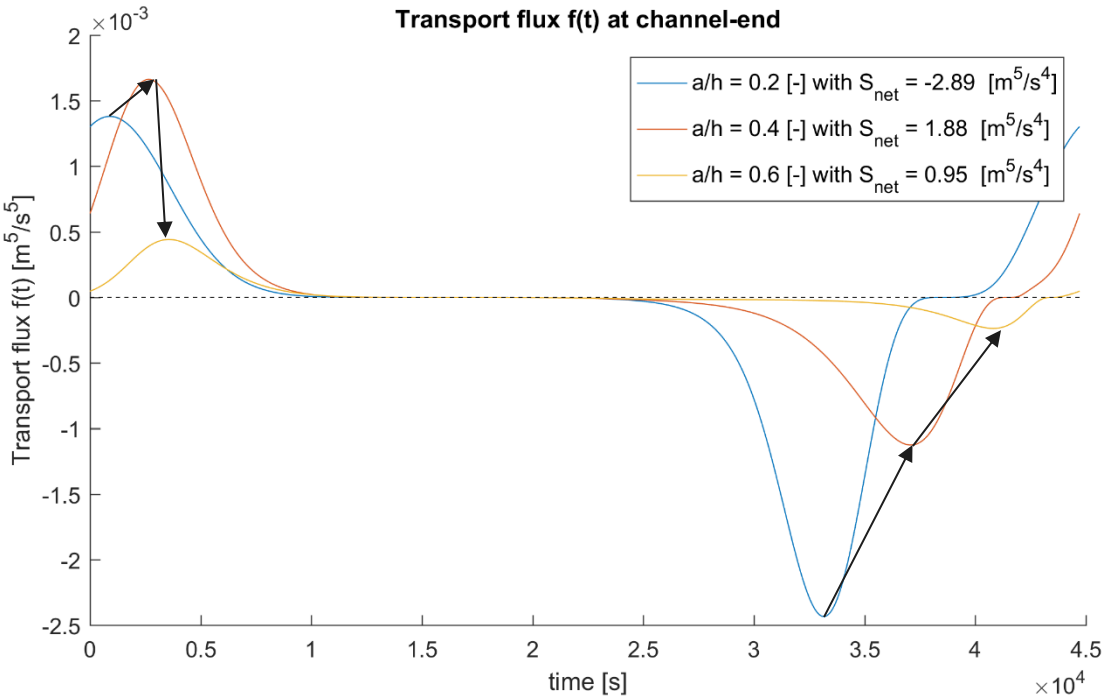

Figure 62 - Transport at the end of the channel as function of varying a/h

For the different values of a/h the tide-residual transport for all channel locations has been determined and visualized in Figure 63. Conclusions:

- there is a large spread in the net transport as function of location and varying values of a/h. Both maxima for, ebb- and flood-transport, are dependent on location along the channel and a/h, depicted with a dot; '.' and plus; '+' sign.
- For values of a/h larger than 0.2 the variability of the net transport over the length of the channel is large. Especially at the seaward boundary the velocities are large. This is not fully visualized as it is out of the colour range and therefore all values of S_{net} < -200 have the same colour.
- For a/h = 0.2, the net transport is in ebb direction over the whole channel. For a/h > 0.2 there is a transition between transport from ebb to flood dominant in channel end direction. This transition is about half channel length for a/h = 0.2. For increasing a/h the transitions ('line of no transport'), moves in seaward direction.
- The variability is larger for larger values of a/h. As the net transport quantities increase for increasing values of a/h, a larger sedimentation rate for a longer part of the channel is expected.

When comparing Figure 63 with Figure 51 for the variations of W_{sluice}, the same effect for the tide-residual transport along the channel can be observed. The effects of the various transport lines are in resemblance with the situations 1 and 3 described in section 5.3.2. For all scenarios a subcritical flow regime is present, because for these scenarios all Froude numbers are smaller than one. A smaller difference between the wave celerity and the current velocities for smaller depths is visible.

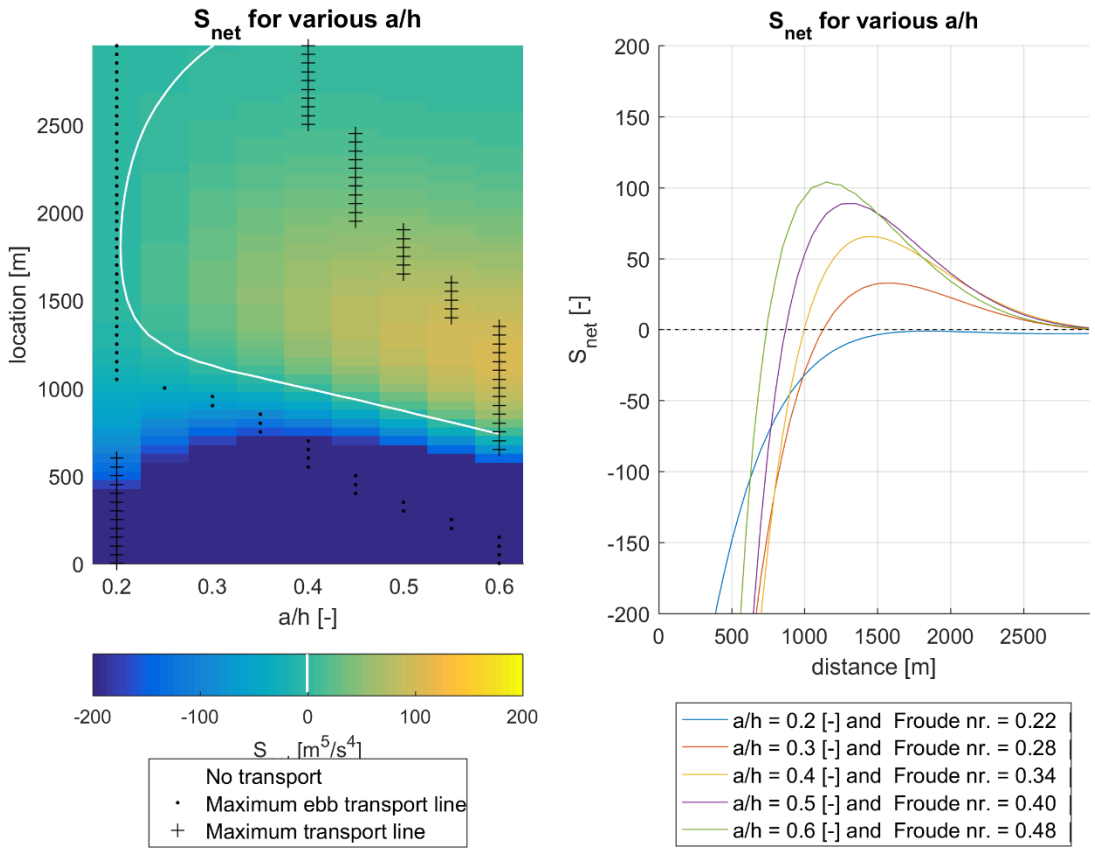

Figure 63 - Net transport as function of varying a/h.

5.4.3 Conclusions

The variation of the relative depth strongly affects the distribution of water levels and current velocities over the length of the channel. The system is ebb dominant at the seaward side and the various scenarios for the relative depth do not affect the dominant sediment direction at the seaward side. The variations have led to an increasing ebb- dominance for decreasing a/h ratios, as is illustrated in Figure 63.

An optimum can be found around a/h = 0.2, when considering the total length of the channel. For a deeper system with a/h < 0.2, the total domain has an ebb dominant behaviour. For shallower channels flood dominance is present at the landward side of the spatial domain, see Figure 63. For decreasing depth (so an; increase in the value of a/h), the location of the transition between ebb and flood directed tide-residual sediment transport moves in seaward direction.

Note:The hypsometric curve determines the depth profile and this has strong implications for the initial dominant sediment transport behaviour of the channel. For this study, the depth-width profile of the reference situation of Noordpolderzijl is chosen and scenarios for different depth-width profile have not been executed.

5.5 Scenarios for A_{basin}

In this section the flushing basin area is the parameter for which various scenarios are discussed. The flushing basin area influences the boundary condition at the channel-end / sluice. With varying basin area, the basin water levels have a different behaviour over time compared to the water levels in the channel and this influences the water levels in the channel. The area of the flushing basin represents the amount of storage capacity. As the amount of capacity increases, an increased phase lag and amplitude reduction of the water levels of the flushing basin compared to the channel is expected.

The various scenarios range from very small values, with minor effects to the water levels, velocities and sediment transport, to large values and effects. All other parameters are kept constant. In Table 12 an overview of the parameters and their values is presented. In the previous sections, a flushing basin of 100 ha is used as a reference value for A_{basin}. The scenarios in this chapter are smaller and larger.

Table 12 - Defined values for the parameters for scenarios of A_{basin}

Parameter	value(s)	dimension
A_{basin}	30 : 30 : 300	[ha]
a/h	0.5	[-]
W_{sluice}	25	[m]
$W_{channel}$	50	[m]
$L_{channel}$	3000	[m]

5.5.1 Water levels & velocities

For the two most extreme scenarios, the water levels and current velocities are illustrated in Figure 64. A strong change in both quantities can be observed as result of the difference in A_{basin}. For the scenario of A_{basin} = 30 ha there is no phase lag in the water levels between the channel-end and the flushing basin. For the scenario of A_{basin} = 300 ha there is a large phase lag between the channel-end and the flushing basin. Considering a basin area of 300 ha, the water level variations of the basin are reduced in range, compared to the situation of a flushing basin of 30 ha. Although the water level in the basin are reduced in range, the larger differences between the water level in the basin and the channel result in larger velocities at the sluice for the large basin (channel-end in Figure 64, the bottom right panel).

The current velocities at the channel-end over time for the situation with A_{basin} = 30 ha. and A_{basin} = 300 ha. for the flood and ebb have almost the same magnitude. There is a difference in the distribution of the velocities over time. For a small flushing basin, the current velocities are slowly decreasing after maximum flood currents until maximum ebb currents and strongly increasing thereafter. The larger flushing basin has strong velocity changes for both slack water periods. For both tidal periods, the velocities are enlarged.

In the situation of a flushing basin of 300 ha. there is a large gradient (water level difference at a certain time) in water levels between the different locations along the channel.

When the basin level is zero (red line), the current velocities are maximum for all locations. When the basin water level has reached its maximum (around t =200.000 s), the current velocities at the channel end and sluice are zero again. However, the current velocities at the seaward boundary are already in ebb tidal direction at that time. There is a direct relation between these two quantities. This relation is influenced by the width of the sluice and the flushing basin area.

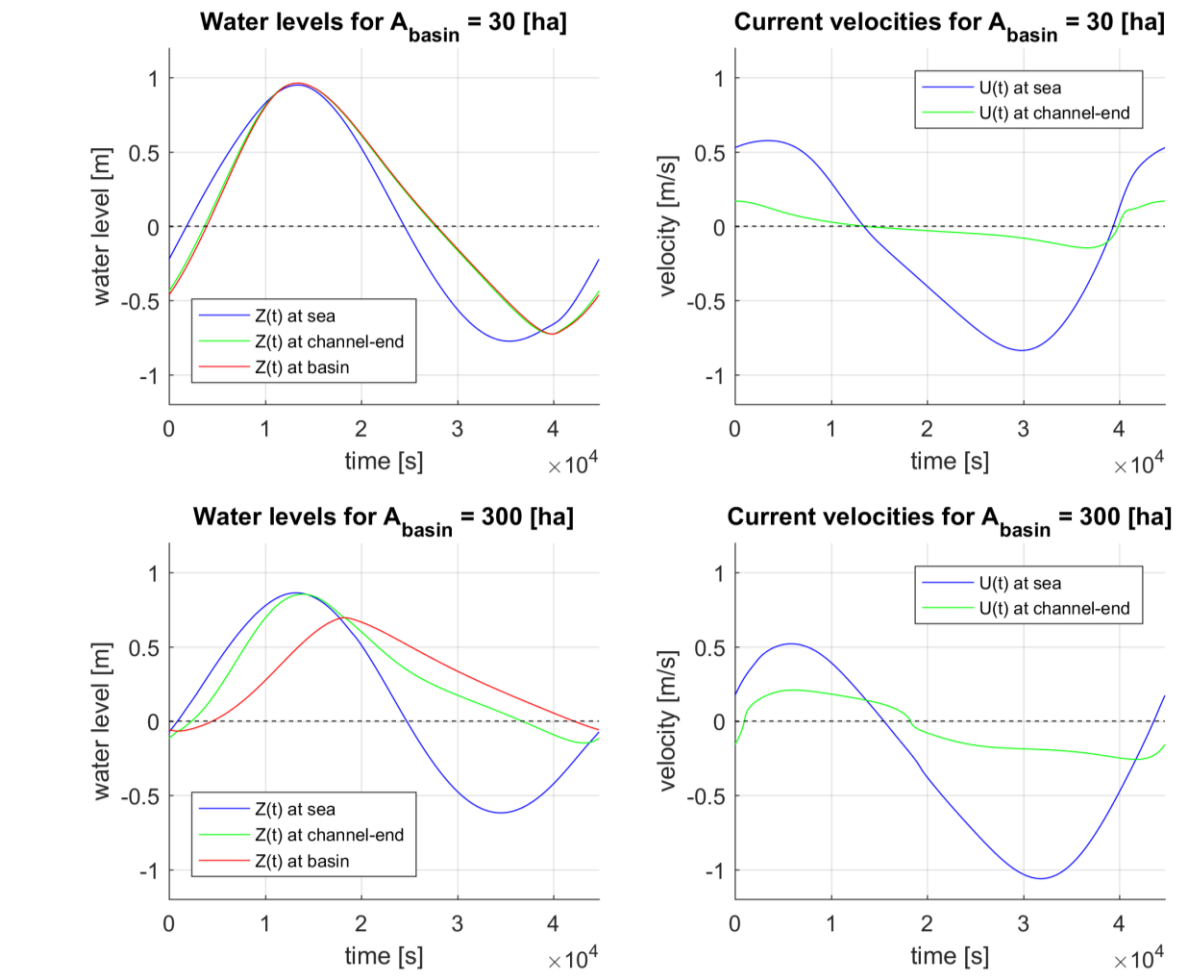

Figure 64 - Water levels and discharges for 30 and 300 ha.

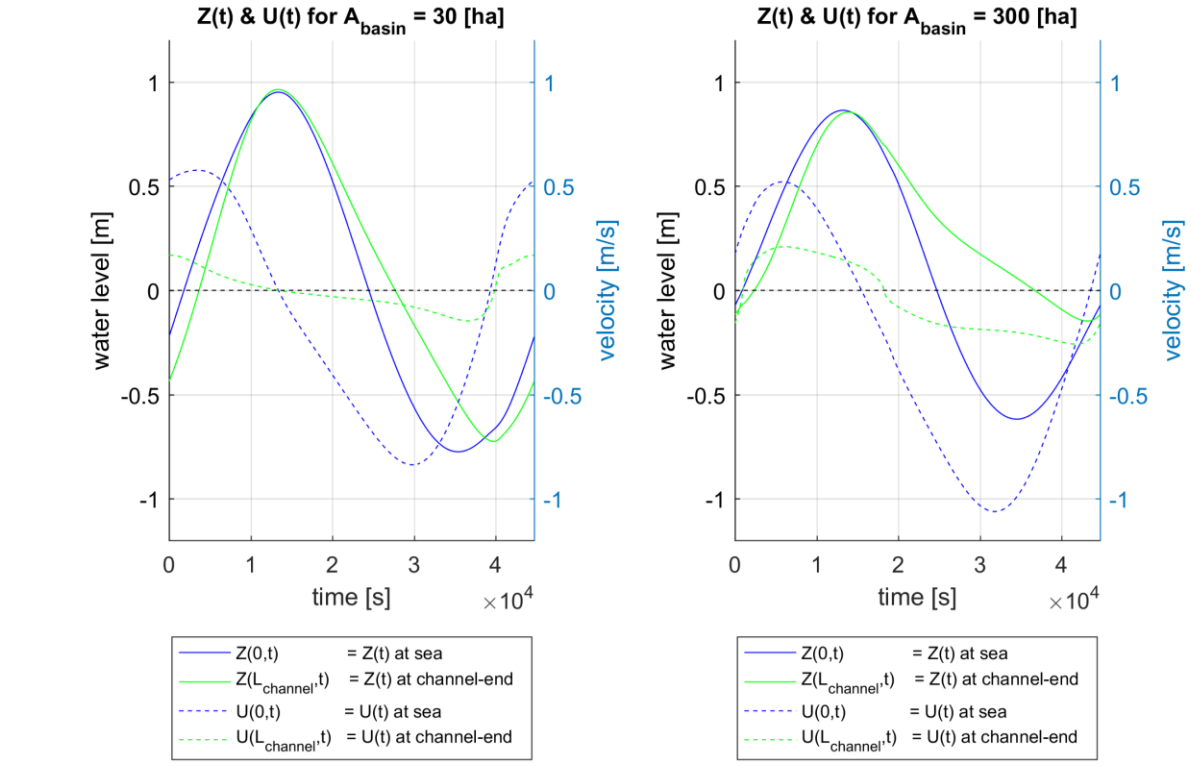

Figure 65 - Water levels; Z(t) and current velocities; U(t), combined for the situation A_{basin} = 30 ha and A_{basin} = 300 ha

In Figure 66 an overview of the current velocities over time and space is given. Comparing the two scenarios, one can observe:

1. a larger delay of the maximum ebb current velocities in channel-end direction along the channel for the flushing basin of 300 ha, depicted by the black dots.
2. that the maximum flood current velocities for all locations along the channel for a flushing basin area of 300 ha, occur at the same time.
3. that the flood current velocities change overall less than the ebb current velocities when varying the flushing basin area. The ebb current velocities at the first part of the channel from sea change much faster for the highest value of the flushing basin. This results in smaller variabilities of the current velocities in the rest of the domain for the large basin area. The transport is therefore also less variable for larger flushing basin areas.

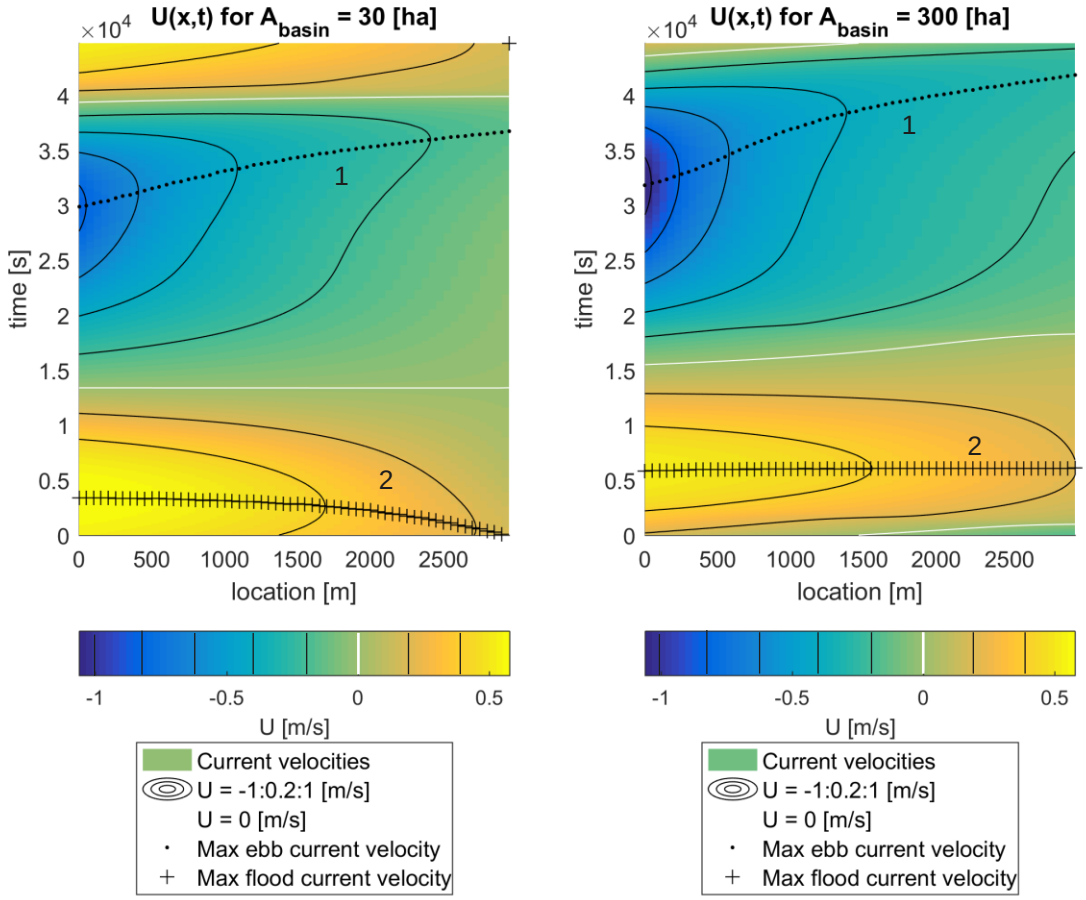

Figure 66 - Current velocities for A_{basin} = 30 ha and A_{basin} = 300 ha

The variability along the channel is illustrated in Figure 67. By comparing the maximum (flood) and minimum (ebb) current velocities at different locations, one can observe smaller maxima than minima at the seaward side of the channel. This has implications for the net transport direction at that location. At the channel-end the maximum ebb current velocities are also larger than the maximum flood current velocities.

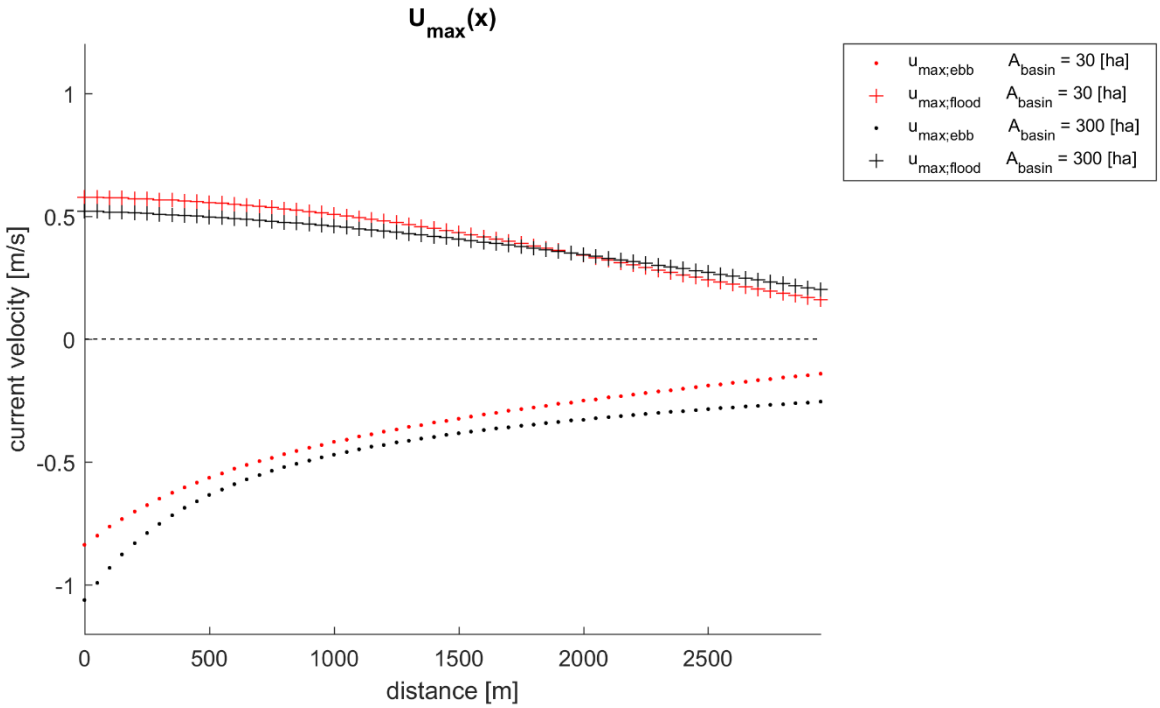

Figure 67 - Maximum and minimum current velocities along the channel, for A_{basin} = 300 ha

For the maximum and minimum current velocities (peak velocities), the ratio is illustrated as function of the location along the channel for various scenarios of the flushing basin area in Figure 68. This ratio of the peak velocities is an indication for the tide-residual transport direction. A reduction in flood dominant transport along the second channel length is observed for smaller basin areas. A change to total ebb-dominance over the total length of the channel cannot be obtained, indicated with the black arrow in Figure 68.

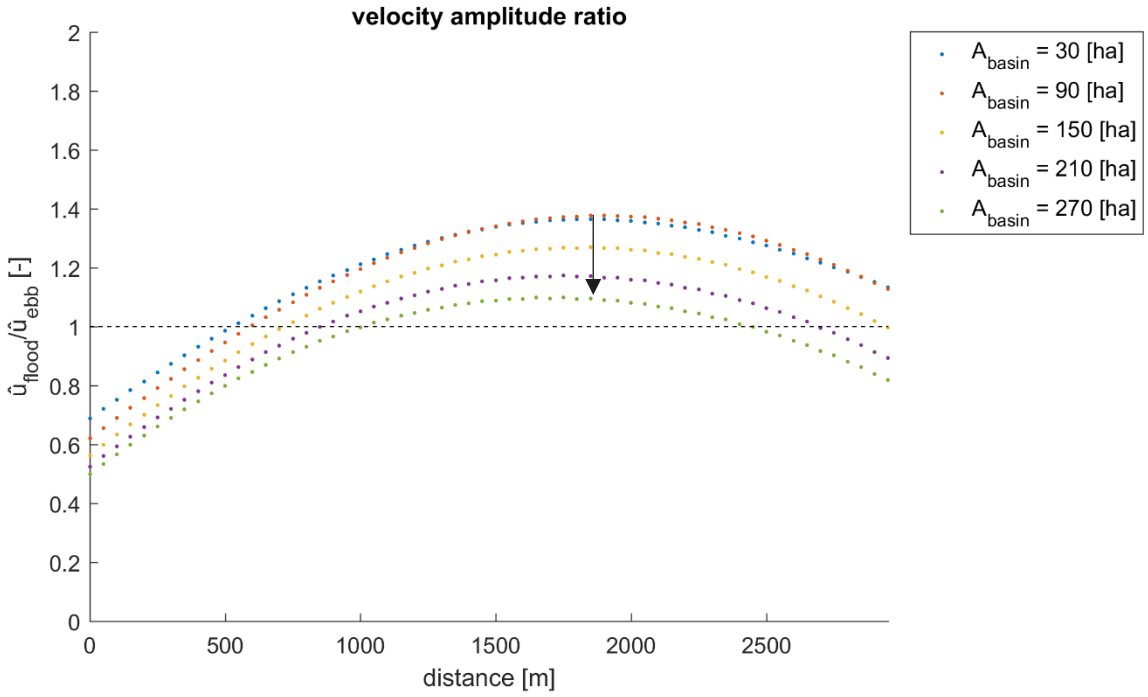

Figure 68 - Velocity amplitude ratio for varying A_{basin}

Conclusion: when increasing the flushing basin, a relative increase of maximum ebb current velocities over the whole domain is present. The effect on the sediment transport is elaborated in the next section.

5.5.2 Sediment Transport

For each value of the basin area the transport as function of place and time can be determined; S(x,t). For the smallest and largest value of basin area; A_{basin} = 300 ha, the transport is illustrated in Figure 69. At the seaward side the largest transport quantities are around t ≈ 30000 s. Integration over time for this location, implies a strong net ebb directed transport. In the rest of the domain the transport quantities are relatively low (green).

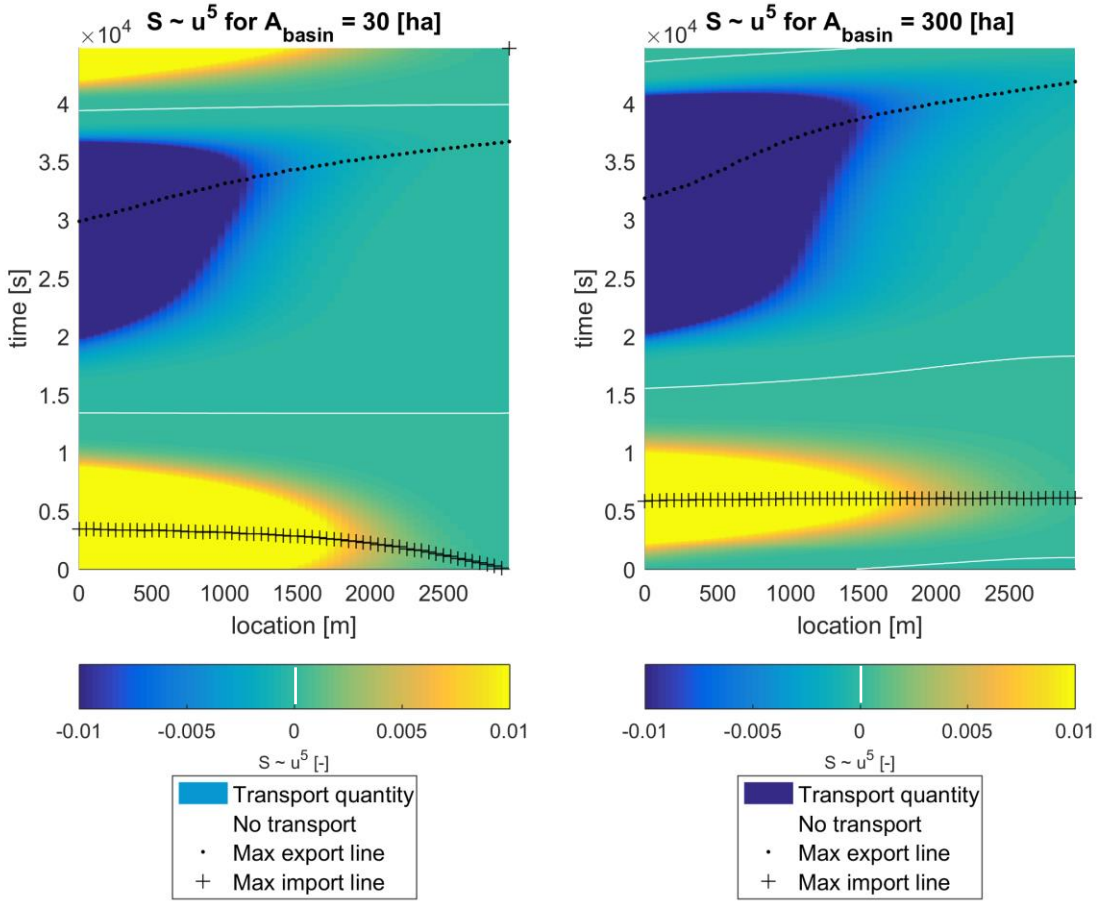

Figure 69 - Transport as function of time and space; S(x,t) for A_{basin} = 30 ha and 300 ha

The net transport direction over the whole domain is important, especially the end of the channel. In Figure 70, the transport is illustrated for the different flushing basin areas. Indicated with a number. It can be observed that:

1. First, the flood transport flux increased as result of an increase of the flushing basins area. The maximum ebb transport flux is also increases by a same amount.
2. Secondly, the flood transport flux decreases, whereas the ebb transport increases further for increased A_{basin}.

The tide-residual transport for the channel-end can therefore considered as ebb dominant for higher values of A_{basin}.

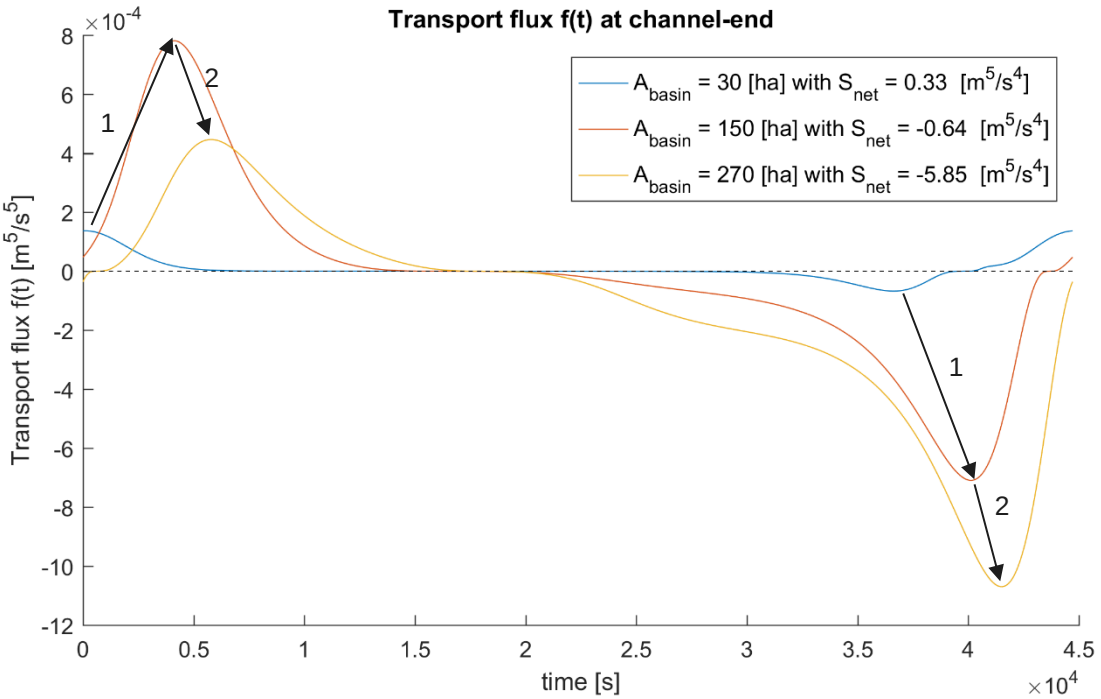

Figure 70 - Transport at the end of the channel for varying A_{basin}.

The above graph can be made for all locations in the channel. Integration of the tide-residual transport over a tidal period for each location and for each value of the varying flushing basin area results in the net transport rate, see Figure 71. In this figure flood dominant transport is observed in the second part of the channel close to the flushing basin above the white line. Ebb dominated transport occurs in the seaward side of the channel below the white line in the graph.

The maximum tide-residual transport in the ebb direction (the negative values) can be obtained by the largest basin area: A_{basin} = 300 ha (black dots). Moreover, the variability of the transport quantities over the second part of the channel decreases with larger basin areas. The chosen colour range visualises the transport differences in the second part of the channel. The first part, where the largest negative transports are present are not visible in the dark blue part. The maximum transport takes place at the seaward side of the channel. The minimum transport occurs for the smallest basin area.

The right panel in Figure 71 illustrates for various values of A_{basin} the tide-residual transport. This is the highest at the seaward side and the lowest at the channel-end. For the other locations the tide-residual transport changes from a maximum-ebb directed at the seaward side, to a maximum-flood directed in the middle and to zero again at the landward side.

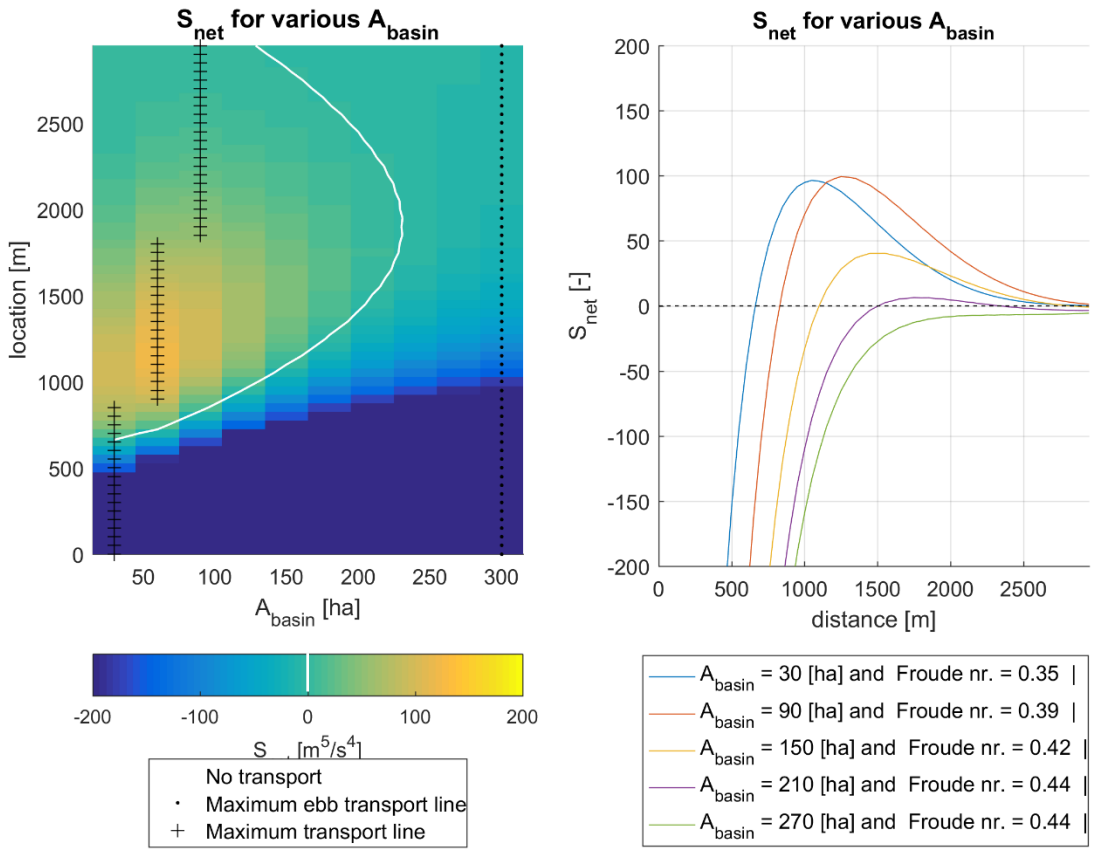

Figure 71 - Net transport quantities for different flushing basin areas

Like the parameter W_{sluice} and a/h, the design parameter A_{basin} needs a minimum value to create a tide-residual transport in seaward direction for the total length of the channel. A minimum basin area: A_{basin} = 240 ha is required as can be seen in Figure 71, this is right-side of the white line. For A_{basin} < 90 ha, the tide-residual transport in flood direction increases. For A_{basin} > 90 ha the tide-residual transport decreases.

5.5.3 Equilibrium cross-section

In section 4.6 the equation for the equilibrium cross-sectional area – tidal prism relation, the required basin area is determined for the reference situation and a channel width of 50 m. The required basin area is about 270 ha to create an equilibrium stable channel. Figure 71 shows that with $A_{basin} = 240$ ha the tide-residual transport along the channel is minimal. It confirms the determined basin area in section 4.6 of A_{basin} = 280 ha.

5.5.4 Conclusion

For the parameter A_{basin} with a variable channel width over height, including tidal flats and no variabilities in longitudinal direction, the net transport increases in ebb direction with increasing flushing basin area, see Figure 71.

For A_{basin} = 30 ha, the second part of the channel, the net transport is in flood dominant direction. For A_{basin} = 300 ha, there is an ebb dominant net sediment transport over the total channel length present.

In conclusion, the net transport changes from being flood dominant to ebb dominant, with increasing basin area. For an ebb-dominant behaviour along the total length of the channel, a minimum basin area can be assigned: 240 ha.

The determined required flushing basin area creating an in the long-term equilibrium channel for the reference situation of Noordpolderzijl is in good resemblance with the in this section determined value of 240 ha. Much smaller or larger flushing basins areas than 240 ha, create an instable channel. The siltation or erosion in the channel would be enlarged.

5.6 Combined scenarios

In the above paragraphs 5.1 – 5.5 scenarios of the individual key design parameters of a tidal flushing basin system have been compared. In Table 13, the results of these variations are summarized.

Table 13 - Overview effect of variations on the tide-residual transport

parameters	values smallest : largest	dimensions	A decrease of the tide-residual transport for:
A_{basin}	100 : 300	[ha]	Larger values
a/h	0.2 : 0.6	[-]	Lower values
W_{sluice}	5.0 : 50	[m]	Lower values

The analysis so far has given insight in the behaviour of the system for individual parameters. In the next part, the combination of the three key parameters is elaborated, to comprehend the combined effect of changing parameters. The quantity that is used for the comparison is the integrated transport quantity given by the velocity in the fifth order. The results of these variations are visualized in Figure 72. These results are discussed in the next section.

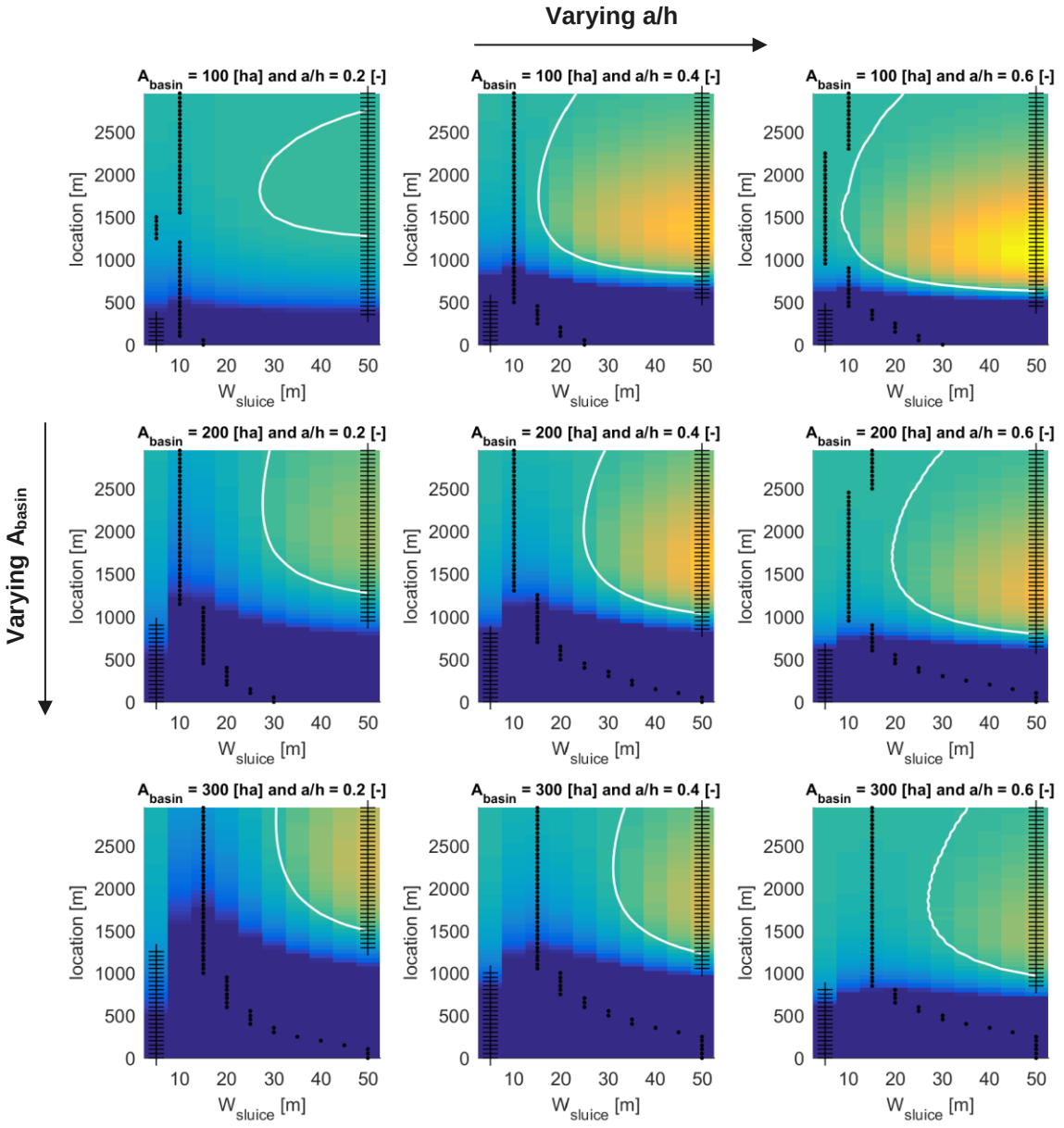

Figure 72 - Combined variations: from left to right: changing a/h. Top to bottom: changing A_{basin}. Variation in W_{sluice} in all plots.

Each of the nine figures in Figure 72 visualizes the integrated transport along the channel for each value of the sluice width; W_{sluice}. The colours indicate the quantity of transport from -200 – 200 [m^5/s^4]. The three indicators, black dots, white line and black plus represents the locations at which maximum ebb transport, zero transport and maximum flood transport takes place.

The first figure in Figure 72 represents the situation with a flushing basin of 100 ha, relative depth (a/h) of 0.2 and variable sluice width. The other figures in right direction have a decreasing relative depth. In the downward direction, the flushing basin area increases.

5.6.1 Combination 1: W_{sluice} – A_{basin}

As already been discussed in section 5.3, the variation of width of the sluice results in a strong variation of the flow. For the lowest values of the sluice width the integrated transport over the total channel length has a net ebb dominant direction for most of the variations. The combined variations depicted in Figure 72 are discussed in the next section considering the vertical direction.

- a/h = 0.2; first column of Figure 72

For the upper left figure, representing the situation with a flushing basin of 100 ha, relative depth (a/h) of 0.2 and variable sluice width, the variability over the second half of the channel is low as can be seen by the almost even colour (green). At the first half of the channel; 0 – 1500 m, there is a strong variance. As at the seaward boundary the current velocities and asymmetry are the highest, this location has the largest transport quantities. With increasing basin area: the net transport is intensified. Larger transport in ebb direction results from increasing basin area. The largest ebb dominant part results from a large basin area with a sluice width of 15 m should be chosen.

- a/h = 0.4; second column of Figure 72

The second column represents the situation with a relative depth of 0.4. The response to a change in basins area a sluice width differs from the first column. For the smallest basin area of 100 ha the variability in transport for different values of the sluice width, is high. Also, the boundary of zero transport shifts to the left. Whereas this boundary for a/h = 0.2 for all values of the basin area lies about 30 m, this boundary lies at 15 m.

For an increasing basin area in case of a/h = 0.4 the boundary of zero transport shifts to higher values of the sluice width. Total ebb-dominant behaviour occurs already at a sluice width of 30 m. With increasing basin areas, the variability over the second half of the channel, decreases. The optimum, in the situation with the largest ebb dominant transport quantity, considering the second half of the channel, shifts from 10 to 15 m.

- a/h = 0.6; third column of Figure 72

The last column in Figure 72 deals with the situations with a relatively shallow channel. The largest variability can be observed for small values of the flushing basin. The second part of the channel is flood dominant for all values of the sluice width, apart from the smallest value of W_{sluice} = 5 m. This minimum required sluice width to create an ebb-dominant channel, increases with for larger flushing basins.

The same effect of decreasing variability of the transport quantities over the channel as for a/h = 0.4, can be observed. This effect is however stronger for this value of the relative depth. For relatively deep situation; a/h = 0.2 there is an opposite effect.

5.6.2 Combination 2: W_{sluice} – a/h

The effect of decreasing relative depth, i.e. the increase of the depth of the shallow channel can be observed when one looks from left to right in Figure 72.

- A_{basin} = 100 ha; first row of Figure 72

For a small basin area (first row of Figure 72) the decreased relative depth results in a strong variability of the transport quantities for larger sluice widths. For A_{basin} < 100 ha and lower values of the sluice width a tide-residual transport in the flood direction is observed over the second half of the channel. The middle graph of

the first row, has the largest tide residual transport in the ebb direction. Low basin areas are therefore most effective in intermediate relative depth (a/h = 0.4).s

- A_{basin} = 200 ha; second row of Figure 72

When considering: A_{basin} = 200 ha and W_{sluice} < 20 m the deeper channels result in larger tide-residual transports in the ebb direction. For W_{sluice} > 20 m, the tide-residual flood transport is for intermediate channel depths largest. For W_{sluice} > 20 m and the deepest channel depths the flood transport is the smallest.

- A_{basin} = 300 ha; third row of Figure 72

For A_{basin} = 300 ha. and W_{sluice} < 25 m, the maximum tide-residual transport in the ebb direction occurs for deeper channels.

The tide-residual transport in the flood direction is maximum for deeper channels. The part with flood transport is however smaller for deeper channels. This is an opposite effect to that of a small flushing basin A_{basin} = 100 ha.

5.6.3 Combination 3: A_{basin} – a/h

The most promising two sluice widths, considering the net sediment transport are: W_{sluice} = 10 and 15 m. These two widths are therefore used as a basis for the next combined variations, visualized in Figure 74 and Figure 73.

- W_{sluice} = 10 m

For W_{sluice} = 10 m, the net transport quantities are different. The situation with the smallest basin area combined with the smallest relative depth; A_{basin} = 100 ha, a/h = 0.6, result in almost net ebb-dominant transport over the total length of the channel. The rest of the situations are all ebb dominant along the total domain. The largest relative effect accomplished by the largest basin.

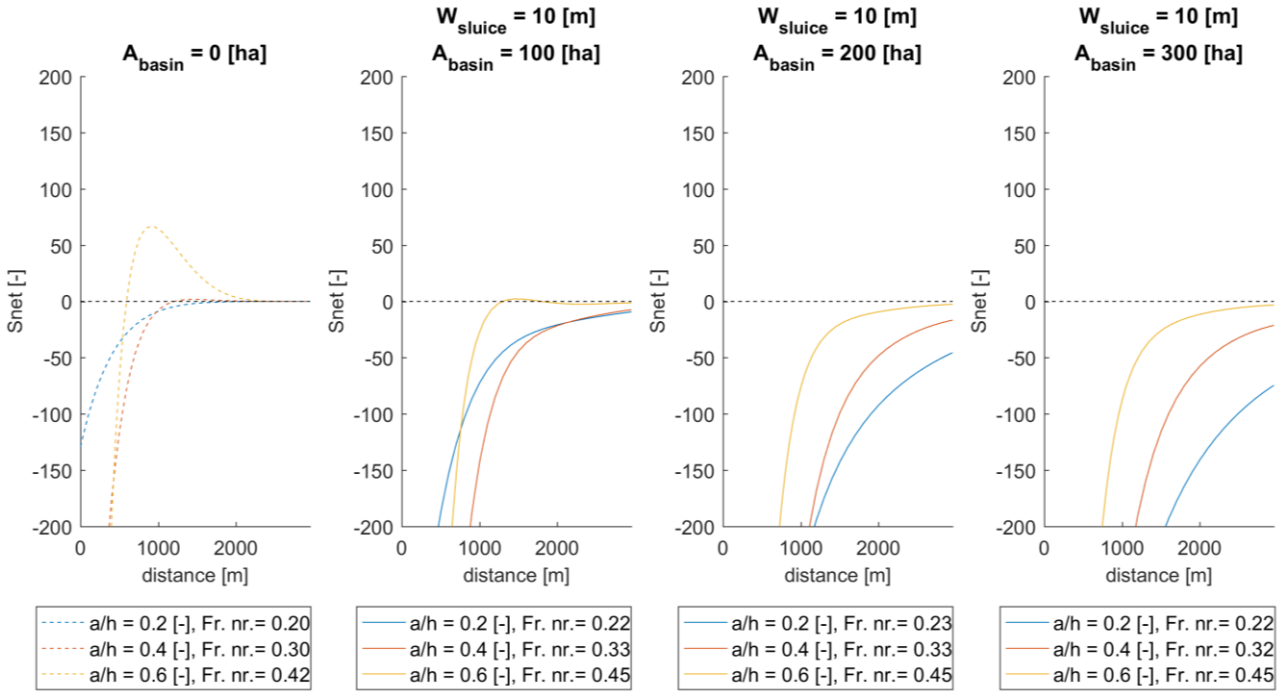

Figure 73 - Net transport quantity for W_{sluice} = 10 m.

- W_{sluice} = 15 m

For W_{sluice} = 15 m, the relative deepest channel in combination with the smallest basin area results in the least preferred situation. The relative shallowest in combination with the largest basin area results in the largest net sediment transport quantities and

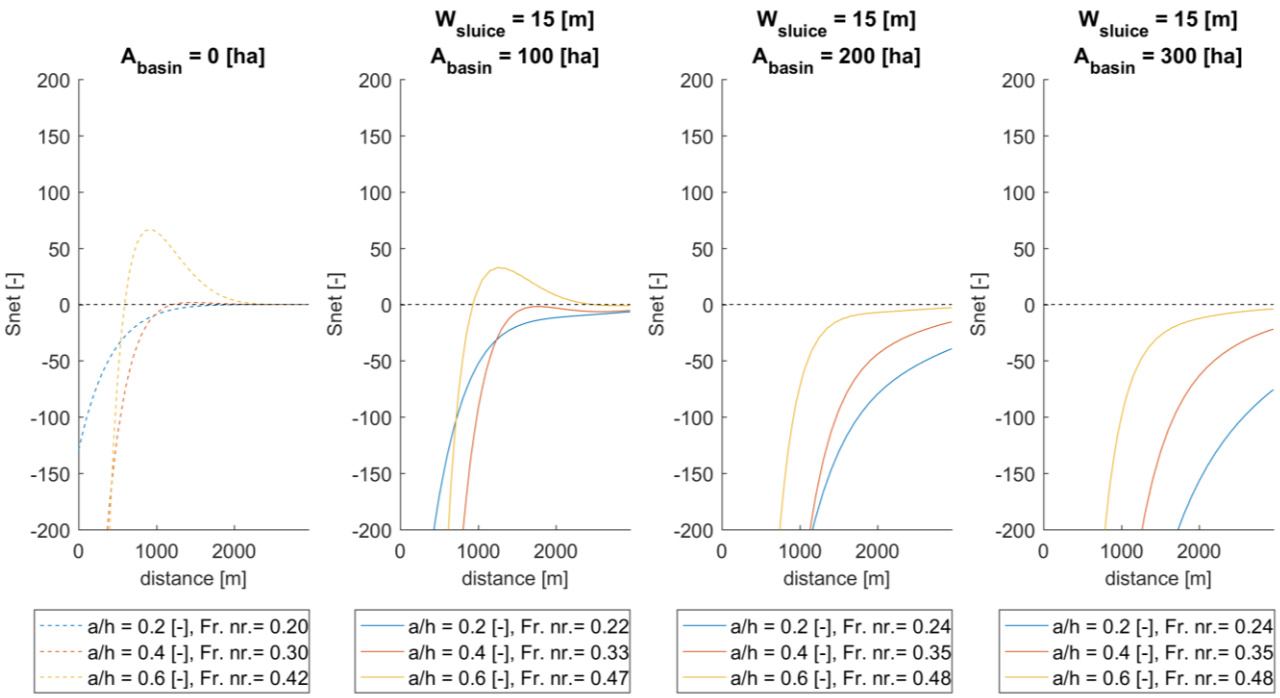

Figure 74 - Net transport quantity for W_{sluice} = 15 m.

When comparing the two most promising configurations of for the sluice width, the four most ebb dominant combined situations do not change.

- W_{sluice} = 50 m

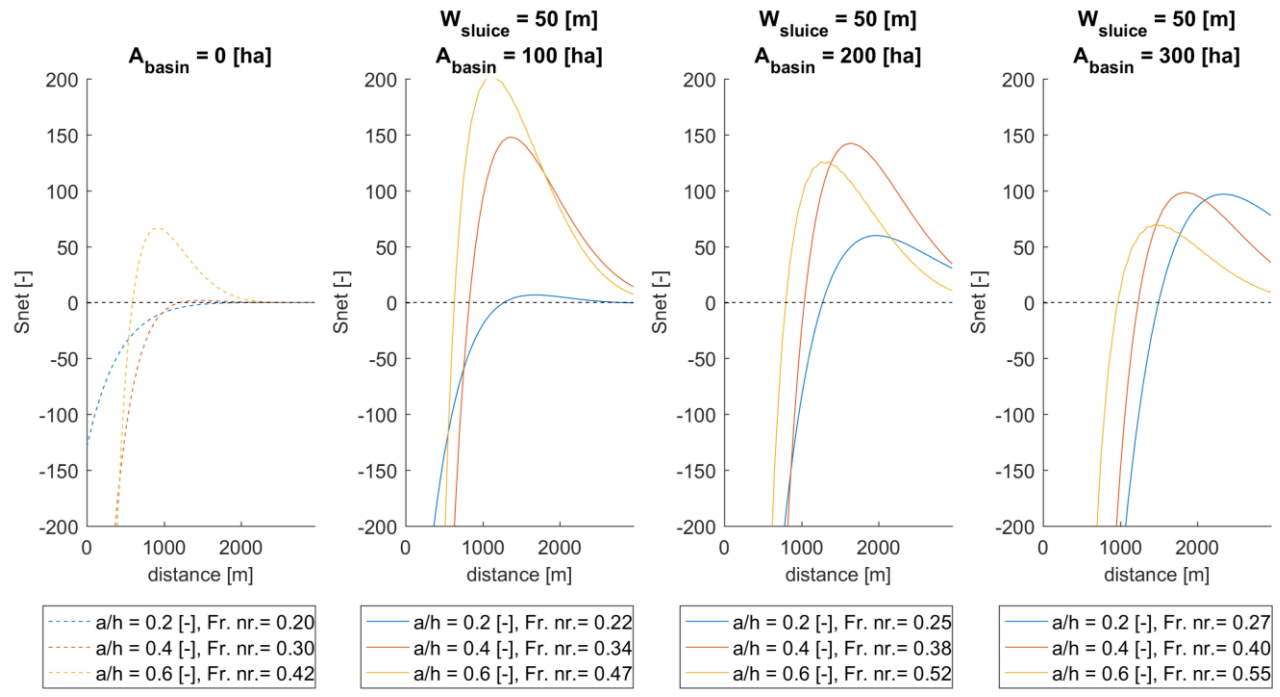

Figure 75 - Net transport quantity for W_{sluice} = 50 m.

5.6.4 Combination 4: A_{basin} – a/h

For this combination, the flushing basin area is visualized in each graph (Figure 76). Three graphs have been made for smallest depth in the right graph.

- W_{sluice} = 10 m

For a relatively deep channel the flushing basin has a large effect on the sediment transport quantities, see Figure 76. Considering a/h = 0.2, 0.4 and a small basin, there is almost no effect of a smaller depth. Only for the shallowest situation of a/h = 0.6, the net tide-residual transport is for a small part in the flood direction. When considering the panel on the right, it can be observed that a flushing basin has almost no effect on the tide residual transport. In general, flushing basins have less effect for shallow channels. A relatively large flushing basin is required for shallow channels to create a tide-residual transport in the ebb direction.

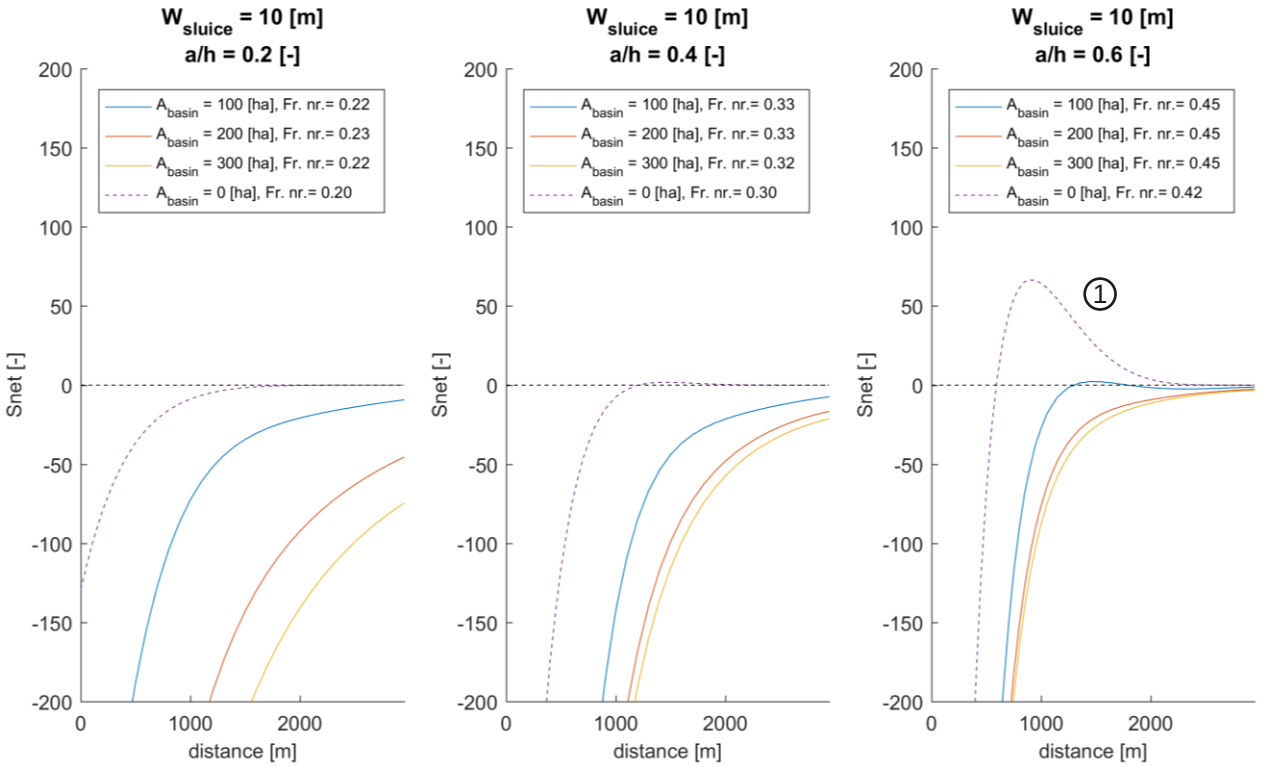

Figure 76 - Snet for the combined variation A_{basin} - a/h and W_{sluice} = 10 m

- W_{sluice} = 15 m

Almost the same effects can be observed as for W_{sluice} = 10 m. The difference: for the shallowest situations and smallest basin area the tide-residual transport in the flood direction is enlarged. There is a larger variability in net transport lines compared to the variations for W_{sluice} = 10 m.

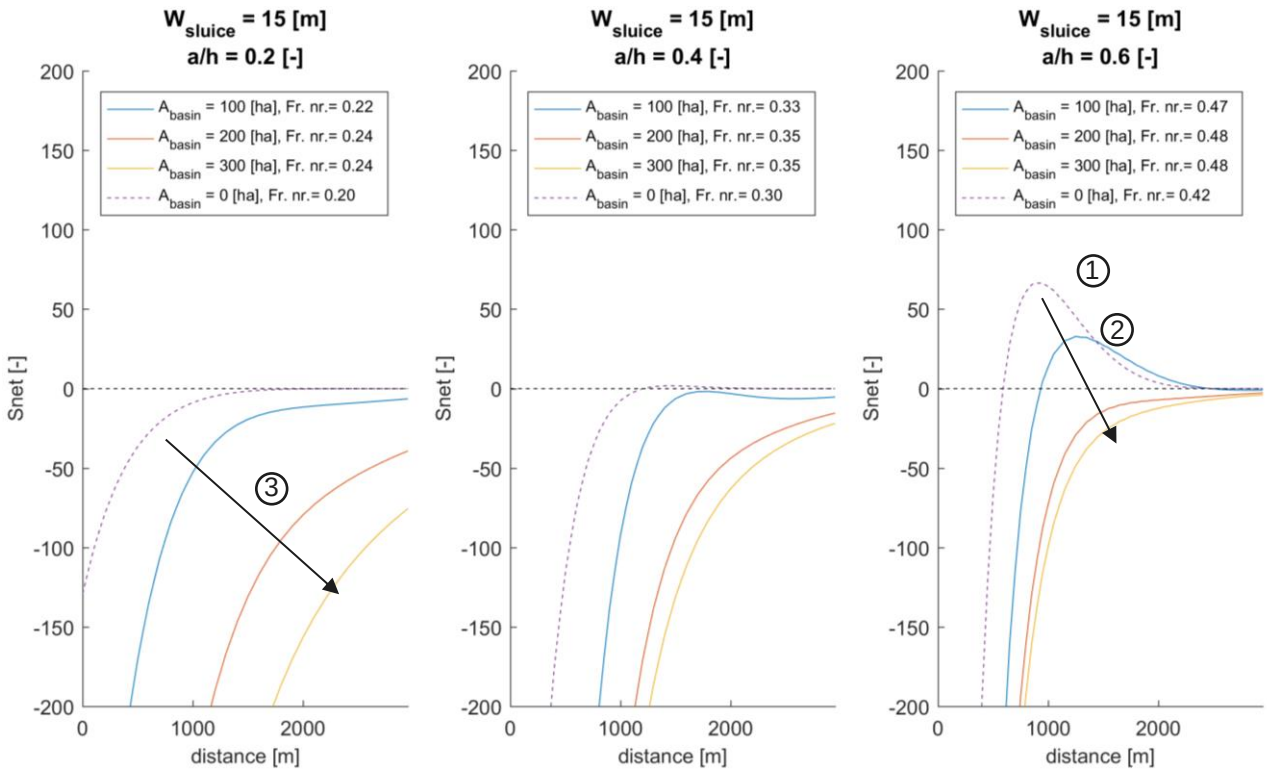

Figure 77 - Snet for the combined variation A_{basin} - a/h and W_{sluice} = 15 m

5.6.5 Practical implications

The channel depth at Noordpolderzijl is small. A relative depth of 0.6 is more likely than 0.4. Considering a/h = 0.6, it can be concluded that (indicated for each number in Figure 76 and Figure 77):

1. Especially for small basins, small sluice widths are preferred.
2. For a sluice width of 15 m and a small basin area A_{basin} = 100 ha, the tide-residual transport is in the flood direction, is reduced compared to the situation without a flushing basin. It is therefore of utmost importance that the flushing basin is sufficiently large enough, otherwise the siltation problem is not solved.
3. The largest change in the tide-residual transport can be obtained for deep channels: a/h = 0.2. However, these channels have already most of the time a tide-residual ebb transport, due to their depth. There is no need for a flushing basin in that situation. Constructing a deeper channel and maintaining the required depth by use of a flushing basin is a possibility. However, the potential influence of tidal cross channel currents can be high. These cross-channel currents could cause unforeseen siltation.

5.7 Conclusions on the scenarios

All the key parameters basin area, channel depth and sluice width have specific effects on the current velocities along the channel and over time. The above sections, illustrates the variations in the tide-residual suspended transport due to various scenarios of the chosen key parameters.

For all key design parameters and their combinations, the net sediment transport is ebb dominant at the seaward side of the domain. For some of the combinations of these parameters there is an undesired transition from ebb to flood dominance in the middle part of the channel.

The reduction of the sluice width (W_{sluice}) results in a change from flood to ebb dominance for the second half of the domain, see Figure 72. For smaller basin areas (the first row of Figure 72) the decrease of the relative depth results in an increase of the net flood dominant sediment transport quantities. Therefore, much smaller sluice widths are required to establish the same effect.

For larger basin areas, the influence of the width of the sluice is marginal, see Figure 72 last row. The transition of an ebb- and flood-dominated system occurs at about W_{sluice} = 30 m. The relative change that results from

each variation of the key parameter, gives an indication of the effectiveness of the key parameter in changing the flow and the resulting sediment transport.

6 DISCUSSION

The ultimate question of this thesis is: Can a flushing basin be an effective alternative in maintaining a required depth in a navigational tidal harbour channel? This study does not give the final answer to that question, but it presents an optimisation of the performance of a channel basin system in a tidal basin. More specifically, the influence of three main key design parameters: Size of the flushing basin A_{basin}, relative depth of the access-channel a/h and size of the sluice W_{sluice} on the performance has been determined. These parameters and their influence on sedimentation in a tidal harbour channel are discussed this chapter.

6.1 Processes

The tidal asymmetry is one of the dominant causes of a tide-residual transport in a tidal basin and is studied in this thesis. Other processes that may influence the sedimentation and erosion have not been included in the analysis.

The sedimentation in harbours and entrance channels in tidal basins results in the need of relatively large and frequent dredging. For the Wadden Sea, investigations of the possible causes of the high sedimentation at several locations has been executed (see for instance R. Hasselaar, et al. (2013) and Cleveringa (2012)). The local situation results in a site-specific combination of sedimentation processes, that are:

- tidal asymmetry: decrease of tidal prism results in an increase of flood-dominance
- horizontal eddy circulation, e.g. recirculation of dredged material
- vertical circulation generated by density differences
- gravity induced circulation currents
- storm/wind induced redistribution of sediment from adjacent tidal flats

The first of these processes is included in this thesis. The other processes can be dominant for a specific location or are incidental. For instance, at several harbours in the Wadden Sea gravity induced circulation currents are present as result of fresh water flushing. These processes cannot be included in the method that is used in this study and additional information (from observations and model simulations) are required to assess their local importance.

6.2 Method

This thesis has a generic approach to develop an understanding of the influence of the chosen key parameters on the performance of a flushing basin in general. The approach is to use a mathematical computer program (Matlab) to facilitate the analysis of multiple situations. The benefits and drawbacks of the chosen method are discussed here.

6.2.1 From 3-dimensional to 1-dimensional

To understand the dominant important processes of the sedimentation on a specific location, measurements in combination with a 2D/3D hydrodynamic model can be used. A flushing basin changes the flow of water locally and therefore the sedimentation. The relative importance of the processes that contribute to sedimentation do change as well. To determine the effect of a flushing basin, a 2D/3D model study fitting to the local conditions, is needed. By measuring effect on several locations, a general theory about dominant contributing processes may result. However, the result of this approach does not guarantee a theoretic/generic understanding, because the local conditions may prevail over the generic processes.

In this thesis, the predominantly longitudinal direction of the tidal wave is considered as one dimensional (1D). This is possible as the lateral variations in a tidal basin along a tidal channel are relatively small. By using a one-dimensional approach, the lateral current and water level variations are excluded and the effects in longitudinal direction are analysed separately.

At specific locations a complete representation of the exchange of water as result of the tide, is preferable and recommended in a 3D approach.

6.2.2 Boundary conditions

6.2.2.1 Flushing basin

The channel and basin interaction is modelled using a boundary condition that describes the exchange of water through the sluice. By using this simplification, local processes in the sluice and the flushing basin are excluded. E.g. the strong confining and thereafter widening of the sluice and flushing basin affects the water levels and current velocities. For the goal of this study the simplification is sufficient. For site specific studies these effects should be included. Inclusion of the effects can be achieved by using engineering rules for flow through construction or by using a flow model that includes the processes.

6.2.2.2 Seaward side

A tidal wave is forced at the seaward side by a semi-diurnal variation with an amplitude of 1 m. This sinusoidal wave is a theoretical representation of the tide. Tidal variations at specific locations in the Wadden Sea deviate from this sinusoidal tide. The tide at the deeper channel in the area at Noordpolderzijl (reference location) has for example a shape that is far from sinusoidal. Changing this boundary condition to a more representative one will give more site-specific results. By considering the spring-neap tidal cycle, the monthly varying transport quantities can be determined. For the generic purpose of this study the sinusoidal wave is used, because it facilitates the demonstration of the principal changes.

6.2.3 Cross channel currents

A consequence of a one-dimensional model is the exclusion of cross-channel directed currents. Especially during the transition of the inundation and drying of the tidal flats, these flows can be significant. One of the assumptions of one-dimensional modelling is a width much smaller than the length of the model: $w/L \ll 1$. Although a large contribution of the flow takes place in the channel, instead of over the tidal flats, the maximum ratio in this model study is about $w/L \approx 0.5$. With this relative large ratio, an extension from one dimensional to a two-dimensional model can be considered.

6.2.4 Alluvial bed

The assumption of an alluvial bed, see paragraph 4.3.2, has strong implications for the net transport of sediment. For an alluvial bed, the availability of sediment is not limited and the transport rate is determined by the integration of the total transport over one tidal period. The velocity asymmetry is therefore crucial for determining the net sediment transport quantities.

When one considers a limited availability of sediment (‘starved bed’), the time needed for settling and mobilization of the sediment is important. The asymmetry in time is the dominant asymmetry that determines the tide-residual transport. For modelling the tide-residual transport for starved bed conditions, the water – bed exchange must be considered too. The transport in this situation is not defined by a transport formula, but by entrainment formula. The sediment mass balance must therefore be solved.

Whether starved or alluvial conditions must be considered, depends on the physical properties of the specific location. For the Wadden Sea, both conditions are possible. For relatively high concentration of fines in the water column the alluvial bed conditions are legitimate. As high concentrations are present predominantly at the lower parts of the tidal basin (close to the shore), an alluvial bed is assumed in this study.

6.2.5 Initial channel bathymetry

The initial bathymetry of the channel is predefined, and is known as an important criterion for the dominant direction of the net transport. For the given bathymetry, the change of velocities as function of the key design parameters has led to significant results. For other predefined bathymetries, this is not necessarily the case.

The strong dependence of the relative depth is an indication for the possible importance of the initial bathymetry. The variability of the hypsometric curves of other locations at which accumulation of sediments takes place in the navigational channel is therefore of importance to investigate the applicability of flushing basins.

6.2.6 Equilibrium channel cross-section

Tidal basins are in equilibrium when there is no net import or export of sediments. The cross-sectional area of the channel is related to the tidal prism. When the tidal basin is in equilibrium, the channel geometry is also in equilibrium. This relation is used to determine the required flushing basin area for a stable channel in section 4.6.

The required basin area from this equilibrium relation matches with the results for the tide-residual transport along the channel for various scenarios of the basin area determined in 5.5.

The hydraulics change in the tidal area of the flushing basin system. How the morphology will respond to this change depends on the dynamic coupling. A stable tidal flushing basin system requires dynamic coupling of the geometric parameters as channel width, channel depth, flat width and flat depth.

6.2.7 Basin siltation

The interaction of the channel and the flushing basin is simulated as a boundary condition at the channel-end. So, one spatial point represents the flushing basin. The water level variations in the basin and the discharge through the sluice are determined with the continuity equation and the discharge formula of Torricelli. Although the exchange of water between the channel and the flushing basin is modelled properly, local- and spatial effects in the flushing basin are excluded. For a detailed description of the water levels and current velocities at the sluice and in the basin this method is not sufficient.

From the sluice to the basin the current velocities seriously decrease as a result from the transition from a small cross-section to a large cross-section of the flushing basin. The change in current velocities results in a tide-residual transport into the basin. For the basin of Nessmersiel (Coldewey et al., 1987), ‘Zwin’ (Huys & Verwaest, 1998) and Ostend (Hubrechtsen, 2000) the net import of sediment has been described and suggestions against sedimentation are given:

- continuous stationary dredging
- to use only the lower part of the water column for flushing and the upper part of the water column for filling. As the concentration of suspended sediment is larger near the bottom, this results in a smaller import of sediment and a larger export of sediment, compared to the situation in which the total water column is used for filling and flushing.

The initial geometry of the flushing basin system determines an optimal function. Siltation of the flushing basin reduces the optimal functioning of the flushing basin and should be prevented. Although this is a recognized problem, it is not considered in this study. This problem can be solved or counteracted, and the rate of siltation and the reducing measures should be quantified for a proper design.

6.2.8 Comparison with transport indicators

The comparison of the tide-residual transport direction determined by the integrated transport flux compared with the direction determined by the relative phase difference between the semi-diurnal tide and the first higher harmonic illustrated larges differences between these two methods. The cause of this difference is the relative large contribution of the second and third higher harmonics to the asymmetry and thus tide-residual transport.

6.3 Applicability

In this model study, the hydraulic conditions are idealized. The semi-diurnal tide is the only forced physical process. The real world is far from ideal and variations of the hydraulic conditions occur. Storms can be destructive. Especially the morphology in the tidal basins is far from constant. An optimum design of a flushing basin is however defined, given a bathymetry and tidal enforcement that is specific for that area.

One incidental event can change the local defined bathymetry and therefore the equilibrium of a flushing basin system. This means that dredging as a back guard is inevitable in a flushing basin system.

7 CONCLUSIONS & RECOMMENDATIONS

In this chapter, the findings of this report are summarized and concluded. Combined with the points elaborated in the discussion, recommendations for further research are presented.

7.1 Conclusions

In tidal basins, tidal asymmetry induces a tide-residual suspended sediment transport. This is one of the reasons of sedimentation within the tidal basins. This sedimentation requires periodically dredging in order to maintain navigability. Recently flushing basins have been studied as possible alternatives for dredging at Holwerd (P.C.P. Vellinga et al., 2016) and Noordpolderzijl (Danel, 2014). For these and other locations optimization of the design of a flushing basin system is meaningful. To determine the optimum geometric dimensions of a flushing basin system it is crucial to determine what the effect is on the tide-residual transport of the dimensions of the flushing basin.

This thesis presents answers to two questions on flushing basins. The first question is:

What is the influence of the geometry (shape and dimensions) of the flushing basin system upon the residual tidal transport in the harbour channel?

To optimize the function of a flushing basin a large tide-residual export (ebb-directed) of sediment should be achieved. To achieve an ebb-directed transport, the design of a flushing basin system must comprise:

- a relatively narrow discharge sluice, compared to the width of the channel. Considering a channel width of 50 m, an optimal effect is obtained for a sluice width of 10 to 15 m for all combined variations of the flushing basin area and ratios of the tidal amplitude/channel depth. For relatively wide discharge sluices a flushing basin has a disadvantageously effect compared to the situation without a flushing basin, because an increase of the tide-residual transport in flood direction can be expected in the second seaward (landward) part of the tidal channel.
- a large flushing basin area. Larger basins result in larger tide-residual export of sediment. However, the nominal effect of an increase of flushing basin area, decreases.
- a relatively deep channel relative to the tidal amplitude, as indicated by the tidal amplitude/channel depth ratio; a/h. For the given conditions, a/h about 0.2 is optimal. For a/h about 0.2, the depth is about 5 m. Further increased depth results in a decreased non-linearity (asymmetry) and therefore, the effect on tide-residual sedimentation reduces.

The second question is:

Could flushing basins be an alternative solution to dredging?

To answer this question, the function and/or design of the flushing basin must be optimized. At Nessmersiel the opening and closure regime of the discharge sluice of the flushing basin is optimized with regard to the already present and invariable/fixed dimensions of the basin and the discharge sluice. This thesis confirms that the tide-residual transport is affected by the key design parameters, thus an optimum situation can be determined. The sedimentation of the flushing basin is a known problem and is not considered of this study. The basin has therefore to be dredged to maintain the required prism.

7.2 Recommendations

This thesis describes the influence of the geometric parameters of a flushing basin system on the hydrodynamics within a tidal channel by use of a 1D model for an idealized situation. For a full understanding of a flushing basin system more research must be done. Recommendations for further research are:

- **From hydrodynamics to bed-exchange and morpho-dynamic change:**
  - The adaptation of the bed as result of the hydrodynamics is not considered in this thesis. The adaptation of the bed could result in a change of transport or a shift in the sediment distribution.
- **Sediment conditions:**
  - Alluvial bed /starved bed. Depending on the availability of the sediment starved bed or alluvial bed conditions are considered. This thesis assumes an alluvial bed. For a full scope of all possibilities, starved bed conditions must be also considered. For starved bed conditions the time asymmetry determines the tide-residual sediment transport quantities and direction. To get a better estimate of the sediment transport, the equation for the sediment balance must

be solved. The resulting product of the concentration and current velocities, results in a formulation of the distribution of the sediment transport over time and distance.

- **Change of the hypsometric curve**
  - The slope of the tidal flats can play a role in the hydraulics within the channel. An increased slope results in a change of the cross-sectional area and hydraulic radius of the channel. This affects the friction term of the shallow water equations. Moreover, an increased slope can induce an increase in cross-channel currents. This effect is not included in this thesis.
  - In this study, the height of the tidal flats is determined by the fixed hypsometric curve of Noordpolderzijl. The height of the tidal flats relative to the average water can vary on various locations. For higher tidal flats, the flushing during ebb is confined by the higher tidal flats for a longer duration. The relative depth might be larger in these situations and therefore, the tide-residual net transport harder to be influenced by a flushing basin system.
- **2D model, reduced flow by the spreading**
  - The spreading of the flow might be an important effect that has a major influence on the optimal function of a flushing basin system. The importance of this effect can be quantified by the extension of the one-dimensional model to a two-dimensional model.
- **Sluice design**
  - The transition from the basin to the channel must be regulated by a sluice. As result of the strong change in the geometry, the current velocities and water levels change over a relatively short distance. The advection is therefore increased around the sluice. The local geometry has a strong influence on the amount of energy dissipation of the flow. Smooth transitions decrease this effect. In addition, scouring should be minimized. Due to the increased current velocities at the sluice, scour protection should be used. A proper sluice design results in an increased function of the flushing basin system.

REFERENCE LIST

Bosboom, J., & Stive, M. J. F. (2015). Coastal Dynamics, lecture notes CIE4305.

Coldewey, H. G., Erchinger, H. F., & Probst, K. (1987). *Forschungsbericht Tiefenstabilisierung von Außentiefs - (AT-S) - mit Naturuntersuchungen am Neßmersieler Außentief. Schlußbericht über das KFKI-Forschungsprojekt. T 2017*. Retrieved from

Danel, H. (2014). *Spoelmeer Noordpolderzijl, Deskundigenraadpleging mogelijkheden spoelzee Noordpolderzijl* Retrieved from

de Lucas, M., Ibanez, M., & Winterwerp, H. (2016). *Analyse Vaargeul HolwerdAmeland; Overview Laboratory Analyses*. Retrieved from

Dronkers, J. J. (1998). *Morphodynamics of the Dutch Delta. 8th International Biennial Conference on Physics of Estuaries and Coastal Seas, The Hague, pp. 297-304*.

Elias, E. P. L., van der Spek, A. J. F., Wang, Z. B., & de Ronde, J. (2012). Morphodynamic development and sediment budget of the Dutch Wadden Sea over the last century. *Netherlands Journal of Geoscience*.

Eysink. (1979). *Morfologie van de Waddenzee, gevolgen van zand- en schelpenwinning*. Retrieved from

Hasselaar, R., de Boer, W. P., & Luijendijk, A. L. (2013). *Optimizing harbour maintenance strategies using Delft3D-FLOW and D-Flow Flexible Mesh*. Paper presented at the Proceedings of Coasts & Ports Conference Sydney, Australia.

Hubrechtsen, F. (2000). *Gespoeld, gespuid, gebaggerd*. Retrieved from Ostend:

Huys, S., & Verwaest, T. (1998). *Spuiwerking in het Zwin*. Retrieved from

Postma, H. (1961). Transport and accumulation of suspended matter in the Dutch Wadden Sea. *Netherlands Journal of Sea Research, 1*(1), 148-190. doi:http://dx.doi.org/10.1016/0077-7579(61)90004-7

Speer, P. E., & Aubrey, D. G. (1984). A Study of Non-linear Tidal Propagation in Shallow Inlet/Estuarine Systems, Part II: Theory.

van Duren, L., Winterwerp, H., van Prooijen, B., Ridderinkhof, H., & Oost, A. (2001). Clear as Mud: understanding fine sediment dynamics in the Wadden Sea – Action Plan.

van Kessel, T. (2016). *Analyse Vaargeul Holwerd-Ameland; Veldmetingen vaargeul Holwerd*. Retrieved from

van Straaten, L. M. J. U. (1957). Accumulation of grained sediments in the Dutch Wadden Sea.

van Straaten, L. M. J. U., & Kuenen, H. (1958). Tidal action as a cause of clay accumulation.

Vellinga, P. C. P., Baptist, M. J., Danel, H., Herman, P., Ietswaart, T., van Kessel, T., . . . van der Zee, W. (2016). *Rapport tweede kennistafel spoelmeer 'Holwerd aan Zee'*. Retrieved from

Vellinga, P. C. P., Cleveringa, J., Danel, J., van Kessel, T., Lofvers, E., Mulder, H., . . . Sas, H. (2015). *Rapport Kennistafel 'Spoelmeer Holwerd aan Zee'* Retrieved from

Wang, Z. B., Jeuken, C., & de Vriend, H. J. (1999). Tidal asymmetry and residual sediment transport in estuaries.

Zheng Bing Wang, Julia Vroom, Bram C. van Prooijen, Robert J. Labeur, Marcel J.F. Stive, & Jansen, M. H. P. (2011). *Development of tidal watersheds in the Wadden Sea*.

Zijlema, M. (2015). Lecture Notes: Computational Modelling of Flow and Transport.

LIST OF SYMBOLS

Symbol	Units	Definition
α_n	[-]	phase angle of component number n
a_0	[m]	mean level
a_n	[m]	amplitude of component number n
a_{M2}	[m]	(harmonic) amplitude of semi-diurnal component
A_c	[m2]	channel cross-sectional area
A_{basin}	[m^2]	flushing basin area
a/h	[m/m]	relative depth: tidal amplitude/channel depth
c	$[m^{2-n}s^{n-1}]$	concentration of $10^{-7} - 10^{-4}$ with n = 3 … 5
c	[m/s]	wave celerity
c_f	[-]	friction coefficient
f	[m^5/s^5]	transport flux
Fr	[-]	Froude number
g	[m/s]	gravitational acceleration
h	[m]	channel depth
Δh	[m]	water level difference between channel-end and basin
i_b	[m/m]	bottom slope
ρ_{water}	[kg/m^3]	density of water
k_s	[-]	equivalent geometrical roughness of Nikuradse
L	[m]	wave length of the tide
$L_{channel}$	[m]	length of the channel
N	[-]	Number of harmonic components
P	[m^3]	tidal prism of the basin.
ϕ	[rad]	relative phase difference
ϕ_{M2}	[rad]	phase of the M2 tide
R	[m]	hydraulic radius
S_{net}	[m^5/s^4]	sediment transport
t	[s]	time
T_{LWS}	[s]	period of low water slack
T_{HWS}	[s]	period of high water slack
T_{M2}	[s]	tidal period of the semi-diurnal tide
Q	[m^3/s]	discharge
U	[m/s]	depth averaged velocity
W	[m]	width
$W_{channel}$	[m]	width of the channel
W_{sluice}	[m]	width of the sluice
ω_n	[1/hr]	angular velocity of component number n
x	[m]	x- coordinate; location along the channel

ζ	[m]	water level elevation above reference plane
Z	[m]	water level elevation above reference plane
Z_m^n	[m]	discretized water level at spatial grid point m and at time n

LIST OF FIGURES

LIST OF TABLES

APPENDIX A - THE WADDEN SEA

In this chapter, the basin dynamics are presented. The tidal flow has a large contribution to the morphological development. In the last part of this chapter, the Dutch locations with siltation problems mentioned in this thesis are described.

A.1. Basin

In short shallow basins, the water level immediately follows the water level in the sea (communicating vessels). Thus, no variation in water level along the channel axis:

$$\frac{\partial \eta}{\partial x} = 0$$

And

$$Q(t,x) = A_s u_s = \frac{\partial \eta_0}{\partial t} \int_x^{L_b} b dx = \frac{\partial \eta_0}{\partial t} A_b \quad \Leftrightarrow \quad u_s(x,t) = \frac{\partial \eta_0}{\partial t} \frac{A_b}{A_s}$$

In the situation of a short tidal basin with a little storage-offering tidal flats and shallow channels, A_s is much larger around HW slack than around LW. As a result, the rate of velocity change at high water slack is smaller; the HW-slack duration is longer than the LW-slack duration. (Bosboom & Stive, 2015)

A.2. Tidal flow

The dominant tidal component in the Wadden Sea is semi-diurnal. The tidal flow propagates along the Dutch coast in northern direction around the two amphidromical-points in the North Sea. The tidal wave enters the Wadden Sea on each side of an island, with a small phase-lag of the northern wave. This phase-lag and as well the tidal amplitude determine the location of the watershed; the location of minimal velocity amplitude.

Tidal asymmetry is one of the main causes sedimentation in the Wadden Sea. This asymmetry results in longer slack water periods during rising periods than during lowering, thus offering the sediment particles have more time to settle. As a result, the net sediment direction into the basin of the Wadden Sea.

A.3. Morphological development, watersheds

The morphological development is dependent on the equilibrium of the tidal basin elements. The Wadden Sea with his barrier islands can be schematized by tidal basins surrounded by barrier islands with tidal inlets in between, called tidal inlet system. Due to the tidal exchange, tidal deltas are formed. The predominant import of the Wadden Sea resulted in intertidal flats (flood tidal deltas) separated by channels. Relative sea-level rise caused expansion of the basin, which increased the volume of sediment accommodation space and generated a net landward sediment transport (see e.g. Van Straaten, 1975; Flemming & Davis, 1994).

The tidal basin can be schematised into large morphological elements of which the equilibrium sizes are related to hydrodynamic parameters like the tidal range and the tidal prism. The tidal prism is strongly dependent on the size of the basin, especially for the short basins like most of the Wadden Sea basins, in which the tidal range is more or less constant and weakly dependent on the morphology. This means that movement of tidal watersheds can have substantial influence on the morphological equilibrium of the Wadden Sea as it influences the size of the basins.

Note that there is a distinction between the morphological tidal watershed and the hydraulic tidal watershed. A morphological tidal watershed is defined as the line between the two basins with the highest bed level. The corresponding hydraulic tidal watershed is the division line between the two basins on the basis of tidal filling. (Zheng Bing Wang et al., 2011)

A.4. Closures

The closures of parts of tidal basins can have significant effects on the morphological state of the basin. For example, the Afsluitdijk and Lauwersmeer. Watershed of Marsdiep, Eyerlandse Gat and Vlie are changing position in eastern direction with the exception of the Vlakte of Oosterbierum. Movements of the watersheds indicate an inbalance of morphological equilibrium.

Closures resulted in rising tidal differences and therefore an accommodation space for sediment, which is the cause of the changing morphology.

A.5. Ratio: sedimentation/erosion

Despite major sedimentation, the large difference in inter - tidal shoal to basin area ratios between the Western (0.3-0.4) and the Eastern Wadden Sea (0.6-0.8) might be an indication of the disequilibrium in the Western Wadden Sea, given that a similar forcing regime exists. Assuming that the eastern Wadden Sea is in or close to equilibrium, a large volume of sediment is needed to obtain a 0.6-0.8 intertidal shoal to basin area ratio in the Western Wadden Sea. (E.P.L. Elias et al. 2012)

For an overview of the zones of sedimentation and erosion see Figure 78 and Figure 79. Sedimentation occurs at large landward areas in the western part of Wadden Sea. At the eastern side of the Wadden Sea, especially the watershed of the Ems-Dollard, less activity can be observed south of the Islands Rottermeroog and Rottermerplaat.

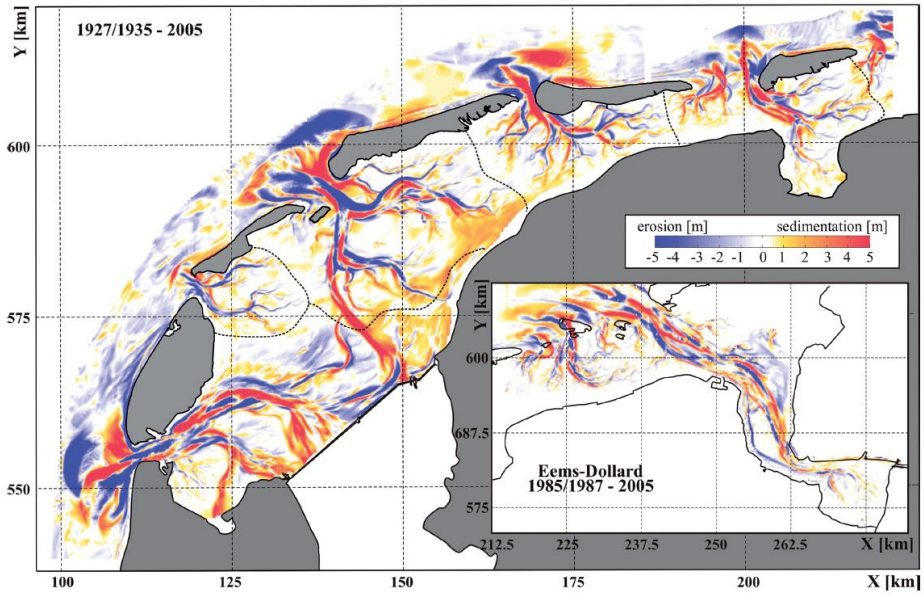

Figure 78 - sedimentation - erosion maps for the periods 1927/1935 till 2005, (Elias, van der Spek, Wang, & de Ronde, 2012)

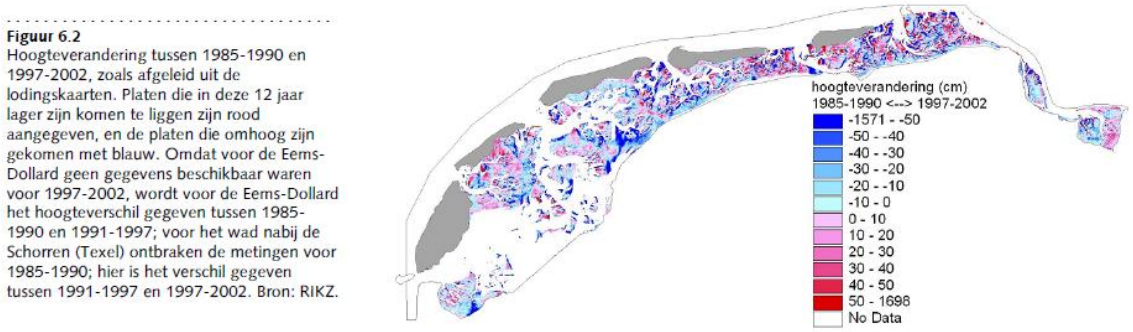

Figure 79 - variation in elevation of the tidal flats. Increasing height (red) decreasing height (blue)

A.6. Channel siltation locations

The sedimentation of the Wadden Sea takes place close to the boundary between sea and land, where several harbours are present. In the next sections, some of these harbours will be described.

Area around Harlingen

The Wadden area at Harlingen is part of the tidal basin Vlie. This is one of the larger tidal basins of the Dutch Wadden Sea; 668 km^2 at mean high water (MHW). The average tidal prism (P) is also one of the largest: 1078 Mm^3. Because of the tidal flow, the tidal inlet between the islands of Vlieland and Terschelling is relatively large, compared to other inlets in the Dutch Wadden system. In the main tidal channel there are several locations of threatening siltation.

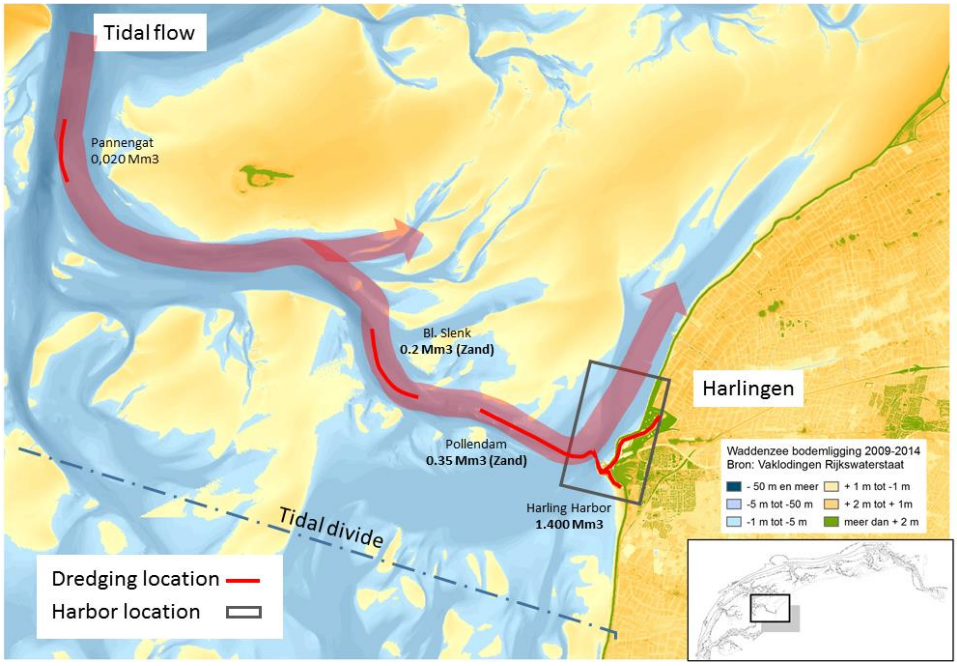

Figure 80 - Area around Harlingen

Harbour siltation Harlingen

Harlingen has a large multifunctional harbour. For centuries, the harbour of Harlingen has been one of the main harbours of the northern Netherlands. The last to be dredged each year: 1.4 Mm3.

Large tidal dynamics are present in front of Harlingen harbour. The rising tide comes in a large deep channel along the Pollendam in southeastern direction. Just in front of the harbour the inflowing water makes a large bend to proceed in north-north eastern direction along the coast to the borders of the watershed. At falling tide, the south-south western flow will split up in front of the harbour in a south-south western direction crossing the tidal divide and a flow following the main tidal channel along the Pollendam. These strong currents bring in sediment.

The tidal dynamics in front of the harbour influence the dynamics within the harbour. These dynamics result in horizontal eddy circulations in front of the harbour and result in resuspension of sediments and possibly afterward sedimentation.

Estuarine circulation

Another cause of sediment is induced by density differences within the harbour basin. In the middle of the harbour, the discharge sluice Tjerkhiddes is situated. This sluice discharges fresh surplus water from a junction canal to maintain the polder water level. This fresh water discharge results in an enforcement of the tidal saline flow, with a large density due to suspended sediment content. Vertical circulation due to density differences

causes sedimentation. The further in the basin, the less dynamic current velocities are present, and hence more sedimentation takes place. Sediment concentration will be less here as well. However, most sedimentation will occur at the seaward side of the harbour Basin. (Hasselaar, de Boer, & Luijendijk, 2013)

Mud Motor

In the recent past, the dredged material has been disposed at different locations on the shallow parts, the intertidal flats. Another method was to dispose it into the channel allowing the ebb-currents to export the dredged material to the sea. One of the locations was in front of the harbour entrance of Harlingen. Both methods don't contribute to a natural system in a positive way. To enhance the development of salt marshes, the Mud Motor project has been started by Ecoshape.

The Ecoshape coproduction of Dutch companies that aims to implement the Building-With-Nature-philosophy started the development of saltmarshes at Koehoal using a Mud Motor. The Mud Motor is a variation of the Sand Motor at the North Sea at Kijkduin of the same consortium. For a period of three years, part of the dredged material, 0.2 Mm^3 is deposited at Koehoal. By redistribution the material, the saltmarsh grows with 2-4 cm/year above reference level (when assuming that 10% of the material will stay in the study area). The dredged material of the harbour of Harlingen is disposed upstream of the Koehoal saltmarshes. The aimed effects of the Mud Motor are:

- less recirculation towards the harbour, hence less maintenance dredging,
- promotion of the growth and stability of salt marshes, improving the Wadden Sea ecosystem,
- stabilizing the foreshore of the dykes, and therefore less maintenance of the dyke.

These effects enhance the natural development of the saltmarshes. Whether these effects are significant hasn't been statistically proved yet.

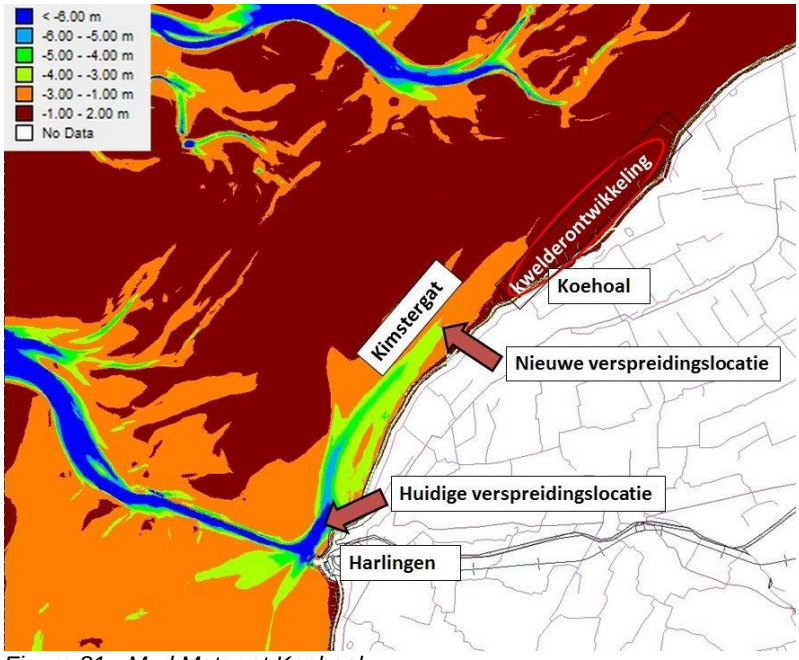

Figure 81 - Mud Motor at Koehoal

Area around Holwerd

The Wadden Sea area around Holwerd is part of the basin Ameland. Within this basin three harbours are located: Ballumerbocht, Nes and Holwerd. All of these three harbours have sedimentation problems close to the harbour. They have in common that the approach channel is relatively narrow and deep and bordered with high intertidal flats.

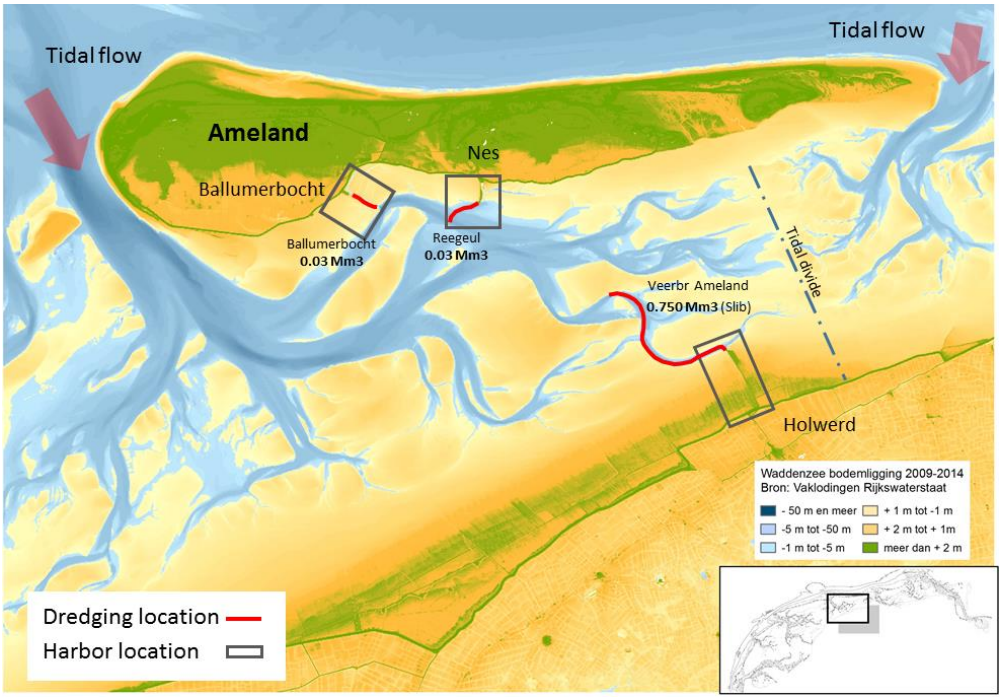

Figure 82 - Area around Holwerd

Siltation at Holwerd

The harbour of Holwerd is located at the end of a tidal channel and connected with the hinterland by a peninsula. In between the end of the peninsula and the mainland salt marshes are present. A gradual transition from intertidal flat to grassland has been obtained by using willow screens to trap the sediments behind them.

The last part of the channel, about 2 km to Holwerd must be dredged yearly -with an amount of 1.750 Mm^3 of dredged material in 2012- to maintain the necessary navigation depth of the ferry. This amount increased significantly over the last years, see Figure 85.

1. *morphological developments;*
2. *mud dynamics and the development of a highly concentrated fluid mud layer in the lower part of the water column;*
3. *nautical factors: changes in the methods of sonar depth measurement, changed requirements for width and depth of the fairway and changes in the dredging practice.*

The analysis of the morphological developments showed that the tidal prism of the channel has been reduced due to a general tendency of accretion in the mudflats and saltmarshes surrounding the channel. This is the most fundamental cause for the changes in the fairway, as physical processes will force the channel to become shallower and narrower as a reaction to this reduction in tidal prism – this tendency was subsequently countered by dredging. In addition, local morphological developments, in particular the heightening of some tidal flats surrounding the fairway and degeneration of a flood-ebb circulation cell, played a certain role. In combination with the reduction in tidal prism, this led to a less ebb-dominant (more flood-dominant) tidal circulation in the fairway, which brings in more sediment to the upstream reaches. (de Lucas, Ibanez, & Winterwerp, 2016)

The tidal prism decreased over the course of the years, and both in current velocity and tidal volumes a tendency towards flood dominance is found.

Simulations with a 1DV column model for mud dynamics suggest that the current velocity in the channel is in the range where formation of fluid mud becomes probable. This conclusion, however, is strongly dependent on the correct estimation of absolute velocity and is therefore in need of confirmation by model calibration/validation, and by field observations.

Figure 83 - Holwerd overview

Figure 84 - Impression ferry harbour Holwerd

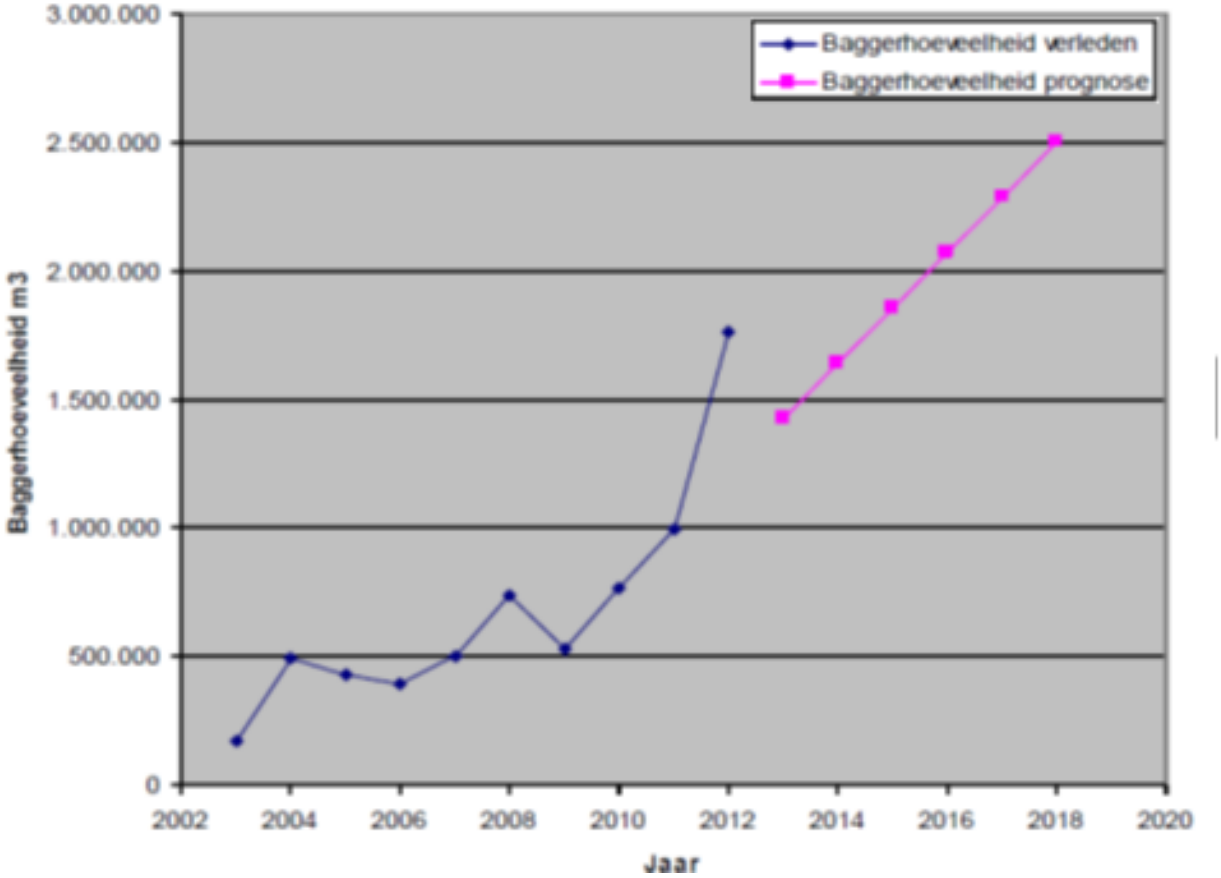

Figure 85 - dredging amounts channel Holwerd – Ameland

Siltation at Nes

The largest harbour of Ameland is Nes. The main purpose of this port is the berthing of the two ferries that navigate to Holwerd. These ferries berth at the end of a peninsula. On the east side of this peninsula a marina is located. Pleasure boats mainly use this marina. Dredging takes place in the 'Reegeul', the main channel in front of the ferry harbour. The amount of dredged material is about 0.3 Mm^3/year.

Figure 86 - Overview Nes

Figure 87 - Impression Ferry Harbour Nes

Siltation at Ballumerbocht

The Harbour of Ballumerbocht is used from the 17th century as a transport harbour to the Frisian coast and other Wadden islands. Until 1948 it was used as a harbour for the ferry to Fryslan. The closure of the IJsselmeer by the Afsluitdijk resulted in different reducing currents and a siltation of the channel. Navigation of larger vessels wasn't possible anymore. Today the harbour is used for smaller ships and is one of the two life boat stations of the Royal Netherlands Sea Rescue Institution (KNRM).

The amount of dredged material is about 0.3 Mm^3/year.

Figure 88 - Overview Ballumerbocht

Figure 89 - Impression Ballumerbocht

Area around Noordpolderzijl

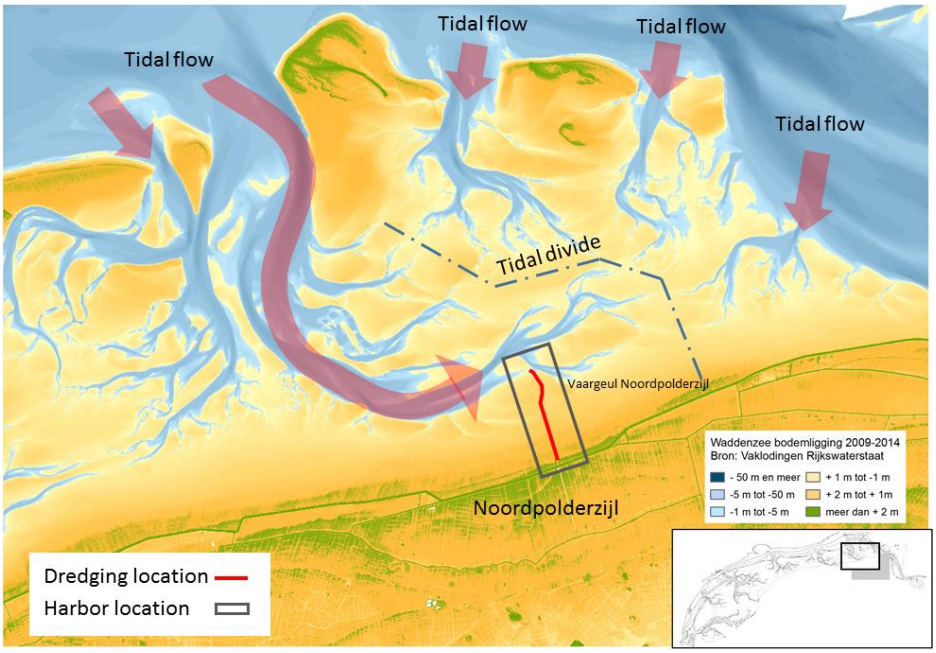

Figure 90 - Area around Noordpolderzijl

Siltation at Noordpolderzijl

Noordpolderzijl is a hamlet at the Wadden Sea coast with the smallest sea harbour of the Netherlands. This harbour has been used by shrimp fishers and had its own fish auction. For reclamation of the Noordpolder, a sluice was built in 1811. In 1985 the sluice had to be replaced by a new discharge sluice, necessary after heightening of the sea dike.

The small and shallow channel to the harbour (Noordpoldermude), has a fixed width and is connected to the deeper tidal channel Zuid-Oost Lauwers. Tidal flats bound both sides of the channel. From the Wadden Sea to the dike saltmarshes are created by willow screens. The chronologically stages of these saltmarshes are clearly visible. See Figure 91 and Figure 92 for an overview and an impression of the area.

Figure 91 - Overview Noordpolderzijl

Figure 92 - Impression Noordpolderzijl

Another feature of Noordpolderzijl is its fish-migration sluice. This sluice has been built in 2014 and enables the migrating fish to swim from salt to brackish water. In this brackish water, fish will spawn. The transition from salt to fresh water is a scarce environment in the Netherlands and therefore has highly added natural value.

Estuarine circulation

The Noordpolderzijl fresh water discharge results in an enforcement of the saline water lens. Due to the difference in densities, the saline water brings in extra sediment at each tidal cycle. This phenomenon is called estuarine circulation and is also observed in the harbour of Harlingen (earlier mentioned in this document).

APPENDIX B – HARMONIC DECOMPOSITION

B.1. Transport indicators

B.1.1. Scenarios for W_{sluice}

The change of the shape of the current velocity signal along the channel can be quantified by the amplitude ratio and relative phase difference of the higher harmonics. In Figure 94, the result of this harmonic decomposition illustrates a decrease of the semi-diurnal tidal amplitude; a_{M2}. For the smallest values of W_{sluice} = 5 m. the amplitude of the semi-diurnal tide is decreasing, see Figure 93 at the upper-left panel. For W_{sluice} = 5 m the first higher harmonic is only decreasing, whereas for W_{sluice} = 50 m depicted in lower left panel in red, first an increase and then a decrease of a_{M4} is visible. The relative amplitude change for both situations is depicted in Figure 94, right panels. For W_{sluice} = 50 m the relative amplitudes are larger and the variability is higher.

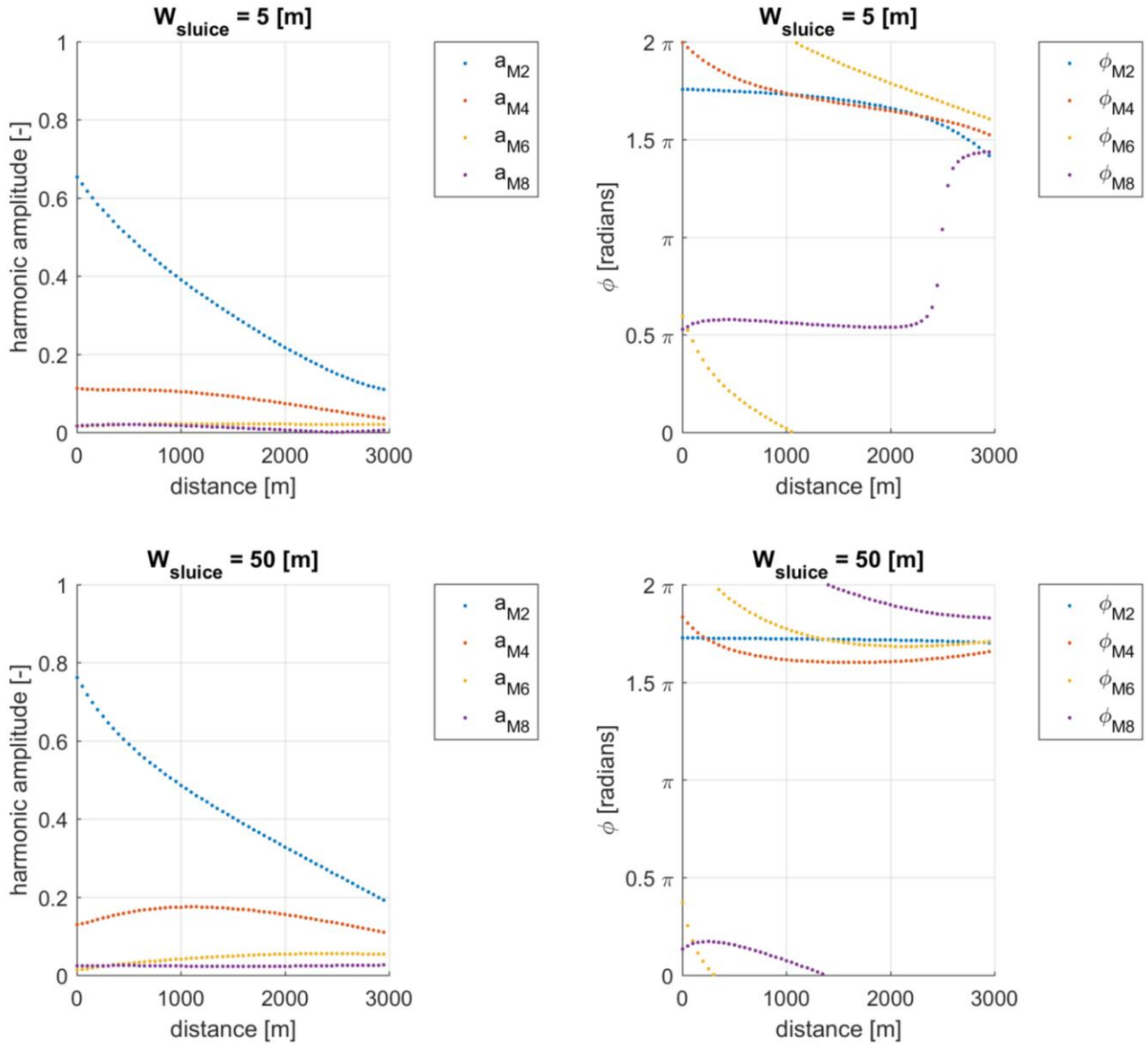

Figure 93 - Amplitudes and phases of the higher harmonics for varying W_{sluice}

The phases of the harmonics decrease, except for a_{M8} for W_{sluice} = 5 m. The relative phase difference $\phi = 2\phi_{M2} - \phi_{M4}$ has a strong decrease of the phase, see Figure 94. This agrees with the decreasing flood dominance as can be seen in Figure 49. Comparing Figure 49 and Figure 94 lower-right panel in blue, a smaller decrease for W_{sluice} = 50 m can be observed.

As the higher harmonics do not decrease that fast, the relative amplitude e.g. a_{M4}/a_{M2} increase, which can be observed in Figure 94. The M4 which is for example introduced by the advection term in the momentum equation, increases from about 0.2 to 0.35.

For W_{sluice} = 5 m the influence at both channel ends can be observed as the relative phase difference has a large variability over the length of the channel. For peak flow asymmetry, the transition from a net ebb to a net flood directed sediment transport is at $1.5\,\pi$. The variability of the asymmetry is larger for W_{sluice} = 5 m than for W_{sluice} = 50 m. Furthermore, for W_{sluice} = 5 m, and considering the relative phase difference of $2\phi_{M2} - \phi_{M4}$ the end of the channel change from a flood directed to an ebb directed net sediment transport direction, indicated by the black arrow.

For W_{sluice} = 50 m, a flood directed net transport is present for the total length of the channel. The variability of the asymmetry is low. Considering peak flow asymmetry, in the middle of the channel almost a maximum of asymmetry of established as $\phi = 2\phi_{M2} - \phi_{M4} \approx 2\pi$.

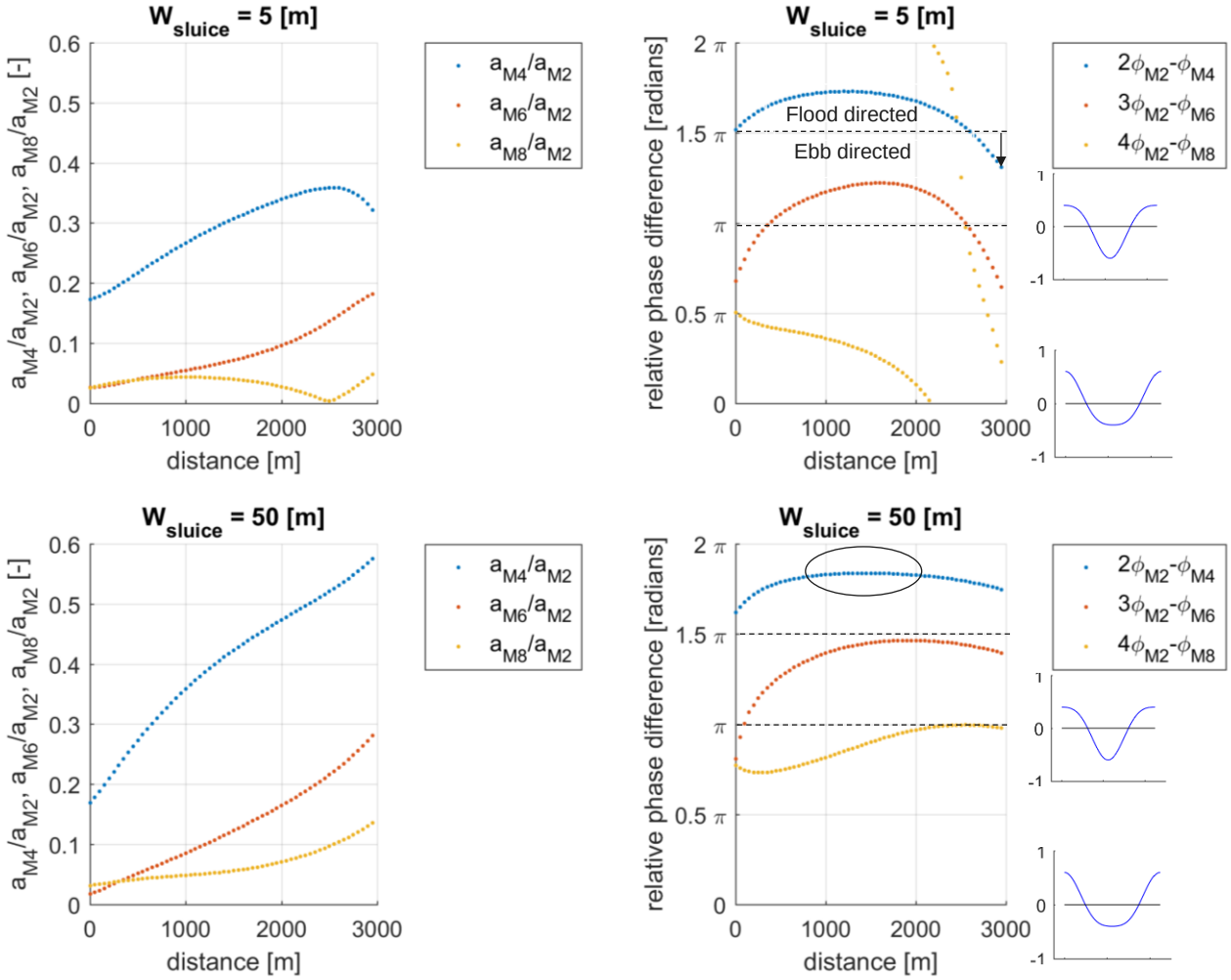

Figure 94 - Amplitude ratio and relative phase difference of the higher harmonics M4, M6 and M8 for varying W_{sluice}

B.1.2. Scenarios for a/h

For the relative deep channel; a/h = 0.2, there is a linear decrease of a_{M2} visible, see Figure 95. a_{M4} slightly increases in longitudinal direction. The higher harmonics a_{M6} and a_{M8} have a minor contribution in the total

signal. Whereas the phase of M_2; ϕ_{M2} is constant along the channel, that of M_4 is slightly changing around $\phi = 2\,\pi$.

For the situation with a relative shallow channel; a/h = 0.6, the flow is much stronger deformed. Especially at the seaward boundary, the rate of change is the highest. There is a decreasing rate of change in channel-end direction for a_{M2}. The first higher harmonic M_4 decreases after an increase. Due to the larger decrease of a_{M2} in relation to a_{M4} the contribution of M_4 becomes larger in channel direction, see Figure 96.

The relative phase difference depicted in Figure 96 for a/h = 0.2, has slightly decreased in comparison to the reference situation in section 5.2. At the end of the channel a small rate in ebb dominant direction is visible from a decreasing relative phase difference.

For a/h = 0.6 this decreasing rate at the end of the channel is also visible, however the relative phase difference has moved up in total, which implies an increased flood dominance. At the seaward side, there is a strong increase.

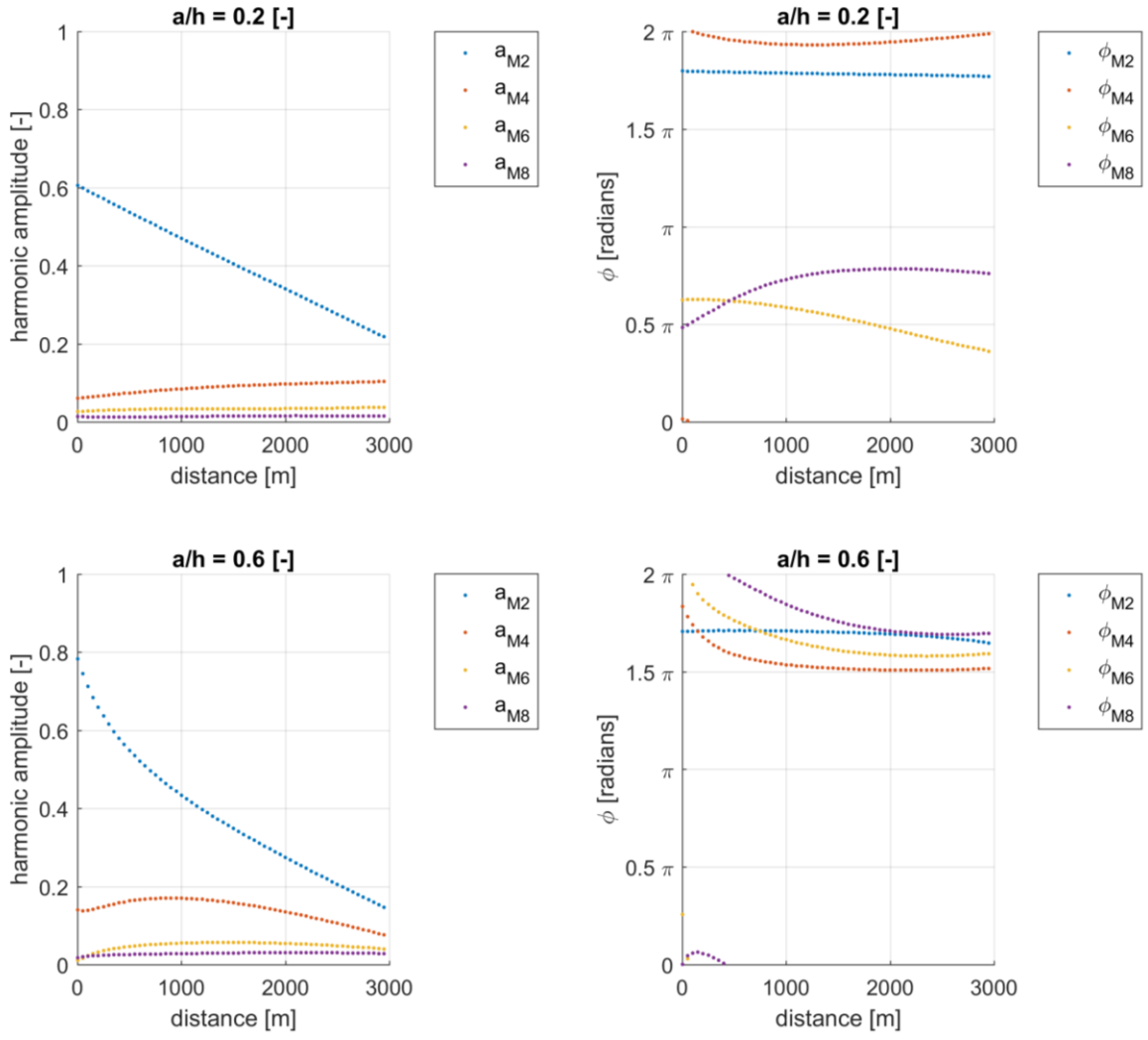

Figure 95 - Harmonic decomposition for smallest and largest value of a/h

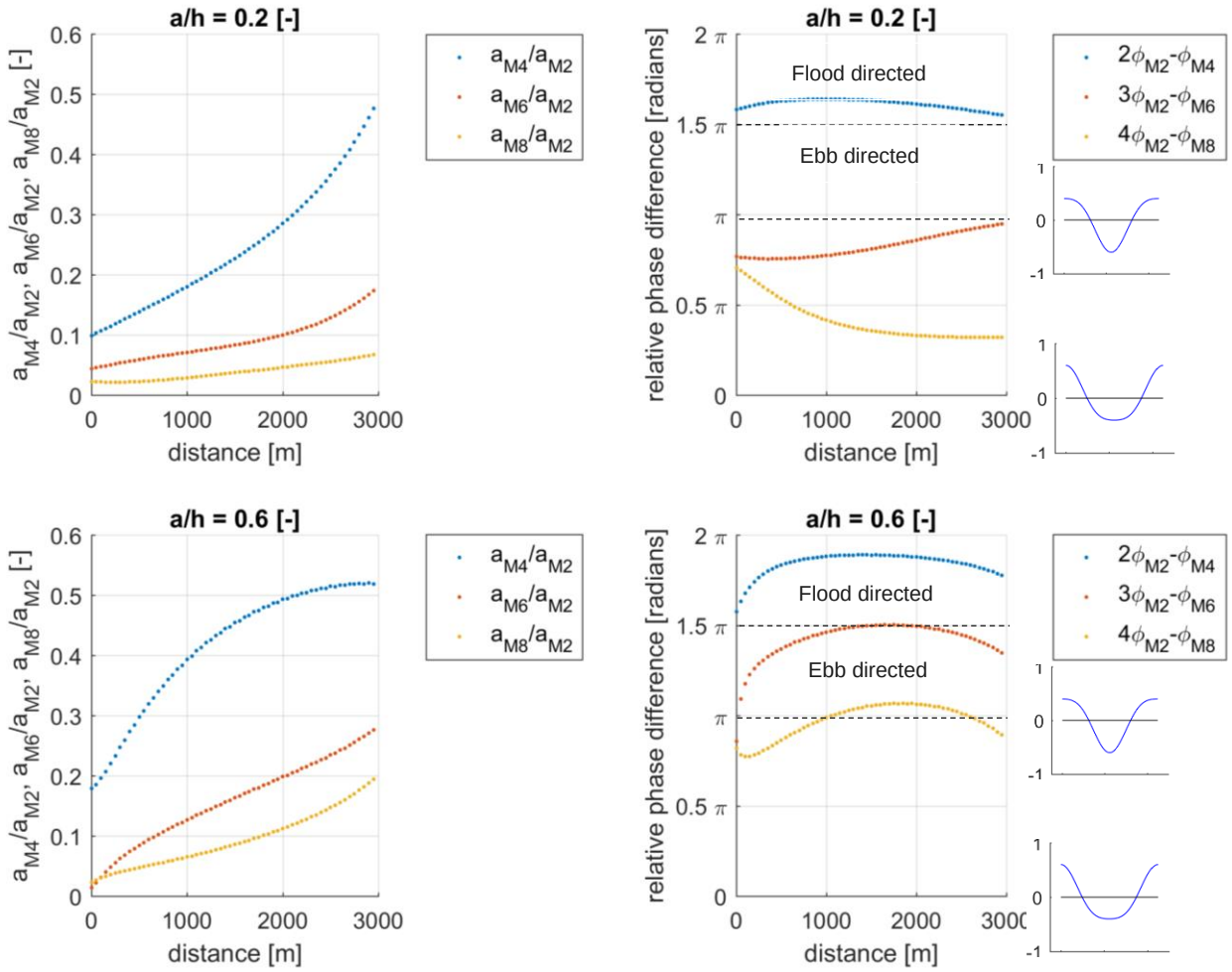

Figure 96 - Relative amplitude and phase differences for varying a/h

B.1.3. Scenarios for A_{basin}

The enlargement of the flushing basin area A_{basin}, results in a stronger change of the velocity signal; U(t) in channel-end direction. This increase in current velocities is also present for larger values of a/h; larger shallowness, see Figure 58 and Figure 66. The amplitudes of the higher harmonics are comparable. The same changes are visible.

The change of the phases is however different, see Figure 95 and Figure 97. For the smallest basin area, the phase of M_2 is constant over the channel length. The phase of the first higher harmonic; M_4 decrease from zero to $1.8\,\pi$ in the middle part and increase to the end of the channel. The same decrease is present for the scenarios of a deep channel.

For the largest basin area; A_{basin} = 300 ha, all phases are decreasing, including M_2, over the length of the channel

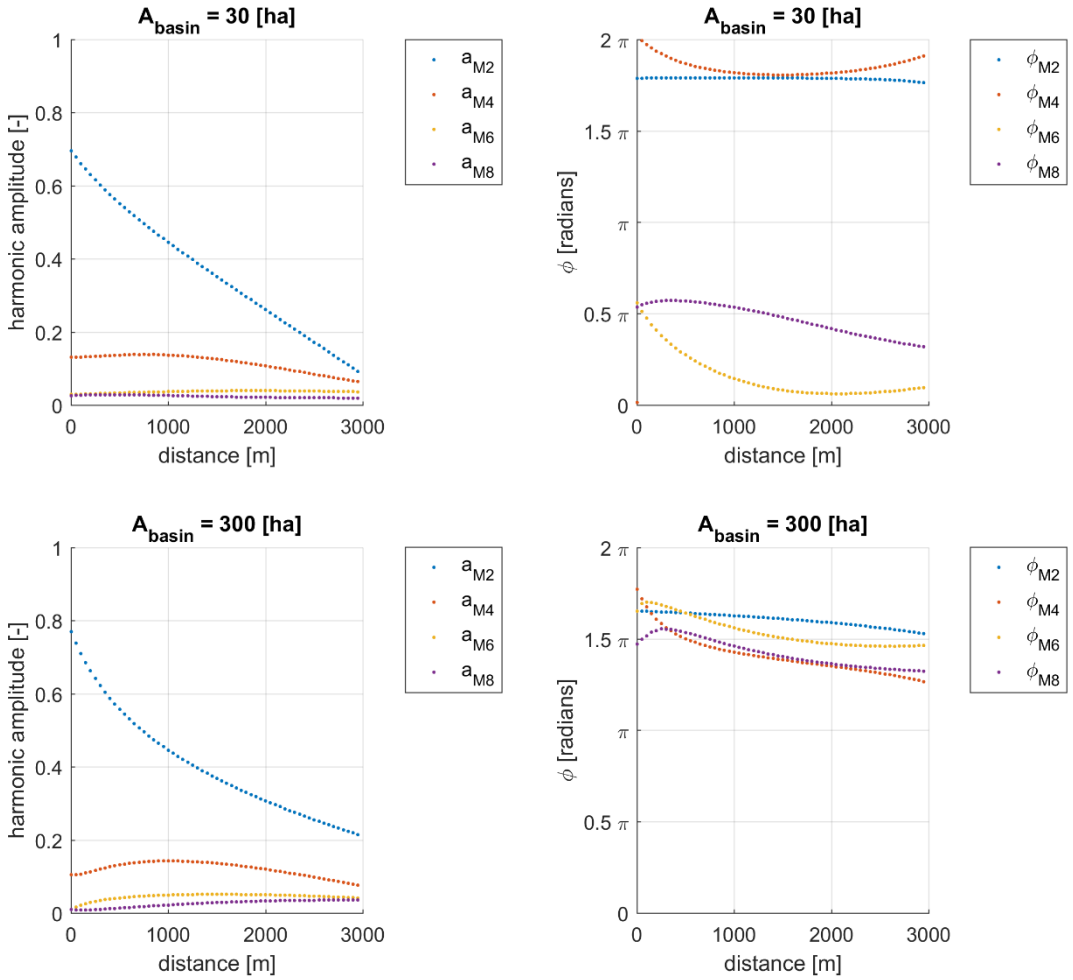

Figure 97 - Harmonic decomposition for smallest and largest value of A_{basin}.

Considering the relative amplitude and phase differences, see Figure 98, a stronger dominance of M_4 can be observed for the smallest basin area. Due to the presence of a larger basin area the relative amplitude decreases at the end of the channel.

The relative phase difference between the semi-diurnal tide and the first higher harmonic, has a larger variation along the channel for the smaller basin area. The relative phase difference for both scenarios: $\phi > \frac{3}{2}\pi$. A flood directed tide-residual transport can be expected.

A decrease of flood dominance that is visible in Figure 71, is also visible in Figure 98 as the relative phase decreases to about $\frac{3}{2}\pi$. However, when considering the harmonic decomposition only, the tide-residual transport is in flood direction. The tide-residual transport direction determined by the transport formula and with the relative phase difference are different. The tide-residual transport direction cannot be determined using only the relative phase difference between M_2 and M_4.

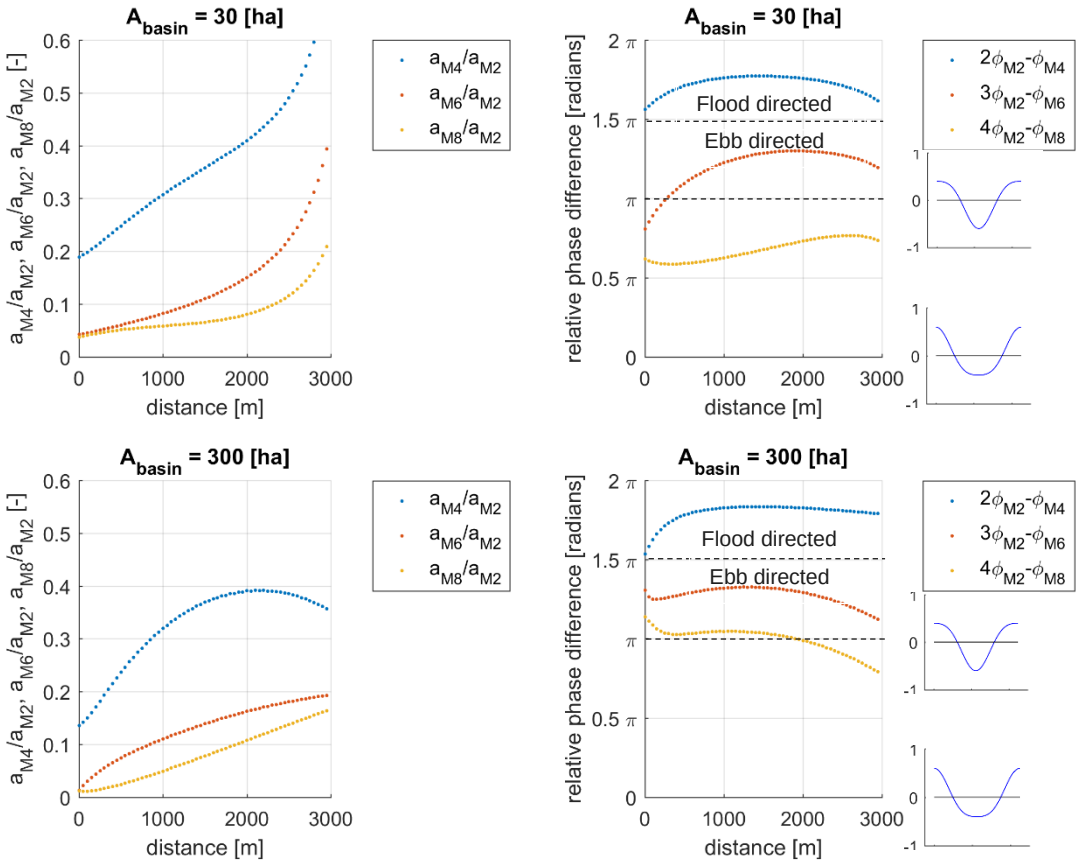

Figure 98 - Relative values for Harmonic decomposition for smallest and largest value of A_{basin}

B.2. Errors

The harmonic analysis is done by harmonic decomposition by using Fourier analysis. For the decomposition the first three higher harmonics are used to represent the original velocity signal. In the following figures for each design variable, the absolute errors are illustrated at the right axis. A maximum absolute error of about 1% can be observed.

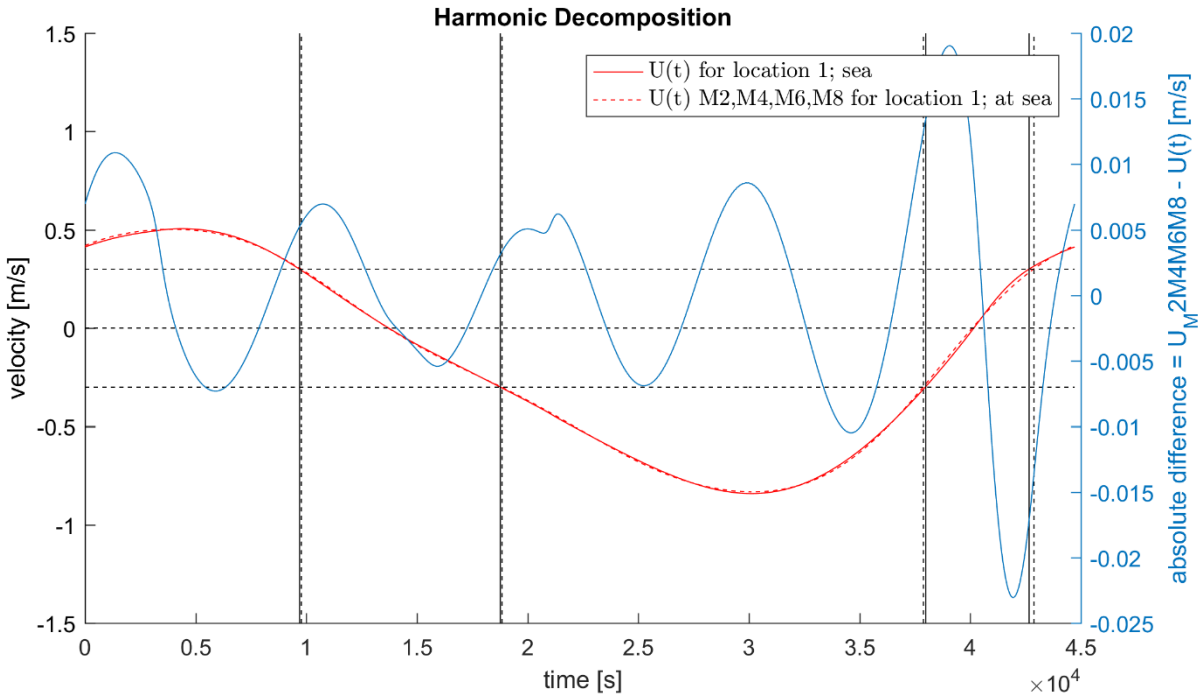

Figure 99 - Absolute error for W_{sluice} = 5 m

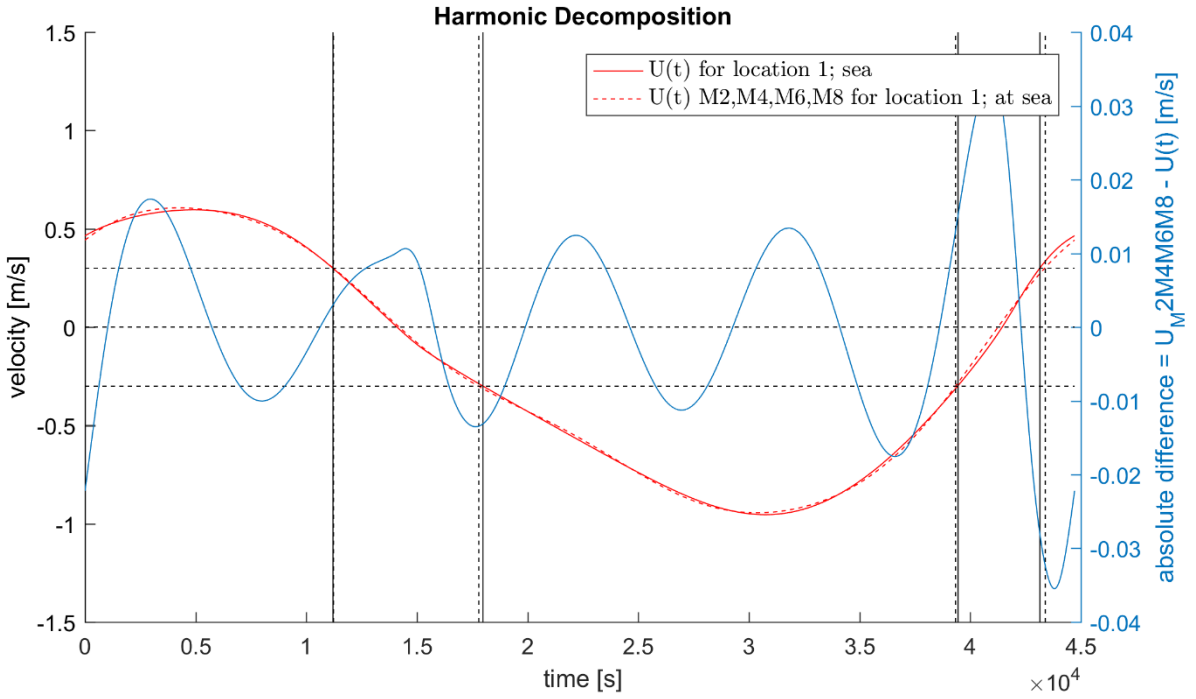

Figure 100 - Absolute error for W_{sluice} = 50 m

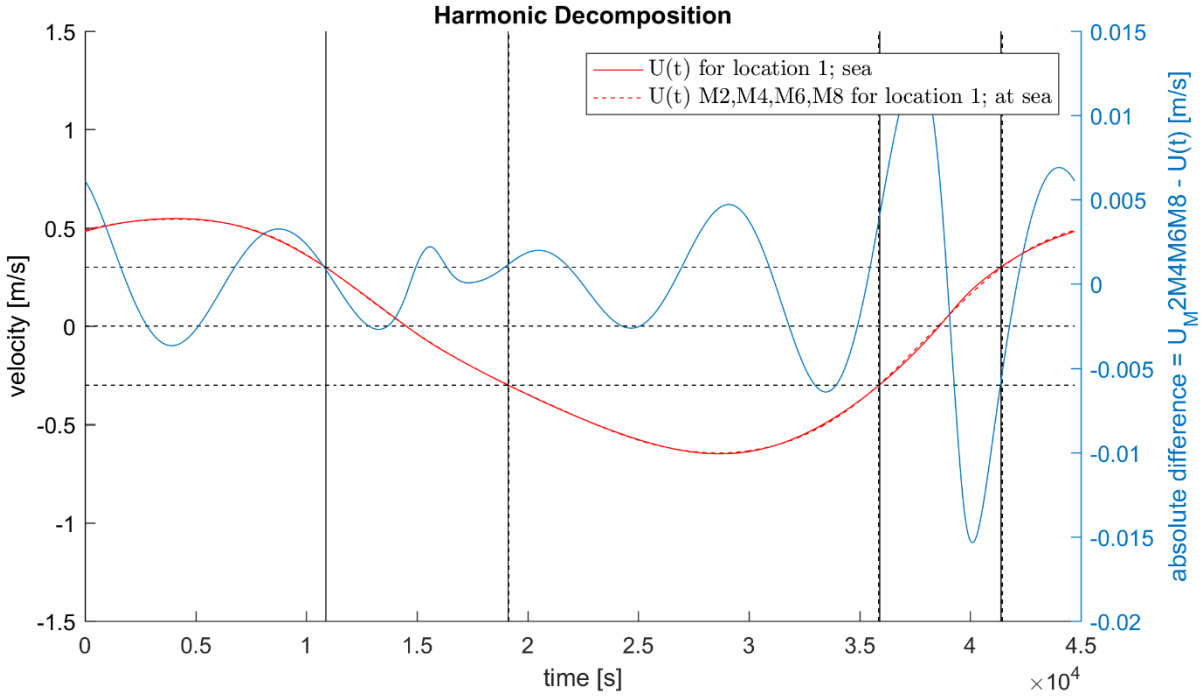

Figure 101 - Absolute error for a/h = 0.2

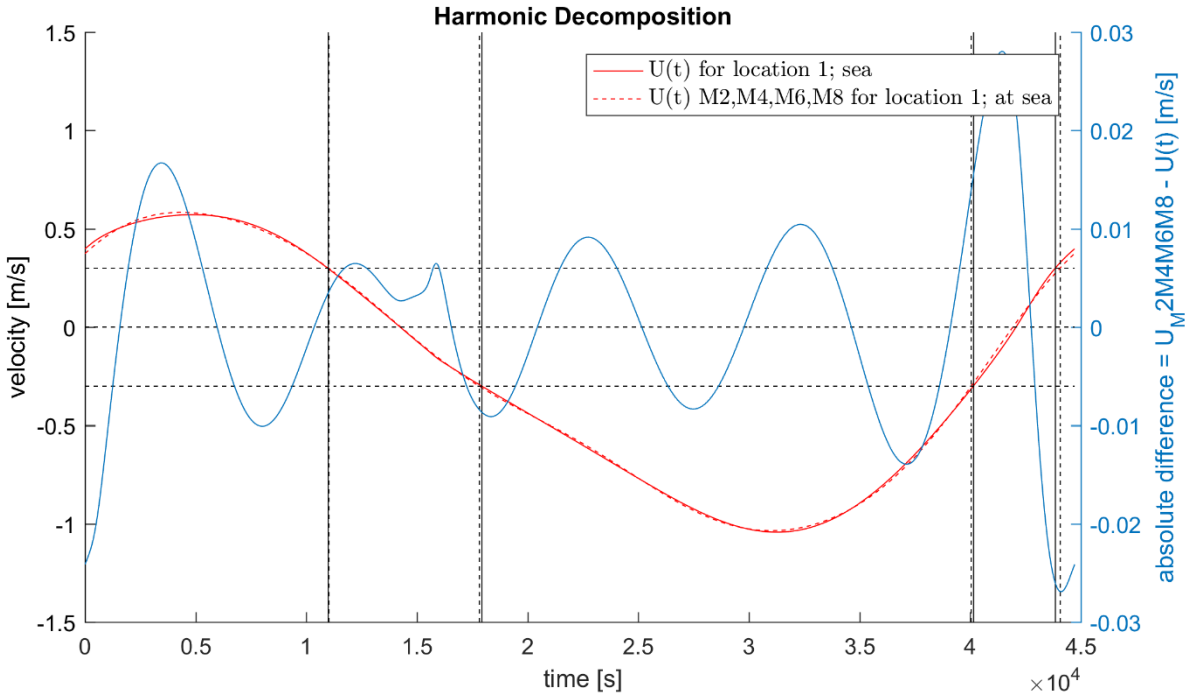

Figure 102 - Absolute error for a/h = 0.6

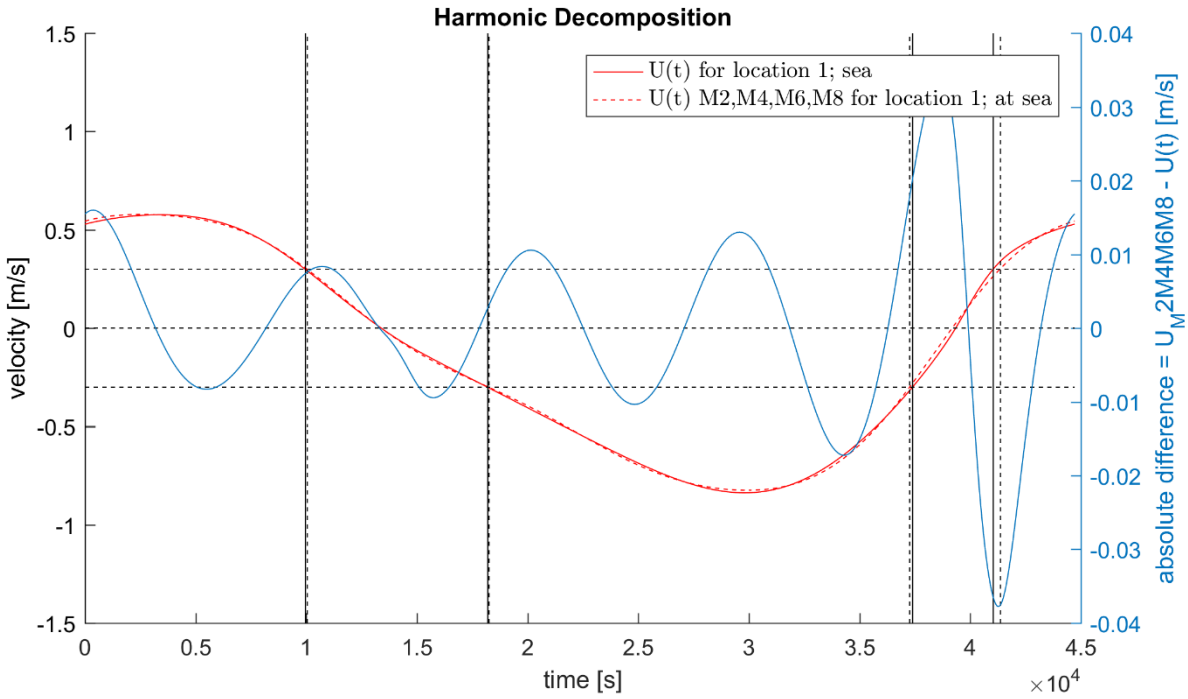

Figure 103 - Absolute error for A_{basin} = 30 ha

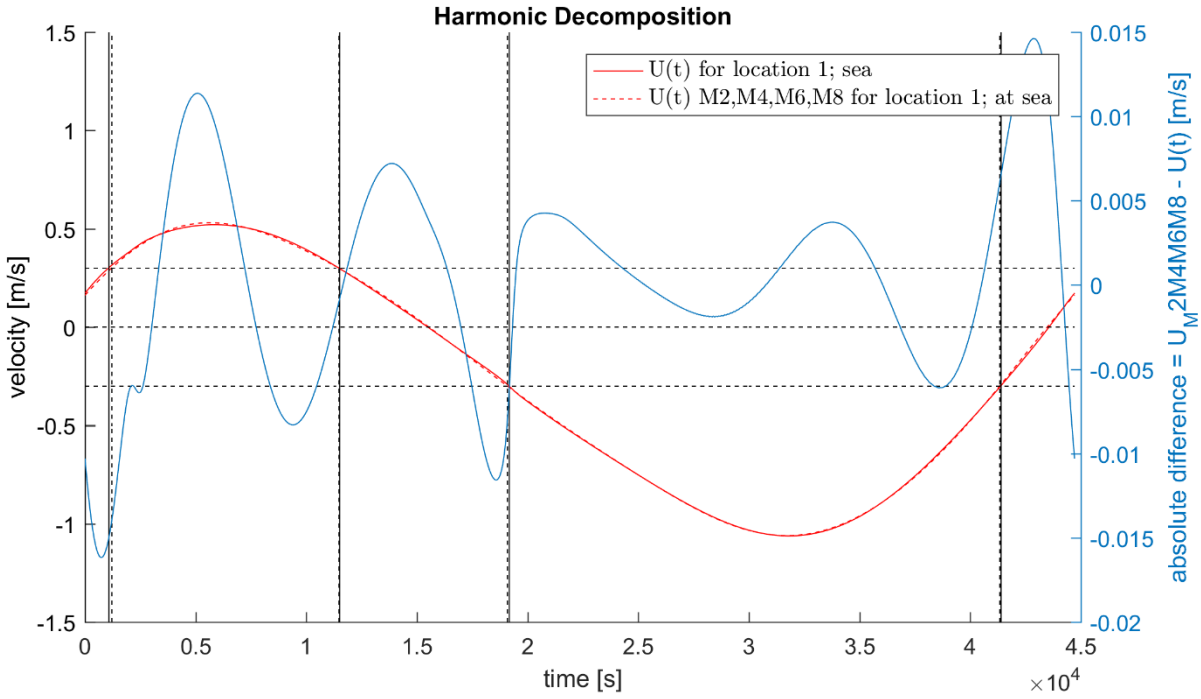

Figure 104 - Absolute error for A_{basin} = 300 ha

Arcadis Nederland B.V.

P.O. Box 137

8000 AC Zwolle

The Netherlands

+31 (0)88 4261 261

www.arcadis.com